VŠB – Technical University of Ostrava
Faculty of Electrical Engineering and Computer Science
Department of Applied Mathematics

Discretization and Numerical Realization of Dynamical Contact Problems with Friction

Diskretizace a numerická realizace dynamických kontaktních úloh se třením

2011 Michal Merta

VŠB - Technical University of Ostrava
Faculty of Electrical Engineering and Computer Science
Department of Applied Mathematics

Diploma Thesis Assignment

Student: **Bc. Michal Merta**

Study Programme: N2647 Information and Communication Technology

Study Branch: 1103T031 Computational Mathematics

Title: Diskretizace a numerická realizace dynamických kontaktních úloh se třením
Discretization and numerical realization of dynamical contact problems with friction

Description:

Pomocí prostředků konvexní analýzy zformulovat dynamické kontaktní úlohy s Coulombovým třením ve tvaru nehladkých rovnic. Provést prostorovou diskretizaci této úlohy pomocí metody konečných prvků. Získanou soustavu obyčejných diferenciálních rovnic, doplněnou inklusemi, jež vyjadřují podmínky nepronikání a tření, řešit pomocí vhodných stabilních a disipativních diferenčních schémat, např. Newmarkova typu. Konečně provést numerické experimenty na jednoduchých úlohách, jejichž cílem bude ověřit teoretické výsledky, týkající se použitých diferenčních metod.
Formulate dynamic contact problems with Coulomb's law of friction in the form of non-smooth equations, using the methods of convex analysis. Perform a spatial discretization of such problems using the finite element method. Solve the obtained system of ordinary differential equations, with inclusions expressing the non-penetration and the friction conditions, by suitable stable and dissipative differential schemes, e.g. of Newmark type. Finally perform numerical experiments to validate theoretical results about used differential methods.

References:

H.B. Khenous: Problemes de contact unilatéral avec frottement de Coulomb en élastostatique et élastodynamique. Etude mathématique et résolution numérique, These de doctorat 2005, l´INSA Toulouse.

T.A. Laursen: Computational Contact and Impact Mechanics, Fundamentals of Modeling Interfacial Phenomena in Nonlinear Finite Element Analysis, Springer 2002.

Extent and terms of a thesis are specified in directions for its elaboration that are opened to the public on the web sites of the faculty.

Supervisor: **prof. RNDr. Jaroslav Haslinger, DrSc.**

Date of issue: 19.11.2011
Date of submission: 06.05.2011

VYSOKÁ ŠKOLA BÁŇSKÁ-TECHNICKÁ UNIVERZITA Fakulta elektrotechniky a informatiky OSTRAVA

Head of Department

prof. RNDr. Václav Snášel, CSc.
Dean of Faculty

I declare that I created this thesis myself. I have stated all sources and publications that I had used.

Ostrava, May 6, 2011 .....

Motto: "... not because it is easy, but because it is hard."

JFK

I would like to express my sincere gratitude to Prof. RNDr. Jaroslav Haslinger, DrSc. for his careful and patient supervision of this work. My thanks also belong to Ing. Oldřich Vlach, PhD. and Ing. Tomáš Brzobohatý, PhD. for their helpful suggestions and advice.

Abstract

This thesis deals with methods for the numerical solution of dynamic contact problems with friction. We present the strong and weak form of the problem, use the finite element method for its spatial discretization and then discuss various methods of the temporal discretization. Then we describe the method of mass redistribution for a stabilization of temporal schemes. Finally the theoretical results are confirmed by several numerical experiments.

Keywords: contact problems, dynamics, Coulomb friction, mass redistribution method

Abstrakt

V této práci se zabýváme metodami numerického řešení dynamických kontaktních úloh se třením. Popisujeme silnou a slabou formulaci problému, následně použijeme metodu konečných prvků pro jeho prostorovou diskretizaci. Dále se zabýváme několika způsoby časové diskretizace problému. Ke stabilizaci vzniklých schémat používáme metodu redistribuce hmotnosti. Teoretické výsledky jsou ověřeny několika numerickými experimenty.

Klíčová slova: kontaktní problémy, dynamika, Coulombovské tření, metoda redistribuce hmotnosti

Notation

$\mathbb{N}$	–	the set of all positive integers
$\mathbb{R}$	–	the set of all real numbers
$\mathbb{R}^n$	–	the set of all n-dimensional real vectors
Ω	–	modeled body
$\partial\Omega$	–	boundary of Ω
Γ_u	–	Dirichlet boundary
Γ_σ	–	Neumann boundary
Γ_c	–	contact boundary
$\boldsymbol{n}$	–	outward unit normal vector to $\partial\Omega$
$\boldsymbol{t}$	–	tangential vector to $\partial\Omega$
$\boldsymbol{\tau}$	–	stress vector
τ_n, τ_t	–	normal and tangential component of $\boldsymbol{\tau}$, respectively
$\boldsymbol{\sigma}$	–	Cauchy stress tensor
$\boldsymbol{\varepsilon}$	–	small strain tensor
$\boldsymbol{f}$	–	body forces vector
$\boldsymbol{u}$	–	continuous displacement vector
$\dot{\boldsymbol{u}}$	–	continuous displacement velocity
u_n, u_t	–	normal and tangential component of $\boldsymbol{u}$, respectively
$\boldsymbol{x}$	–	spatial variable
t	–	time variable
$\mathbb{T}$	–	time interval
g, g_0	–	gap function and initial gap function, respectively
$\mathcal{F}$	–	coefficient of friction
λ_n, λ_t	–	normal and tangential Lagrange multipliers, respectively
$H^1(\Omega)$	–	Sobolev space $W^{1,2}(\Omega)$
$H^{1/2}(\Gamma)$	–	space of traces on Γ of functions from $H^1(\Omega)$, $\Gamma \subset \partial\Omega$
$\mathcal{U}$	–	solution set
$\mathcal{V}$	–	space of virtual displacements
K	–	convex set of admissible displacements
N_K	–	normal cone to K

∂f	–	subdifferential of a function f
Ω^h	–	triangulation of Ω
$\mathcal{U}^h, \mathcal{V}^h$	–	finite dimensional counterparts of $\mathcal{U}, \mathcal{V}$, respectively
$\mathcal{T}^h$	–	set of all triangular elements
$\mathcal{P}^h$	–	set of all nodes
$\mathcal{I}_c$	–	set of indexes of contact nodes
$\boldsymbol{x}_i$	–	node of triangulation
$\tilde{\boldsymbol{u}}$	–	vector function from $\mathcal{U}^h$
φ_i	–	i-th Courant basis function
$\boldsymbol{U}$	–	discretized displacement vector
$\boldsymbol{V}$	–	discretized displacement velocity vector
M	–	mass matrix
K	–	stiffness matrix
$\boldsymbol{L}$	–	discretized load vector
Δt	–	time-step
J	–	energy functional
ΔJ	–	energy variation
$\boldsymbol{u}^k$	–	$\boldsymbol{U}(t_k)$
$\boldsymbol{v}^k$	–	$\dot{\boldsymbol{U}}(t_k)$
$\boldsymbol{a}^k$	–	$\ddot{\boldsymbol{U}}(t_k)$
$\boldsymbol{\lambda}_n^k$	–	vector of normal Lagrange multipliers at $t = t_k$
$\boldsymbol{\lambda}_t^k$	–	vector of tangential Lagrange multipliers at $t = t_k$
$\hat{\mathsf{K}}$	–	effective stiffness matrix
MPRGP	–	Modified Proportioning with Reduced Gradient Projections
$\mathcal{A}(\boldsymbol{x})$	–	active set
$\mathcal{F}(\boldsymbol{x})$	–	free set
$\kappa(\mathsf{A})$	–	spectral number of a matrix A
$\ker(\mathsf{A})$	–	kernel (null space) of a matrix A
M_r	–	redistributed mass matrix
$\|\cdot\|_F$	–	Frobenius norm of a matrix
$\operatorname{supp} f$	–	support of a function f

Contents

Introduction

Contact mechanics is an important part of the computational mechanics which deals with modeling of interfacial phenomena between bodies in mutual contact. Such situations may eventually occur in any complex mechanical system, therefore the real world applications may range from the design of mechanical bearing to modeling of an artificial joint.

A theory of static contact problems is now well-established and there exist numerical procedures for both, frictionless as well as frictional problems. However for several reasons there is a demand for a simulation of dynamical contact problems. One of them is that the frictional behavior may depend on the history of loading. A problem must be discretized both in space and time and it turns out that the classical time discretization algorithms are usually unstable when modeling the contact between bodies. For this reason a lot of effort has been paid to the development of stable time-stepping methods in the last twenty years. In this work we will present some of these results.

In this thesis we study the dynamical form of the Signorini problem, i.e. the contact between an elastic body and a rigid foundation. For the sake of simplicity we restrict ourselves to the case of small deformations. The friction is modeled by Coulomb's law.

This work draws mainly from the monograph by Laursen [19] and from the work of Khenous [13] which extensively studies some of time discretization methods. The theory of variational inequalities and its application in contact mechanics is described in [11]. Methods for contact stabilization of time-stepping algorithms are presented e.g. in [9, 13, 14] or [4, 17].

The outline of this thesis is as follows: in Section 0 we recall some basic principles of the elasticity theory and convex analysis. In the first part of Section 1 we present the strong formulation of frictionless contact problems and extend it to the frictional case. The next part of this section deals with the derivation of the weak formulation of the problem. The last part describes the reformulation of the unilateral and friction conditions in the form of variational inclusions. In Section 2 we present the spatial discretization by the finite element method and several time discretization schemes. These schemes reduce a dynamic problem to a sequence of static contact problems, therefore at the end of the section we briefly describe the solution of static contact problems with Coulomb friction. One of the possible treatment of the numerical instability is described in Section 3. Finally in the last section we present results of several numerical experiments illustrating properties of presented methods.

0 Preliminaries

0.1 Preliminaries from continuum mechanics

Within this section we will briefly recall some basic ideas and principles of continuum mechanics of elastic bodies. Reader interested in more comprehensive explanation should consult e.g. [22] or [1].

Forces acting on an elastic body can be divided into two categories. Volume forces, like gravitational or centrifugal forces, act on each element of a body and their size is proportional to the volume of an element. Surface forces that are created on a surface of the body e.g. by a contact with another body belong to the second category.

Given a plane passing through an arbitrary point of the body we can express a stress (i.e. force per unit area) in this plane by a stress vector $\boldsymbol{\tau}$ which can be evaluated using the Cauchy stress tensor $\boldsymbol{\sigma}$

$$\tau_i = \sigma_{ji} n_j \quad \forall i,$$

where $\boldsymbol{n}$ is a unit normal vector to the given plane[1]. Indexes i and j have a meaning of spatial dimensions.

When no deformation occurs, volume and surface forces acting on body are in an equilibrium state. In the static case this can be expressed as

$$\sigma_{ij,j} + f_i = 0 \quad \forall i,$$

whereas in the dynamical case inertia forces must be taken into consideration:

$$\sigma_{ij,j} + f_i = \varrho \ddot{u}_i \quad \forall i.$$

Here $\boldsymbol{f} = (f_i)$ is a volume force vector, ϱ stands for the density of a material, $\ddot{\boldsymbol{u}}$ means the second partial derivative of a displacement $\boldsymbol{u}$ with respect to time t and $\boldsymbol{\sigma}$ is the above mentioned stress tensor.

Strains in a material are characterized by a strain tensor $\boldsymbol{\epsilon}(\boldsymbol{u}) = (\epsilon_{ij}(\boldsymbol{u}))$, where

$$\epsilon_{ij}(\boldsymbol{u}) := \frac{1}{2}(u_{i,j} + u_{j,i} + u_{i,j}u_{j,i}).$$

If partial derivatives of $\boldsymbol{u}$ are sufficiently small, the last term of $\boldsymbol{\epsilon}(\boldsymbol{u})$ can be neglected:

$$\varepsilon_{ij}(\boldsymbol{u}) := \frac{1}{2}(u_{i,j} + u_{j,i}).$$

We call this tensor a small (linearized) strain tensor.

To complete our model, we need a constitutive relation between $\boldsymbol{\sigma}$ and $\boldsymbol{\varepsilon}$. In this work we will assume a linear dependence between these two quantities which is expressed by linear Hooke's law:

$$\sigma_{ij} = c_{ijkl}\varepsilon_{kl},$$

where $\boldsymbol{c} = (c_{ijkl})$ is a fourth order elasticity tensor, which posses many symmetries that significantly reduce a number of its independent components.

[1] Einstein's summation convention is adopted in this work.

0.2 Preliminaries from convex analysis

Besides the classical expression of non-penetration and friction conditions as inequalities, it is often convenient to state these conditions in the form of inclusions. For this reason, this section provides definitions of some basic terms of convex analysis (for details see [8]).

Definition 0.1 (Normal cone)**.** Let V be a Banach space with the dual space V' and the duality pairing denoted by $\langle , \rangle$. Further let K be a convex closed subset of V and $x \in K$ be given. We define the normal cone to K at x by

$$N_K(x) := \left\{ \mu \in V' \mid \langle \mu, z - x \rangle \leq 0 \quad \forall z \in K \right\}.$$

Example of the normal cone of a convex subset in $\mathbb{R}^2$ is shown in Figure 0.1a.

Definition 0.2 (Indicator function)**.** The indicator function of a subset K of a Banach space V is defined by

$$I_K(x) = \begin{cases} 0, & \text{if } x \in K, \\ \infty, & \text{if } x \notin K. \end{cases}$$

Definition 0.3 (Subdifferential)**.** Let $f \colon V \to \mathbb{R}$ be a convex function and $u \in V$ be given. Then the set

$$\partial f(u) = \left\{ \mu \in V' \mid \langle \mu, v - u \rangle \leq f(v) - f(u) \quad \forall v \in V \right\}$$

is called the subdifferential of f at u.

Definition 0.4 (Polar function)**.** Let $f \colon V \to \mathbb{R} \cup \{-\infty, \infty\}$ and let $u' \in V'$. Then the function

$$f^*(u') := \sup_{u \in V} \left\{ \langle u', u \rangle - f(u) \right\}$$

is called the polar function of f.

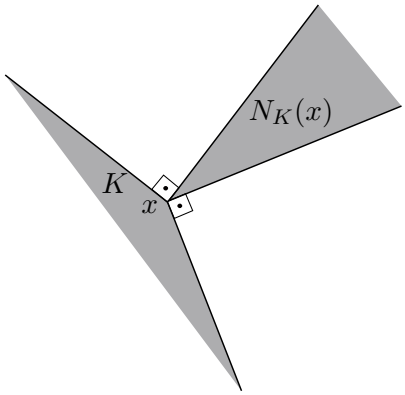

(a) Convex set K and its normal cone

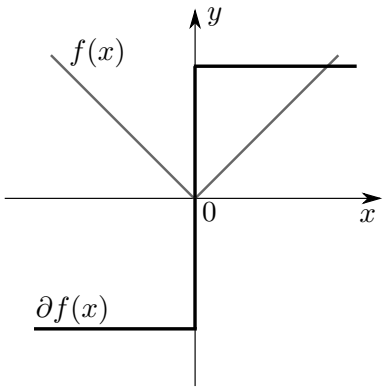

(b) Function $f(x) = |x|$ and the graph of its subdifferential

Figure 0.1: Basic terms of convex analysis

Theorem 0.1. Let $f\colon V \mapsto \mathbb{R}$ be a convex, lower semi-continuous function. Then

$$\mu \in \partial f(u) \Leftrightarrow u \in \partial f^*(\mu).$$

1 Model problem

Problem that will be studied in this thesis is illustrated in Figure 1.1. A deformable body represented by a bounded domain $\Omega \subset \mathbb{R}^2$ with the Lipschitz boundary $\partial\Omega$ comes into a contact with a rigid obstacle S. The boundary of Ω is divided into three non-overlapping relatively open subsets Γ_u, Γ_σ and Γ_c, thus

$$\begin{cases} \partial\Omega = \overline{\Gamma_u} \cup \overline{\Gamma_\sigma} \cup \overline{\Gamma_c}, \\ \Gamma_u \cap \Gamma_\sigma = \Gamma_u \cap \Gamma_c = \Gamma_\sigma \cap \Gamma_c = \emptyset. \end{cases} \tag{1.1}$$

The portion Γ_u represents the part of the boundary where displacements are prescribed, while tractions are prescribed on Γ_σ. Finally Γ_c is the part of the boundary where we expect contact with the obstacle S. Note that the exact part of $\partial\Omega$ where the contact will really occur is not known beforehand. In dynamical problems the contact area will in fact be changing in time.

This kind of problems is called the Signorini problem after the Italian mathematician Antonio Signorini, who as the first formulated its static version. Our intention is to numerically simulate a dynamic contact problem during a time interval $\mathbb{T} := [0, T]$. In the next paragraphs we will derive a strong and weak formulation of the corresponding initial boundary value problems.

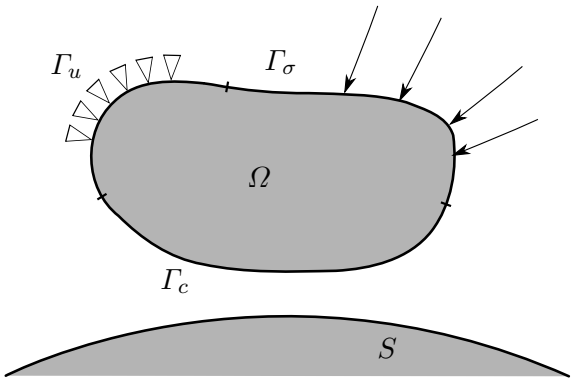

Figure 1.1: Contact between a deformable body Ω and a rigid obstacle S

1.1 Strong formulation of the contact problem without friction

At first we will provide the strong formulation of the initial boundary value problem when friction between the body and the obstacle is neglected. Let $\Omega \subset \mathbb{R}^2$ be a bounded domain with the Lipschitz boundary $\partial\Omega$ that satisfies (1.1) and let the domain $S \subset \mathbb{R}^2$ represent the rigid, immobile obstacle. Ω is said to be a reference configuration of the body, i.e. a state of the body at time $t = 0$.

A displacement vector field $\boldsymbol{u}\colon \Omega \times \mathbb{T} \to \mathbb{R}^2$ is called the strong solution of a contact problem without friction, if it satisfies the following equations and boundary conditions:

$$\begin{cases} \sigma_{ij,j}(\boldsymbol{u}) + f_i = \varrho \ddot{u}_i & \text{in } \Omega \times \mathbb{T}, \quad i = 1,2, \\ \sigma_{ij}(\boldsymbol{u}) = c_{ijkl}\varepsilon_{kl}(\boldsymbol{u}) & \text{in } \Omega \times \mathbb{T}, \quad i,j,k,l = 1,2, \\ u_i = \hat{U}_i & \text{in } \Gamma_u \times \mathbb{T}, \quad i = 1,2, \\ \sigma_{ij}(\boldsymbol{u}) n_j = P_i & \text{in } \Gamma_\sigma \times \mathbb{T}, \quad i = 1,2, \\ g \leq 0 & \text{in } \Gamma_c \times \mathbb{T}, \\ \tau_n \leq 0 & \text{in } \Gamma_c \times \mathbb{T}, \\ g\tau_n = 0 & \text{in } \Gamma_c \times \mathbb{T}, \\ u_{i|t=0} = u_i, \dot{u}_{i|t=0} = v_i & \text{in } \Omega, \quad i = 1,2. \end{cases} \tag{1.2}$$

Let us remind (see Section 0.1) that the first equation expresses the equilibrium of the elastic body; $\boldsymbol{\sigma}$ is the stress tensor, $\boldsymbol{f} = (f_i)$ represents the body forces with $f_i \in L^2(\Omega)$, $\varrho \in L^\infty, \varrho \geq 0$, is a material density. The meaning of g and τ_n is explained below. The second equation is Hooke's law of linear elasticity. Here $c_{ijkl} \in L^\infty(\Omega)$ are material coefficients and $\varepsilon_{ij}(\boldsymbol{u}) := \frac{1}{2}(u_{i,j} + u_{j,i})$ is the linearized strain tensor. The Dirichlet and Neumann boundary condition, respectively, are stated by the third and the fourth equation. Here $\boldsymbol{n}$ stands for an outward unit normal vector to $\partial\Omega$.

Before explaining the remaining conditions in (1.2) we need to define the following decomposition of the displacement $\boldsymbol{u}$ and the stress vector $\boldsymbol{\tau}$ on $\partial\Omega$ into their normal and tangential components:

$$\begin{aligned} u_n &:= u_i n_i, \qquad & u_t &:= u_i t_i \\ \tau_n &:= \sigma_{ij} n_i n_j, \qquad & \tau_t &:= \sigma_{ij} n_j t_i. \end{aligned} \tag{1.3}$$

with $\boldsymbol{t} := (-n_2, n_1)$ being the unit tangential vector to $\partial\Omega$. As friction is neglected, therefore $\tau_t = 0$ on Γ_c.

The correspondence between the points of Γ_c and the points of the obstacle is given by the mapping $\boldsymbol{\Phi}\colon \Gamma_c \to S$. This mapping uniquely assigns a contact point on S for each point $\boldsymbol{x} \in \Gamma_c$. We define it (e.g. as in [19]) as

$$\boldsymbol{\Phi}(\boldsymbol{x}) := \arg\min_{\boldsymbol{y} \in S} \|\boldsymbol{x} - \boldsymbol{y}\|, \quad \boldsymbol{x} \in \Gamma_c.$$

It is necessary to point out that we assume the mapping $\boldsymbol{\Phi}$ to be independent of the solution $\boldsymbol{u}$. Corresponding points are determined only at time $t = 0$ and remain the same for every $t \in \mathbb{T}$. Such a simplification however usually cannot be used in the case of large deformations. Let us also define the unit outward normal vector $\boldsymbol{\nu}$ to ∂S at $\boldsymbol{\Phi}(\boldsymbol{x})$. In the case of small deformations we will approximate $\boldsymbol{\nu}$ by $-\boldsymbol{n}$.

Using this $\boldsymbol{\Phi}$ we next define the initial gap function between the body and the obstacle as

$$g_0(\boldsymbol{x}) := (\boldsymbol{x} - \boldsymbol{\Phi}(\boldsymbol{x})) \cdot \boldsymbol{n}.$$

The gap between Ω and S at time $t \in \mathbb{T}$ is then expressed as

$$g(\boldsymbol{x}, t) := g_0(\boldsymbol{x}) + \boldsymbol{u}(\boldsymbol{x}, t) \cdot \boldsymbol{n}. \tag{1.4}$$

Note that this "gap" is, according to convention [19], negative when no contact occurs and positive in the case of penetration. Finally we can also linearize the contact condition by approximating

$$\boldsymbol{n} \approx \frac{\boldsymbol{x} - \boldsymbol{\Phi}(\boldsymbol{x})}{\|\boldsymbol{x} - \boldsymbol{\Phi}(\boldsymbol{x})\|}. \tag{1.5}$$

Relations $(1.2)_5$ – $(1.2)_7$ express unilateral contact conditions. The first one says that the body does not penetrate into the obstacle. The second one means that the contact stresses are compressive. Finally the third one implies that when the normal stress is non-zero, then there is no gap between Ω and S (contact occurs). On the contrary, when a part of Γ_c is not in contact with the obstacle (the gap function is negative), no stress is induced by contact. These three relations have the form of the Karush-Kuhn-Tucker optimality conditions and during the computational process will be enforced by the methods of nonlinear programming.

The situation is simplified when there is no initial gap between Ω and S, i.e. the initial gap function g_0 is zero. In this particular case we can write conditions $(1.2)_5$ – $(1.2)_7$ in the form

$$\begin{cases} u_n \leq 0 & \text{in } \Gamma_c \times \mathbb{T}, \\ \tau_n \leq 0 & \text{in } \Gamma_c \times \mathbb{T}, \\ u_n \tau_n = 0 & \text{in } \Gamma_c \times \mathbb{T}. \end{cases} \tag{1.6}$$

Finally, because the whole problem is time dependent, we need initial conditions for $\boldsymbol{u}$. Thus the last row of (1.2) gives us an initial displacement and an initial velocity, respectively.

1.2 Coulomb's law of friction

Up to now we assumed that the contact interface between Ω and S is perfectly lubricated and the effects of frictional response of materials in contact are neglected. But in real situations the dissipation of energy due to the frictional effects is significant enough to be taken into consideration.

Unfortunately, due to complexity of frictional effects, it is not possible to describe them by a single model (see [16, 19]). Situation may be complicated e.g. by involving thermomechanical effects to the model. In this work we will use Coulomb's law of friction in the form (see [11])

$$\begin{cases} |\tau_t| \leq \mathcal{F}|\tau_n| & \text{in } \Gamma_c \times \mathbb{T}, \\ (\mathcal{F}\,|\tau_n| - |\tau_t|)\, u_t = 0 & \text{in } \Gamma_c \times \mathbb{T}, \\ u_t \tau_t \leq 0 & \text{in } \Gamma_c \times \mathbb{T}, \end{cases} \tag{1.7}$$

or in the form more convenient for dynamic problems:

$$\begin{cases} \dot{u}_t = 0 \;\Rightarrow\; |\tau_t| \leq -\mathcal{F}\tau_n & \text{in } \Gamma_c \times \mathbb{T}, \\ \dot{u}_t \neq 0 \;\Rightarrow\; \tau_t = \mathcal{F}\tau_n \operatorname{sgn} \dot{u}_t & \text{in } \Gamma_c \times \mathbb{T}. \end{cases} \tag{1.8}$$

Here $\mathcal{F} \geq 0$ is a coefficient of friction, $\mathcal{F} \in L^\infty(\Gamma_c)$. The interpretation of (1.7) is as follows: when the tangential stress is lower than the friction force $-\mathcal{F}\tau_n$, points of Γ_c and the obstacle S stick together. But when the tangential stress attains the friction force, the surfaces of Γ_c and the obstacle may slip on each other. Similarly $(1.8)_1$ implies that the displacement velocity is zero when the tangential stress is bellow the friction force. Relation $(1.8)_2$ says that in the case of slip, the tangential stress has the opposite direction as the actual displacement velocity.

We say that a sufficiently smooth vector field $\boldsymbol{u}\colon \Omega \to \mathbb{R}^2$ is a *strong solution* of dynamical Signorini problem with friction, if it satisfies (1.2) together with (1.7) or (1.8).

1.3 Weak formulation

In this section we will derive a weak form of frictional contact problems in the form of a variational inequality. Let us define for all $t \in \mathbb{T}$ the solution set

$$\mathcal{U}(t) := \left\{ \boldsymbol{v} \in (H^1(\Omega))^2 \,|\, \gamma\boldsymbol{v} = \hat{\boldsymbol{U}}(t) \text{ on } \Gamma_u \right\},$$

and the the space of virtual displacements:

$$\mathcal{V} := \left\{ \boldsymbol{v} \in (H^1(\Omega))^2 \,|\, \gamma\boldsymbol{v} = \boldsymbol{0} \text{ on } \Gamma_u \right\},$$

where $H^1(\Omega)$ denotes the Sobolev space $W^{1,2}(\Omega)$ and $\gamma\colon (H^1(\Omega))^2 \to (L^2(\partial\Omega))^2$ is the trace operator. We also introduce the space of traces of functions from $H^1(\Omega)$ denoted by $H^{1/2}(\partial\Omega)$ and its restriction $H^{1/2}(\Gamma_c) = H^{1/2}(\partial\Omega)_{|\Gamma_c}$.

The set of admissible displacements of Ω is defined by

$$K(t) := \{ \boldsymbol{v} \in \mathcal{U}(t) \,|\, g_0(\boldsymbol{x}) + \boldsymbol{v}(\boldsymbol{x}, t) \cdot \boldsymbol{n} \leq 0 \text{ on } \Gamma_c \}.$$

Note that $K(t)$ is not a linear subset of $\mathcal{U}(t)$; it is a convex set of functions satisfying the non-penetration condition $(1.2)_5$.

Let $\boldsymbol{u}$ be a strong solution of the problem (1.2). Multiplying the equilibrium equation by a test function $\boldsymbol{w} \in \mathcal{V}$ and integrating over Ω we get for all $t \in \mathbb{T}$:

$$\int_\Omega \varrho \ddot{u}_i w_i \,\mathrm{d}\boldsymbol{x} - \int_\Omega \sigma_{ij,j}(\boldsymbol{u}) w_i \,\mathrm{d}\boldsymbol{x} = \int_\Omega f_i w_i \,\mathrm{d}\boldsymbol{x} \qquad \forall \boldsymbol{w} \in \mathcal{V}.$$

We use Green's formula and substitute from Hooke's law to modify the previous equation into the form

$$\int_\Omega \varrho \ddot{u}_i w_i \,\mathrm{d}\boldsymbol{x} + \int_\Omega c_{ijkl}\varepsilon_{ij}(\boldsymbol{u})\varepsilon_{kl}(\boldsymbol{w}) \,\mathrm{d}\boldsymbol{x} - \int_{\partial\Omega} \sigma_{ij}(\boldsymbol{u}) w_i n_j \,\mathrm{d}\boldsymbol{s} = \int_\Omega f_i w_i \,\mathrm{d}\boldsymbol{x} \qquad \forall \boldsymbol{w} \in \mathcal{V}.$$

Taking into account the boundary condition $\sigma_{ij}(\boldsymbol{u})n_j = P_i$ on Γ_σ and the fact that functions from $\mathcal{V}$ are such that $\gamma\boldsymbol{v} = \boldsymbol{0}$ on Γ_u we get

$$\int_\Omega \varrho \ddot{u}_i w_i \,\mathrm{d}\boldsymbol{x} + \int_\Omega c_{ijkl}\varepsilon_{ij}(\boldsymbol{u})\varepsilon_{kl}(\boldsymbol{w}) \,\mathrm{d}\boldsymbol{x} - \int_{\Gamma_c} \tau_i(\boldsymbol{u}) w_i \,\mathrm{d}\boldsymbol{s} = \int_\Omega f_i w_i \,\mathrm{d}\boldsymbol{x} + \int_{\Gamma_\sigma} P_i w_i \,\mathrm{d}\boldsymbol{s} \qquad \forall \boldsymbol{w} \in \mathcal{V}. \quad (1.9)$$

In the next step we decompose the contact stress into its normal and tangential component defined in (1.3):

$$\int_{\Gamma_c} \tau_i(\boldsymbol{u}) w_i \,\mathrm{d}\boldsymbol{s} = \int_{\Gamma_c} (\tau_n(\boldsymbol{u}) n_i w_i + \tau_t(\boldsymbol{u}) t_i w_i) \,\mathrm{d}\boldsymbol{s} = \int_{\Gamma_c} (\tau_n(\boldsymbol{u}) w_n + \tau_t(\boldsymbol{u}) w_t) \,\mathrm{d}\boldsymbol{s}.$$

From this and (1.9) we get following identity:

$$\begin{aligned}\int_\Omega \varrho \ddot{u}_i w_i \,\mathrm{d}\boldsymbol{x} + \int_\Omega c_{ijkl}\varepsilon_{ij}(\boldsymbol{u})\varepsilon_{kl}(\boldsymbol{w}) \,\mathrm{d}\boldsymbol{x} - \int_{\Gamma_c} \tau_t(\boldsymbol{u}) w_t \,\mathrm{d}\boldsymbol{s} \\ - \int_\Omega f_i w_i \,\mathrm{d}\boldsymbol{x} - \int_{\Gamma_\sigma} P_i w_i \,\mathrm{d}\boldsymbol{s} = \int_{\Gamma_c} \tau_n(\boldsymbol{u}) w_n \,\mathrm{d}\boldsymbol{s} \qquad \forall \boldsymbol{w} \in \mathcal{V}. \quad (1.10)\end{aligned}$$

We will now focus on the right-hand side of (1.10). Let $\boldsymbol{v} \in K(t)$ and $\boldsymbol{w} := \boldsymbol{v} - \boldsymbol{u}$. Then $\boldsymbol{w} \in \mathcal{V}$ for all $t \in \mathbb{T}$. Using the definition of the gap function, the non-penetration conditions $(1.2)_5$ – $(1.2)_7$ and the definition of $K(t)$ we see that for such test functions it holds:

$$\begin{aligned}\int_{\Gamma_c} \tau_n(\boldsymbol{u}) w_n \,\mathrm{d}\boldsymbol{s} &= \int_{\Gamma_c} \tau_n(\boldsymbol{u})(v_n - u_n) \,\mathrm{d}\boldsymbol{s} \overset{(1.4)}{=} \int_{\Gamma_c} \tau_n(\boldsymbol{u})(v_n - g + g_0) \\ &= -\underbrace{\int_{\Gamma_c} \tau_n(\boldsymbol{u}) g \,\mathrm{d}\boldsymbol{s}}_{=0} + \underbrace{\int_{\Gamma_c} \tau_n(\boldsymbol{u})(v_n + g_0) \,\mathrm{d}\boldsymbol{s}}_{\geq 0} \geq 0 \qquad \forall \boldsymbol{v} \in K(t). \quad (1.11)\end{aligned}$$

To replace the term with the tangential stress we will prove the following inequality using Coulomb's law (1.7):

$$\tau_t(\boldsymbol{u})(v_t - u_t) - \mathcal{F}\tau_n(\boldsymbol{u})(|v_t| - |u_t|) \geq 0 \quad \text{ on } \Gamma_c \quad \forall \boldsymbol{v} \in K(t). \qquad (1.12)$$

For the sake of simplicity, we will write τ_n, τ_t instead of $\tau_n(\boldsymbol{u}), \tau_t(\boldsymbol{u})$ respectively. We have

$$\begin{aligned}\tau_t v_t - \mathcal{F}\tau_n |v_t| &= \tau_t v_t + \mathcal{F}|\tau_n| \cdot |v_t| \\ &\geq -|\tau_t| \cdot |v_t| + \mathcal{F}|\tau_n| \cdot |v_t| \\ &= (\mathcal{F}|\tau_n| - |\tau_t|)|v_t| \overset{(1.7)_1}{\geq} 0 \qquad \forall \boldsymbol{v} \in K(t),\end{aligned}$$

whereas for the remaining terms of inequality (1.12) we get from (1.6) and $(1.7)_2$:

$$-(\tau_t u_t - \mathcal{F}\tau_n |u_t|) = -(-|\tau_t||u_t| + \mathcal{F}|\tau_n||u_t|) = -(\mathcal{F}|\tau_n| - |\tau_t|)|u_t| = 0.$$

Thus

$$\tau_t(v_t - u_t) - \mathcal{F}\tau_n(|v_t| - |u_t|) = \underbrace{\tau_t v_t - \mathcal{F}\tau_n |v_t|}_{\geq 0} \underbrace{-\tau_t u_t + \mathcal{F}\tau_n |u_t|}_{=0} \geq 0 \qquad \forall \boldsymbol{v} \in K(t).$$

Finally, using (1.11) and (1.12) we can modify equation (1.10) into the form

$$\underbrace{\int_\Omega \varrho\ddot{u}_i(v_i-u_i)\,\mathrm{d}\boldsymbol{x}}_{=:\langle\varrho\ddot{\boldsymbol{u}},\boldsymbol{v}-\boldsymbol{u}\rangle}+\underbrace{\int_\Omega c_{ijkl}\varepsilon_{ij}(\boldsymbol{u})\varepsilon_{kl}(\boldsymbol{v}-\boldsymbol{u})\,\mathrm{d}\boldsymbol{x}}_{=:A(\boldsymbol{u},\boldsymbol{v}-\boldsymbol{u})}\underbrace{-\int_{\Gamma_c}\mathcal{F}\tau_n(\boldsymbol{u})|v_t|\,\mathrm{d}\boldsymbol{s}}_{=:j(\tau_n(\boldsymbol{u}),v_t)}$$
$$+\underbrace{\int_{\Gamma_c}\mathcal{F}\tau_n(\boldsymbol{u})|u_t|\,\mathrm{d}\boldsymbol{s}}_{=:j(\tau_t(\boldsymbol{u}),v_t)}\geq\underbrace{\int_\Omega f_i(v_i-u_i)\,\mathrm{d}\boldsymbol{x}+\int_{\Gamma_\sigma}P_i(v_i-u_i)\,\mathrm{d}\boldsymbol{s}}_{=:L(\boldsymbol{v}-\boldsymbol{u})}\qquad\forall\boldsymbol{v}\in K(t).\quad(1.13)$$

Using previous notation we arrive at the formulation of the dynamic contact problem with friction law (1.7) in the form of the variational inequality (the meaning of the symbols is seen from (1.13)):

$$\begin{cases}\text{Find } \boldsymbol{u}\colon\mathbb{T}\mapsto(H^1(\Omega))^2 \text{ such that } \boldsymbol{u}(\cdot,t)\in K(t)\quad\forall t\in\mathbb{T} \text{ and}\\ \langle\varrho\ddot{\boldsymbol{u}},\boldsymbol{v}-\boldsymbol{u}\rangle+A(\boldsymbol{u},\boldsymbol{v}-\boldsymbol{u})+j(\tau_n(\boldsymbol{u}),v_t)-j(\tau_n(\boldsymbol{u}),u_t)\geq L(\boldsymbol{v}-\boldsymbol{u})\ \forall\boldsymbol{v}\in K(t)\,\forall t\in\mathbb{T},\\ \boldsymbol{u}(\boldsymbol{x},0)=\boldsymbol{u}_0,\dot{\boldsymbol{u}}(\boldsymbol{x},0)=\boldsymbol{v}_0.\end{cases}\tag{1.14}$$

Coulomb's law (1.8) is more complicated because the tangential stress depends on the *velocities* of the displacement. Thus the non-penetration conditions also have to be formulated in velocities instead of displacements. For this reason it is obvious to assume the initial gap function and the displacement on Γ_u to be zero (see [17]).

Under these assumptions (i.e. $g_0(\boldsymbol{x})=0,\hat{\boldsymbol{U}}=\boldsymbol{0}$ for all $t\in\mathbb{T}$) we replace the non-penetration conditions (1.6) by

$$\begin{cases}\dot{u}_n\leq 0 & \text{on } \Gamma_c\times\mathbb{T},\\ \tau_n\leq 0 & \text{on } \Gamma_c\times\mathbb{T},\\ \dot{u}_n\tau_n=0 & \text{on } \Gamma_c\times\mathbb{T}.\end{cases}\tag{1.15}$$

Note, that this formulation implies constraints (1.6), but is physically less accurate. According to these conditions, once the bodies detach, no further contact between them is possible. Next, we present the new definition of the set of admissible displacements:

$$\dot{K}(t):=\{\boldsymbol{v}\in\mathcal{U}(t)\,|\,\boldsymbol{v}(\boldsymbol{x},t)\cdot\boldsymbol{n}\leq 0 \text{ on } \Gamma_c\}\,.$$

By applying the process similar to the one above, one can derive the following weak formulation of the Signorini problem with the non-penetration conditions (1.15) and Coulomb's law (1.8):

$$\begin{cases}\text{Find } \boldsymbol{u}\colon\mathbb{T}\mapsto(H^1(\Omega))^2 \text{ such that } \dot{\boldsymbol{u}}(\cdot,t)\in\dot{K}(t)\quad\forall t\in\mathbb{T} \text{ and}\\ \langle\varrho\ddot{\boldsymbol{u}},\boldsymbol{v}-\dot{\boldsymbol{u}}\rangle+A\,(\boldsymbol{u},\boldsymbol{v}-\dot{\boldsymbol{u}})+j(\tau_n(\boldsymbol{u}),v_t)-j(\tau_n(\boldsymbol{u}),\dot{u}_t)\geq L(\boldsymbol{v}-\dot{\boldsymbol{u}})\ \forall\boldsymbol{v}\in\dot{K}(t)\,\forall t\in\mathbb{T},\\ \boldsymbol{u}(\boldsymbol{x},0)=\boldsymbol{u}_0,\dot{\boldsymbol{u}}(\boldsymbol{x},0)=\boldsymbol{v}_0.\end{cases}\tag{1.16}$$

The main difficulty with (1.14) and (1.16) from the algorithmic point of view is the presence of the non-differentiable term j. To overcome this problem, in the next section we present more convenient formulations.

1.4 Formulation of unilateral and friction conditions by means of inclusions

To complete the first part of this chapter we will derive a hybrid formulation of the problem (for the static case see [15]) and discuss the reformulation of the contact and friction conditions in the form of inclusions. We will consider the contact conditions (1.15) and Coulomb's law (1.8). For this purpose let us define (following [13]) these trace spaces:

$$X := \left\{ \boldsymbol{v}_{|\Gamma_c} \,|\, \boldsymbol{v} \in \mathcal{V} \right\},$$

$$X_n := \left\{ v_{n|\Gamma_c} \,|\, \boldsymbol{v} \in \mathcal{V} \right\} \subset H^{1/2}(\Gamma_c),$$

$$X_t := \left\{ v_{t|\Gamma_c} \,|\, \boldsymbol{v} \in \mathcal{V} \right\} \subset H^{1/2}(\Gamma_c),$$

together with their dual spaces X', X_n' and X_t', respectively. In other words, X_n and X_t are the spaces of all normal and tangential components of functions from X. Elements of the dual spaces X', X_n' and X_t' represent contact forces and their components. The duality pairing between X_n, X_n' and X_t, X_t' will be denoted by $\langle\,,\,\rangle$ in what follows.

The derivation of the contact conditions in the form of inclusions is similar to the one as for the static case described in [13]. We start with the equation (1.10) and replace the unknown stresses on Γ_c by multipliers $\lambda_n \in X_n'$ and $\lambda_t \in X_t'$. The non-penetration constraint may be stated in the weak form as follows:

$$\begin{cases} \dot{u}_n \le 0 & \text{on } \Gamma_c, \forall t \in \mathbb{T}, \\ \int_{\Gamma_c} \lambda_n v_n \,\mathrm{d}\boldsymbol{s} \ge 0 & \forall t \in \mathbb{T}\, \forall v_n \in X_n, v_n \le 0 \text{ on } \Gamma_c, \\ \int_{\Gamma_c} \lambda_n \dot{u}_n \,\mathrm{d}\boldsymbol{s} = 0 & \forall t \in \mathbb{T}. \end{cases}$$

The set of admissible functions from X_n is denoted by

$$K_n := \left\{ v_n \in X_n \,|\, v_n \le 0 \text{ on } \Gamma_c \right\}. \tag{1.17}$$

This definition and the weak form of the non-penetration condition imply

$$-\int_{\Gamma_c} \lambda_n w_n \,\mathrm{d}\boldsymbol{s} \le 0 \qquad \forall t \in \mathbb{T}\, \forall w_n \in K_n.$$

Subtracting $\int_{\Gamma_c} \lambda_n \dot{u}_n \,\mathrm{d}\boldsymbol{s} = 0$ from both sides of this inequality, we get

$$-\int_{\Gamma_c} \lambda_n (w_n - \dot{u}_n) \,\mathrm{d}\boldsymbol{s} \le 0 \qquad \forall t \in \mathbb{T}\, \forall w_n \in K_n.$$

From Section 0.2 we know that

$$N_{K_n}(\dot{u}_n) := \left\{ \mu_n \in X_n' \,|\, \langle \mu_n, w_n - \dot{u}_n \rangle \le 0 \quad \forall w_n \in K_n \right\}$$

is the normal cone to K_n at $\dot{u}_n$. Thus the previous inequality means that $-\lambda_n \in N_{K_n}(\dot{u}_n)$, taking into account that the duality pairing $\langle\,,\,\rangle$ is represented by the $L^2(\Gamma_c)$-scalar product.

To derive the weak formulation of the friction conditions, we start with the equality

$$\langle \varrho\ddot{\boldsymbol{u}}, \boldsymbol{v}-\dot{\boldsymbol{u}}\rangle + A(\boldsymbol{u}, \boldsymbol{v}-\dot{\boldsymbol{u}}) = L(\boldsymbol{v}-\dot{\boldsymbol{u}}) + \langle \lambda_n, v_n - \dot{u}_n\rangle + \langle \lambda_t, v_t - \dot{u}_t\rangle \quad \forall \boldsymbol{v}\in\mathcal{V}\,\forall t\in\mathbb{T}$$

and add the term $j(\lambda_n, v_t) - j(\lambda_n, \dot{u}_t)$ to the left and the right side. This together with (1.16) lead to the expression

$$\langle \lambda_n, v_n - \dot{u}_n\rangle + \langle \lambda_t, v_t - \dot{u}_t\rangle + j(\lambda_t, v_t) - j(\lambda_n, \dot{u}_t) \geq 0 \quad \forall v\in\mathcal{V}\,\forall t\in\mathbb{T}.$$

If we choose $v\in\mathcal{V}$ such that $v_n = \dot{u}_n$ on Γ_c and $v_t\in X_t$ arbitrary then we get

$$\int_{\Gamma_c} \lambda_t(v_t - \dot{u}_t)\,\mathrm{d}\boldsymbol{s} - \int_{\Gamma_c} \mathcal{F}\lambda_n(|v_t| - |\dot{u}_t|)\,\mathrm{d}\boldsymbol{s} \geq 0 \qquad \forall v_t\in X_t\,\forall t\in\mathbb{T}. \tag{1.18}$$

Denote

$$\partial_2 j(\lambda_n, \dot{u}_t) := \left\{\mu_t\in X_t' \,|\, \langle \mu_t, v_t - \dot{u}_t\rangle \leq j(\lambda_n, v_t) - j(\lambda_n, \dot{u}_t) \quad \forall v_t\in X_t\right\}$$

the partial subdifferential of $j(\lambda_n, \cdot)$ with respect to the second variable. Thus dynamic contact problems with Coulomb's law of friction (1.8) and unilateral conditions (1.15) can be expressed in the form

$$\begin{cases} \text{Find } \boldsymbol{u}\colon \mathbb{T}\mapsto (H^1(\Omega))^2, \lambda_n\colon \mathbb{T}\mapsto X_n', \lambda_t\colon \mathbb{T}\mapsto X_t' \text{ such that} \\ \langle \varrho\ddot{\boldsymbol{u}}, \boldsymbol{v}\rangle + A(\boldsymbol{u}, \boldsymbol{v}) = L(\boldsymbol{v}) + \langle \lambda_n, v_n\rangle + \langle \lambda_t, v_t\rangle \quad \forall \boldsymbol{v}\in\mathcal{V}\,\forall t\in\mathbb{T}, \\ -\lambda_n \in N_{K_n}(\dot{u}_n) \quad \forall t\in\mathbb{T}, \\ -\lambda_t \in \partial_2 j(\lambda_n, \dot{u}_t) \quad \forall t\in\mathbb{T}, \\ \boldsymbol{u}(\boldsymbol{x}, 0) = \boldsymbol{u}_0, \dot{\boldsymbol{u}}(\boldsymbol{x}, 0) = \boldsymbol{v}_0. \end{cases} \tag{1.19}$$

The problem now has the form of the non-smooth equation with three unknowns – the displacement $\boldsymbol{u}$, the normal stress λ_n and the tangential stress λ_t. The last two inclusions play the role of the constitutive laws among these three quantities.

So far it has been show that (1.16) implies (1.19). To prove the equivalence of these two formulations we have to show that (1.19) implies (1.16). We substitute the test function $\boldsymbol{w}-\dot{\boldsymbol{u}}$, $\boldsymbol{w}\in\dot{K}(t)$, into the equation $(1.19)_2$, use the definition of the normal cone and of the subdifferential and obtain

$$\langle \varrho\ddot{\boldsymbol{u}}, \boldsymbol{w}-\dot{\boldsymbol{u}}\rangle + A(\boldsymbol{u}, \boldsymbol{w}-\dot{\boldsymbol{u}}) = L(\boldsymbol{w}-\dot{\boldsymbol{u}}) + \underbrace{\langle \lambda_n, w_n - \dot{u}_n\rangle}_{\geq 0} + \underbrace{\langle \lambda_t, w_t - \dot{u}_t\rangle}_{\geq j(\lambda_n, v_t) - j(\lambda_t, \dot{u}_t)} \quad \forall \boldsymbol{w}\in\dot{K}(t)\,\forall t\in\mathbb{T},$$

i.e.,

$$\langle \varrho\ddot{\boldsymbol{u}}, \boldsymbol{w}-\dot{\boldsymbol{u}}\rangle + A(\boldsymbol{u}, \boldsymbol{w}-\dot{\boldsymbol{u}}) + j(\lambda_t, w_t) - j(\lambda_n, \dot{u}_t) \geq L(\boldsymbol{w}-\dot{\boldsymbol{u}}) \quad \forall \boldsymbol{w}\in\dot{K}(t)\,\forall t\in\mathbb{T}.$$

From (1.19) we get that $\dot{u}_n\in K_n$, thus $\dot{u}_n\leq 0$ on Γ_c. Now if $\boldsymbol{w}\in\dot{K}(t)$ then $w_n\in K_n$ for all $t\in\mathbb{T}$. The definition of the normal cone $N_{K_n}(\dot{u}_n)$ says that:

$$-\int_{\Gamma_c} \lambda_n(w_n - \dot{u}_n)\,\mathrm{d}\boldsymbol{s} \leq 0 \qquad \forall w_n\in K_n,$$

Inserting $w_n = 0$ and $w_n = 2\dot{u}_n$ into the previous inequality we obtain

$$\int_{\Gamma_c} \lambda_n \dot{u}_n \, \mathrm{d}\boldsymbol{s} = 0. \tag{1.20}$$

Therefore

$$0 \leq \int_{\Gamma_c} \lambda_n w_n \, \mathrm{d}\boldsymbol{s} \qquad \forall w_n \in K_n,$$

implying $\lambda_n \leq 0$ on Γ_c. From this we see that the integrand of (1.20) is non-negative on Γ_c, thus $\lambda_n \dot{u}_n = 0$ on Γ_c.

Further from $-\lambda_t \in \partial_2 j(\lambda_n, \dot{u}_t)$ and the definition of the subdifferential we get:

$$-\int_{\Gamma_c} \lambda_t (v_t - \dot{u}_t) \, \mathrm{d}\boldsymbol{s} \leq -\int_{\Gamma_c} \mathcal{F}\lambda_n |v_t| \, \mathrm{d}\boldsymbol{s} + \int_{\Gamma_c} \mathcal{F}\lambda_n |\dot{u}_t| \, \mathrm{d}\boldsymbol{s} \qquad \forall v_t \in X_t. \tag{1.21}$$

Let us choose $v_t = 0$ and $v_t = 2\dot{u}_t$. We obtain $\int_{\Gamma_c} \lambda_t \dot{u}_t \, \mathrm{d}\boldsymbol{s} \leq \int_{\Gamma_c} \mathcal{F}\lambda_n |\dot{u}_t| \, \mathrm{d}\boldsymbol{s}$ and $\int_{\Gamma_c} \lambda_t \dot{u}_t \, \mathrm{d}\boldsymbol{s} \geq \int_{\Gamma_c} \mathcal{F}\lambda_n |\dot{u}_t| \, \mathrm{d}\boldsymbol{s}$, respectively. Thus

$$\int_{\Gamma_c} \lambda_t \dot{u}_t \, \mathrm{d}\boldsymbol{s} = \int_{\Gamma_c} \mathcal{F}\lambda_n |\dot{u}_t| \, \mathrm{d}\boldsymbol{s}.$$

From this and (1.21) we arrive at

$$-\int_{\Gamma_c} \lambda_t v_t \, \mathrm{d}\boldsymbol{s} \leq -\int_{\Gamma_c} \mathcal{F}\lambda_n |v_t| \, \mathrm{d}\boldsymbol{s} \quad \forall v_t \in X_t,$$

or equivalently

$$\int_{\Gamma_c} (\lambda_t v_t - \mathcal{F}\lambda_n |v_t|) \, \mathrm{d}\boldsymbol{s} \geq 0 \quad \forall v_t \in X_t.$$

From this it follows that $|\lambda_t| \leq -\mathcal{F}\lambda_n$ on Γ_c.

Remark 1.1. Both variational inclusions in (1.19) may be replaced by

$$\begin{cases} -\lambda_n \in N_{K_n}(u_n) & \forall t \in \mathbb{T}, \\ -\lambda_t \in \partial_2 j(\lambda_n, u_t) & \forall t \in \mathbb{T}, \end{cases} \tag{1.22}$$

for the non-penetration condition (1.6) and friction conditions (1.7), respectively, or by physically more realistic laws

$$\begin{cases} -\lambda_n \in N_{K_n}(u_n) & \forall t \in \mathbb{T}, \\ -\lambda_t \in \partial_2 j(\lambda_n, \dot{u}_t) & \forall t \in \mathbb{T}. \end{cases} \tag{1.23}$$

Remark 1.2. Let us define the sets of the Lagrange multipliers

$$\Lambda_n = \left\{ \mu \in X_n' \mid \langle \mu, v_n \rangle \geq 0 \quad \forall v_n \in K_n \right\},$$

and

$$\Lambda_t(c) = \left\{ \mu \in X_t' \,|\, \langle \mu, v_t \rangle - \langle c, |v_t| \rangle \leq 0 \quad \forall v_t \in X_t \right\}.$$

Using Theorem 0.1, it is possible to show, that

$$-\lambda_n \in N_{K_n}(\dot{u}_n) \quad \Leftrightarrow \quad -\dot{u}_n \in N_{\Lambda_n}(\lambda_n), \tag{1.24}$$

and

$$-\lambda_t \in \partial_2 j(\lambda_n, \dot{u}_t) \quad \Leftrightarrow \quad -\dot{u}_t \in N_{\Lambda_t(-\mathcal{F}\lambda_n)}(\lambda_t). \tag{1.25}$$

This formulation will be useful for numerical realization based on the duality approach.

2 Numerical realization of time dependent contact problems with friction

For numerical realization of dynamic contact problems, the weak formulations presented in the previous section have to be discretized. There are basically two possible ways how to discretize dynamic problems depending on the order of the spatial and time discretization. In methods of Rothe's type the time discretization precedes the discretization in space. The time derivative of the displacement is replaced by its finite difference and the initial boundary value problem is converted to a sequence of static problems. The advantage of this approach is the possibility to choose different accuracy for the solution of resulting problem at each time level. However in this work we will use the semi-discretization of Galerkin's type – first in space then in time.

It should be mentioned beforehand that there are many difficulties arising in modelling of dynamic contacts between bodies. First of all, there is no general proof of the existence and uniqueness of a solution, thus it is not possible to state conditions for numerical convergence. Secondly, although there are well established methods for numerical simulation of dynamic problems in linear elasticity, they usually fail in case of contact problems. One of the reasons of this failure is that classical schemes (e.g. the Newmark scheme) are designed to conserve the total energy of a body, whereas in reality a contact with an obstacle leads to the dissipation of the kinetic energy of contact nodes. This causes artificial oscillations of the energy on the contact boundary (see [4, 14]).

Recently, several approaches have been developed to overcome this problem. In the case of Rothe's type discretization a contact–stabilized modification of the Newmark method is described in [4, 17]. For a discretization first in space, then in time the method of mass redistribution has been presented in [13, 14].

In the first part of this section the finite element discretization in space is discussed. For simplicity we will consider a plane domain Ω and S to be already in contact, i.e. $g \equiv 0$. For the simulation of the contact interactions, we will use the constitutive law (1.23). The displacements will be approximated by P_1 polynomials on triangles. The next part deals with classical time discretization schemes which reduce the problem to the sequence of static contact problems with friction. Therefore the third part describes the realization of static frictional problems as searching for a fixed point of some operator.

2.1 Finite element discretization

In this paragraph we will describe a spatial discretization by semi-discrete Galerkin method. By 'semi-discrete' we mean that the time dimension remains continuous at this moment. The domain Ω is replaced by its conformal triangulation Ω^h (see Figure 2.1a). Similarly, the parts $\Gamma_u, \Gamma_\sigma, \Gamma_c$ are replaced by $\Gamma_u^h, \Gamma_\sigma^h$, and Γ_c^h, respectively. The set of all triangular elements is denoted $\mathcal{T}^h := \{T_i\}_{i=1}^{n_e}$; the set of all nodes is $\mathcal{P}^h := \{\boldsymbol{x}_i\}_{i=1}^{n}$. The superscript h has a meaning of the 'diameter' of the largest triangular element, n is the number of the nodes and n_e is the number of the elements. The nodes of every triangle are numbered

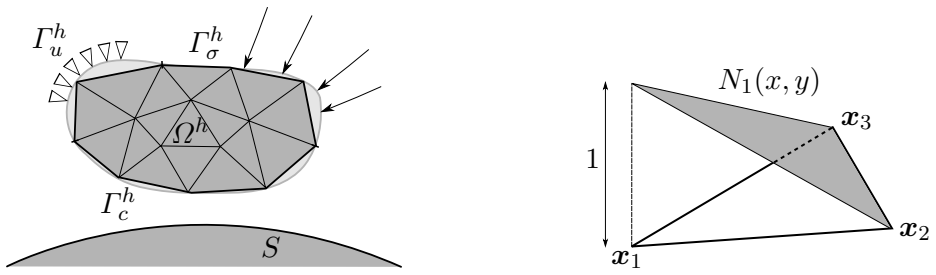

(a) Discretization of the domain Ω

(b) Shape function over the triangular element

Figure 2.1: Finite element discretization

$1, 2, 3$ counterclockwise and the global nodes indexes are assigned by the connectivity table (see Table 1).

The solution set $\mathcal{U}(t)$ is approximated by $\mathcal{U}^h(t)$, a finite dimensional subset of $(H^1(\Omega))^2$. The finite dimensional counterpart of the space $\mathcal{V}$ of virtual displacements is denoted by $\mathcal{V}^h$. The set $\mathcal{U}^h(t)$ consists of vector functions $\tilde{\boldsymbol{u}}(\boldsymbol{x}, t) = (\tilde{u}(\boldsymbol{x}, t), \tilde{v}(\boldsymbol{x}, t))$ whose components $\tilde{u}, \tilde{v} \colon \mathbb{R}^2 \times \mathbb{T} \to \mathbb{R}$ are piecewise linear functions over $\mathcal{T}^h$ representing displacements in the direction of the x and y axis, respectively.

Let $\{\varphi_1(\boldsymbol{x}), \varphi_2(\boldsymbol{x}), \ldots, \varphi_n(\boldsymbol{x})\}$ be the set of Courant basis functions over Ω^h, i.e. φ_i are piecewise linear over Ω^h and $\varphi_i(\boldsymbol{x_j}) = \delta_{ij}$, where δ_{ij} is Kronecker's delta[2]. The main idea of the Galerkin method is to express $\tilde{\boldsymbol{u}}(\boldsymbol{x}, t)$ as a linear combination of the basis function, i.e.

$$\tilde{u}(\boldsymbol{x}, t) = \sum_{i=1}^{n} U_i(t)\varphi_i(\boldsymbol{x}), \qquad \tilde{v}(\boldsymbol{x}, t) = \sum_{i=1}^{n} V_i(t)\varphi_i(\boldsymbol{x})$$

and to choose the basis functions as the test functions. After substitution to the weak formulation of the problem we will derive its matrix form for the coefficients

$$\boldsymbol{U}(t) = (U_1(t), V_1(t), \ldots, U_n(t), V_n(t))^\top$$

of linear combination as unknowns[3]. Due to the choice of the basis functions which have a small support, the resulting matrices are sparse. Because of an easy implementation, the assembling of matrices and vectors is usually performed over individual elements. In the next paragraphs we will adopt this approach.

Let us focus on a single triangular element $T \in \mathcal{T}^h$ with the vertices $\boldsymbol{x_1} = (x_1, y_1), \boldsymbol{x_2} = (x_2, y_2)$ and $\boldsymbol{x_3} = (x_3, y_3)$. Over this element we define three basis (linear) functions N_1, N_2, N_3 such that $N_i(\boldsymbol{x}_j) = \delta_{ij}$ (see Figure 2.1b). It can be easily shown that if $\boldsymbol{x}_a \notin \Gamma_u^h$ the basis functions have following form (see [24]):

$$N_a(x, y) := \frac{a_a + b_a x + c_a y}{2\Delta}, \qquad a = 1, 2, 3,$$

[2] $\delta_{ij} = 1$ if $i = j$, $\delta_{ij} = 0$ otherwise

[3] Actually the coefficients in the nodes on the Dirichlet boundary are known. Their enforcement will be discussed later.

with

$$\begin{array}{lllllllll} a_1 &=& x_2y_3 - x_3y_2, & a_2 &=& x_3y_1 - x_1y_3, & a_3 &=& x_1y_2 - x_2y_1, \\ b_1 &=& y_2 - y_3, & b_2 &=& y_3 - y_1, & b_3 &=& y_1 - y_2, \\ c_1 &=& x_3 - x_2, & c_2 &=& x_1 - x_3, & c_3 &=& x_2 - x_1, \end{array}$$

and

$$2\Delta = \det \begin{bmatrix} 1 & x_1 & y_1 \\ 1 & x_2 & y_2 \\ 1 & x_3 & y_3 \end{bmatrix} \tag{2.1}$$

where Δ is the area of the given triangle. Since we consider 2-D problems, each node has two degrees of freedom (the displacement in the direction of x-axis and y-axis) and we need six shape functions over each element. We arrange them in the matrices

$$\mathsf{N}_1(x,y) := N_1(x,y)\mathsf{I}_2, \qquad \mathsf{N}_2(x,y) := N_2(x,y)\mathsf{I}_2, \qquad \mathsf{N}_3(x,y) := N_3(x,y)\mathsf{I}_2,$$

$$\mathsf{N}(\boldsymbol{x}) := \begin{bmatrix} \mathsf{N}_1(\boldsymbol{x}) & \mathsf{N}_2(\boldsymbol{x}) & \mathsf{N}_3(\boldsymbol{x}) \end{bmatrix},$$

where I_2 is the identity matrix of order two. For simplicity, we will omit the spatial variable and write N instead of $\mathsf{N}(\boldsymbol{x})$. We can now approximate the displacement $\boldsymbol{u}$ over T by the linear combination of the element basis functions

$$\boldsymbol{u}(\boldsymbol{x},t) \approx \sum_{i=1}^{3} \mathsf{N}_i(\boldsymbol{x})\hat{\boldsymbol{u}}_i(t) = \mathsf{N}\hat{\boldsymbol{u}}(t). \tag{2.2}$$

Here the coefficients of the linear combination have the form $\hat{\boldsymbol{u}}_i(t) := (\hat{u}_i(t), \hat{v}_i(t))^\top$ and $\hat{\boldsymbol{u}}(t) := (\hat{u}_1(t), \hat{v}_1(t), \hat{u}_2(t), \hat{v}_2(t), \hat{u}_3(t), \hat{v}_3(t))^\top$. They represent the displacement of the vertices of T in the directions of the coordinate axis. Note that they depend on time.

	Nodes			
Element	1	2	3	Local nodes indexes
1	1	2	4	Global nodes indexes
2	2	3	4	
⋮				
20	17	19	15	

Table 1: Element connectivity table

2.1.1 Assembling the mass and the stiffness matrices

First, we will derive the classical mass and stiffness matrices, i.e. we will discretize the terms $\langle \varrho\ddot{\boldsymbol{u}}, \boldsymbol{v}\rangle$ and $A(\boldsymbol{u},\boldsymbol{v})$ in (1.19). Recall that

$$\langle \rho\ddot{\boldsymbol{u}}, \boldsymbol{v}\rangle := \int_\Omega \varrho\ddot{u}_i v_i \,\mathrm{d}\boldsymbol{x}, \quad A(\boldsymbol{u},\boldsymbol{v}) := \int_\Omega c_{ijkl}\varepsilon_{ij}(\boldsymbol{u})\varepsilon_{kl}(\boldsymbol{v}) \,\mathrm{d}\boldsymbol{x}.$$

Because the integral over the domain Ω^h may be split into the sum of integrals over all triangles from $\mathcal{T}^h$, i.e.

$$\int_\Omega \varrho \ddot{u}_i v_i \,\mathrm{d}\boldsymbol{x} = \sum_{i=1}^{n_e} \int_{T_i} \varrho \ddot{u}_i v_i \,\mathrm{d}\boldsymbol{x}, \quad A(\boldsymbol{u},\boldsymbol{v}) = \sum_{i=1}^{n_e} \int_{T_i} c_{ijkl}\varepsilon_{ij}(\boldsymbol{u})\varepsilon_{kl}(\boldsymbol{v}) \,\mathrm{d}\boldsymbol{x},$$

we will derive the element mass and stiffness matrices and map their elements to appropriate positions in the global mass and stiffness matrices.

The term $\ddot{\boldsymbol{u}}$ will be approximated on each $T_i \in \mathcal{T}^h$ in the same manner as in (2.2):

$$\ddot{\boldsymbol{u}}(\boldsymbol{x},t) \approx \mathsf{N}\ddot{\hat{\boldsymbol{u}}}(t)$$

Using this approximation and using the shape functions as test functions, the inertia term becomes

$$\int_{T_i} \varrho \mathsf{N}^\top \mathsf{N} \ddot{\hat{\boldsymbol{u}}}(t) \,\mathrm{d}\boldsymbol{x} = \underbrace{\int_{T_i} \varrho \mathsf{N}^\top \mathsf{N} \,\mathrm{d}\boldsymbol{x}}_{=:\mathsf{M}^e} \ddot{\hat{\boldsymbol{u}}}(t) = \mathsf{M}^e \ddot{\hat{\boldsymbol{u}}}(t),$$

where M^e denotes the element mass matrix. Since $\int_{T_i} N_a N_b \,\mathrm{d}\boldsymbol{x} = \frac{1}{6}\Delta$ if $a = b$ and $\int_{T_i} N_a N_b \,\mathrm{d}\boldsymbol{x} = \frac{1}{12}\Delta$ if $a \neq b$, the element mass matrix has the form

$$\mathsf{M}^e = \frac{\varrho\Delta}{12} \begin{bmatrix} 2 & 0 & 1 & 0 & 1 & 0 \\ 0 & 2 & 0 & 1 & 0 & 1 \\ 1 & 0 & 2 & 0 & 1 & 0 \\ 0 & 1 & 0 & 2 & 0 & 1 \\ 1 & 0 & 1 & 0 & 2 & 0 \\ 0 & 1 & 0 & 1 & 0 & 2 \end{bmatrix}.$$

Recall that Δ is the area of the triangle T_i which is easily computable from (2.1).

Introducing the operator

$$\boldsymbol{\epsilon} := \begin{bmatrix} \frac{\partial}{\partial x} & 0 \\ 0 & \frac{\partial}{\partial y} \\ \frac{\partial}{\partial y} & \frac{\partial}{\partial x} \end{bmatrix}$$

and the linearized elasticity matrix for a homogenous isotropic body

$$\mathsf{D} := \frac{E}{(1+\nu)(1-2\nu)} \begin{bmatrix} 1-\nu & \nu & 0 \\ \nu & 1-\nu & 0 \\ 0 & 0 & \frac{1-2\nu}{2} \end{bmatrix}$$

with Young's modulus E and Poisson's ratio ν (for details see [24]) we may write the term $A(u,v)$ in the matrix form as

$$\int_{T_i} (\boldsymbol{\epsilon}\mathsf{N})^\top \mathsf{D}\boldsymbol{\epsilon}(\mathsf{N}\hat{\boldsymbol{u}}(t)) \,\mathrm{d}\boldsymbol{x} = \int_{T_i} \mathsf{B}^\top \mathsf{D}\mathsf{B} \,\mathrm{d}\boldsymbol{x}\, \hat{\boldsymbol{u}}(t) = \mathsf{B}^\top \mathsf{D}\mathsf{B} \int_{T_i} \mathrm{d}\boldsymbol{x}\, \hat{\boldsymbol{u}}(t) = \underbrace{\mathsf{B}^\top \mathsf{D}\mathsf{B}\Delta}_{=:\mathsf{K}^e} \hat{\boldsymbol{u}}(t).$$

Here we denoted

$$\mathsf{B} := \boldsymbol{\epsilon}\mathsf{N} = \begin{bmatrix} \frac{\partial N_1}{\partial x} & 0 & \frac{\partial N_2}{\partial x} & 0 & \frac{\partial N_3}{\partial x} & 0 \\ 0 & \frac{\partial N_1}{\partial y} & 0 & \frac{\partial N_2}{\partial y} & 0 & \frac{\partial N_3}{\partial y} \\ \frac{\partial N_1}{\partial y} & \frac{\partial N_1}{\partial x} & \frac{\partial N_2}{\partial y} & \frac{\partial N_2}{\partial x} & \frac{\partial N_3}{\partial y} & \frac{\partial N_3}{\partial x} \end{bmatrix}$$
$$= \begin{bmatrix} y_2 - y_3 & 0 & y_3 - y_1 & 0 & y_1 - y_2 & 0 \\ 0 & x_3 - x_2 & 0 & x_1 - x_3 & 0 & x_2 - x_1 \\ x_3 - x_2 & y_2 - y_3 & x_1 - x_3 & y_3 - y_1 & x_2 - x_1 & y_1 - y_2 \end{bmatrix} \frac{1}{2\Delta}$$

and used the fact that due to linearity of the shape functions, their derivatives are constants on elements. Finally K^e stands for the element stiffness matrix.

The global mass and stiffness matrices M, K, respectively, are then assembled by summing the elements of local matrices to appropriate positions (defined by the connectivity table) in global matrices.

Remark 2.1. From the finite element analysis it is well-known, that the matrices K and M are symmetric and positive definite [24].

2.1.2 Discretization of the load forces

In this section we will discretize volume forces and surface integrals represented by the term

$$L(\boldsymbol{v}) := \int_\Omega f_i v_i \,\mathrm{d}\boldsymbol{x} + \int_{\Gamma_\sigma} P_i v_i \,\mathrm{d}\boldsymbol{s}.$$

We may again decompose the previous integrals into the sum over all elements and substitute the shape functions as test functions. The volume force $\boldsymbol{f}$ is replaced over every element T_i by its value in the center of gravity $\boldsymbol{x}_T$ of T_i, $\hat{\boldsymbol{f}} = (\hat{f}_1, \hat{f}_2)^\top := \boldsymbol{f}(\boldsymbol{x}_T)$. This leads to the expression

$$\boldsymbol{L}^e := \int_{T_i} \mathsf{N}^\top \hat{\boldsymbol{f}} \,\mathrm{d}\boldsymbol{x} = \frac{\Delta}{3} \begin{bmatrix} \hat{\boldsymbol{f}} \\ \hat{\boldsymbol{f}} \\ \hat{\boldsymbol{f}} \end{bmatrix}.$$

Using the element connectivity table we assemble the global load vector $\boldsymbol{L}(t)$.

Similarly, the contribution of the prescribed tractions on Γ_σ is expressed by the vector

$$\boldsymbol{p}^e := \frac{1}{2} \begin{bmatrix} \hat{\boldsymbol{P}} \\ \hat{\boldsymbol{P}} \end{bmatrix} \ell,$$

where $\hat{\boldsymbol{P}} = (\hat{P}_1, \hat{P}_1)^\top := \boldsymbol{P}(\boldsymbol{x}_s, t)$ is the value of the traction in the middle of the corresponding edge and ℓ is the length of this edge. The components of this vector are summed to the appropriate components of the global load vector.

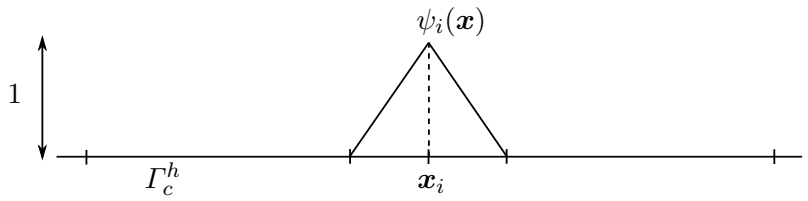

Figure 2.2: Basis functions over one contact boundary element

2.1.3 Discretization of the contact forces

To discretize the terms $\langle \lambda_n, v_n \rangle$ and $\langle \lambda_t, v_t \rangle$ we present the finite element counterparts of the spaces X_n, X_t and X_n', X_t' defined on the contact part Γ_c, which will be denoted by adding the superscript h. There are two possible ways how to define these spaces. We may either use different finite elements for the discretization of X_n, X_t and X_n', X_t' or use the same finite elements for both displacements and forces on the contact boundary. Since there are no greater differences between these methods [13], we will use the latter one (thus $X_n^h = {X'}_n^h$ and $X_t^h = {X'}_t^h$).

Let $\mathcal{I}_c := \left\{ i \,|\, \boldsymbol{x}_i \in \overline{\Gamma_c^h} \setminus \overline{\Gamma_u^h} \right\}$ be the set of indexes of the contact nodes. For the approximation of the normal and tangential contact displacements and forces we use continuous piecewise linear scalar functions. The basis functions of these spaces, denoted by $\{\psi_i\}_{i \in \mathcal{I}_c}$ for the approximation of the normal displacements and stresses and $\{\xi_i\}_{i \in \mathcal{I}_c}$ for the tangential quantities, are such that $\psi_i(\boldsymbol{x}_j) = \xi_i(\boldsymbol{x}_j) = \delta_{ij}$.[4]

Unlike to the previous paragraphs we will not discretize the terms $\langle \lambda_n, v_n \rangle$ and $\langle \lambda_t, v_t \rangle$ element by element. Instead, let us have a look what happens if we substitute the basis functions of the form $(\varphi_i, 0)^\top$ and $(0, \varphi_i)^\top$, where $i \in \mathcal{I}_c$, as the test functions (recall from the introductory paragraph to this subsection that $\varphi_1, \ldots, \varphi_n$ are the Courant basis functions defined over Ω^h). The term $\langle \lambda_n, v_n \rangle$ becomes

$$\int_{\Gamma_c^h} \tilde{\lambda}_n(\boldsymbol{x}, t)(\varphi_i(\boldsymbol{x}), 0) \cdot \boldsymbol{n_i} \,\mathrm{d}\boldsymbol{s} = \int_{\Gamma_c^h} \tilde{\lambda}_n(\boldsymbol{x}, t)\varphi_i(\boldsymbol{x}) n_{i_1} \,\mathrm{d}\boldsymbol{s} = n_{i_1} \int_{\Gamma_c^h} \tilde{\lambda}_n(\boldsymbol{x}, t)\psi_i(\boldsymbol{x}) \,\mathrm{d}\boldsymbol{s}, \quad (2.3)$$

and

$$\int_{\Gamma_c^h} \tilde{\lambda}_n(\boldsymbol{x}, t)(0, \varphi_i(\boldsymbol{x})) \cdot \boldsymbol{n_i} \,\mathrm{d}\boldsymbol{s} = \int_{\Gamma_c^h} \tilde{\lambda}_n(\boldsymbol{x}, t)\varphi_i(\boldsymbol{x}) n_{i_2} \,\mathrm{d}\boldsymbol{s} = n_{i_2} \int_{\Gamma_c^h} \tilde{\lambda}_n(\boldsymbol{x}, t)\psi_i(\boldsymbol{x}) \,\mathrm{d}\boldsymbol{s}, \quad (2.4)$$

where $\tilde{\lambda}_n$ is the approximation of the normal contact stress. Since φ_i is non-zero only on the elements sharing the node $\boldsymbol{x}_i$, we approximate the unit outward normal vector $\boldsymbol{n}$ by its value in this node and denote it as $\boldsymbol{n}_i := (n_{i_1}, n_{i_2})^\top$. In order to present the matrix formulation of (2.3) and (2.4), let $\boldsymbol{N}_i$ be the vector with the following property:

$$\tilde{u}_n(\boldsymbol{x}_i, t) := \tilde{\boldsymbol{u}}(\boldsymbol{x}_i, t) \cdot \boldsymbol{n}_i = \boldsymbol{U}(t)^\top \cdot \boldsymbol{N}_i \quad \forall i \in \mathcal{I}_c \, \forall t \in \mathbb{T}.$$

[4] One may see that ψ_i and ξ_i are in fact restrictions of φ_i on Γ_c^h.

In other words, $\boldsymbol{N}_i$ contains on appropriate positions the coordinates of the unit outward normal vector $\boldsymbol{n}_i$ at $\boldsymbol{x}_i, i \in \mathcal{I}_c$ and zeros elsewhere. Further, let B_n denote a $(\operatorname{card}\mathcal{I}_c \times 2n)$ matrix with the rows composed from the vectors $\boldsymbol{N}_i^\top$, and let $\Lambda_{n_i}(t) := \int_{\Gamma_c^h} \tilde{\lambda}_n(\boldsymbol{x},t)\psi_i(\boldsymbol{x})\,\mathrm{d}\boldsymbol{s}$. The integrals (2.3) and (2.4) may be expressed in the matrix form as $\mathsf{B}_n^\top \boldsymbol{\lambda}_n(t)$ where $\boldsymbol{\lambda}_n(t)$ is the vector constructed from $\Lambda_{n_i}(t)$.[5]

We will now rephrase the contact conditions by means of the new discrete variables. Using $\boldsymbol{N}_i$ we may write the non-penetration condition in the form

$$\boldsymbol{U}(t)^\top \cdot \boldsymbol{N}_i \le 0 \quad \forall i \in \mathcal{I}_c\, \forall t \in \mathbb{T}. \tag{2.5}$$

This corresponds to the following discretization of K_n defined by (1.17):

$$K_n^h := \left\{ \tilde{u}_n \in X_n^h \,|\, \tilde{u}_n(\boldsymbol{x}_i) \le 0 \quad \forall i \in \mathcal{I}_c \right\}.$$

Using the basis functions $\{\psi_i(\boldsymbol{x})\}_{i\in\mathcal{I}_c}$ we may rewrite the discrete form of the condition $\int_{\Gamma_c^h} \tilde{\lambda}_n \tilde{v}_n \,\mathrm{d}\boldsymbol{s} \ge 0, \forall \tilde{v}_n \in K_n^h$ as

$$\int_{\Gamma_c^h} \tilde{\lambda}_n(\boldsymbol{x},t)\psi_i(\boldsymbol{x})\,\mathrm{d}\boldsymbol{s} =: \Lambda_{n_i}(t) \le 0 \quad \forall i \in \mathcal{I}_c\, \forall t \in \mathbb{T}. \tag{2.6}$$

Finally, since the condition $\int_{\Gamma_c^h} \tilde{\lambda}_n \tilde{u}_n \,\mathrm{d}\boldsymbol{s} = 0$ may be written as

$$\int_{\Gamma_c^h} \tilde{\lambda}_n \tilde{u}_n \,\mathrm{d}\boldsymbol{s} = \int_{\Gamma_c^h} \tilde{\lambda}_n \sum_{i\in\mathcal{I}_c} \boldsymbol{U}(t)^\top \cdot \boldsymbol{N}_i \psi_i(\boldsymbol{x})\,\mathrm{d}\boldsymbol{s} = \sum_{i\in\mathcal{I}_c} \boldsymbol{U}(t)^\top \cdot \boldsymbol{N}_i \int_{\Gamma_c^h} \tilde{\lambda}_n \psi_i(\boldsymbol{x})\,\mathrm{d}\boldsymbol{s} = 0,$$

its matrix form is given by

$$\Lambda_{n_i}(t) \left(\boldsymbol{U}(t)^\top \cdot \boldsymbol{N}_i \right) = 0 \quad \forall i \in \mathcal{I}_c\, \forall t \in \mathbb{T}. \tag{2.7}$$

The conditions (2.5), (2.6) and (2.7) can be written in the form $-\boldsymbol{\lambda}_n(t) \in N_{\mathbb{R}_-^{\operatorname{card}\mathcal{I}_c}}(\mathsf{B}_n \boldsymbol{U}(t))$.

Similarly, in the tangential direction we may define $\Lambda_{t_i}(t) := \int_{\Gamma_c^h} \tilde{\lambda}_t(\boldsymbol{x},t)\xi_i(\boldsymbol{x})\,\mathrm{d}\boldsymbol{s}$ and the vectors $\boldsymbol{T}_i$ such that

$$\tilde{u}_t(\boldsymbol{x}_i,t) = \boldsymbol{U}(t)^\top \cdot \boldsymbol{T}_i, \quad \forall i \in \mathcal{I}_c, \forall t \in \mathbb{T}.$$

To present the matrix form of the friction conditions, we substitute the test functions $\tilde{w}_t := \sum_{i\in\mathcal{I}_c} w_t(\boldsymbol{x}_i)\xi_i, w_t \in X_t$ into (1.18) and denote $\dot{U}_{t_i}(t) := \dot{\boldsymbol{U}}(t)^\top \cdot \boldsymbol{T}_i$.

[5] The vector $\boldsymbol{\lambda}_n(t)$ is constructed from elements $\Lambda_{n_i}(t)$ by ordering them in the ascending order depending on the index i.

Assumption In what follows we assume that the coefficient of friction $\mathcal{F}$ is a positive constant over the whole contact boundary.

We obtain:

$$\int_{\Gamma_c^h} \tilde{\lambda}_t \sum_{i\in\mathcal{I}_c} (w_t(\boldsymbol{x}_i) - \dot{U}_{t_i}(t))\xi_i \,\mathrm{d}\boldsymbol{s}$$

$$- \mathcal{F}\int_{\Gamma_c^h} \tilde{\lambda}_n \sum_{i\in\mathcal{I}_c} \big(\,|w_t(\boldsymbol{x}_i)| - \big|\dot{U}_{t_i}(t)\big|\big)\xi_i \,\mathrm{d}\boldsymbol{s} \geq 0 \qquad \forall w_t \in X_t \,\forall t \in \mathbb{T}, \quad (2.8)$$

where we approximated the problematic terms $\big|\sum_{i\in\mathcal{I}_c} \dot{U}_{t_i}(t)\xi_i\big| \approx \sum_{i\in\mathcal{I}_c} \big|\dot{U}_{t_i}(t)\big|\xi_i$ and $\big|\sum_{k\in\mathcal{I}_c} w_t(\boldsymbol{x}_i)\xi_i\big| \approx \sum_{i\in\mathcal{I}_c} |w_t(\boldsymbol{x}_i)|\,\xi_i$. Expression (2.8) is equivalent with

$$\int_{\Gamma_c^h} \tilde{\lambda}_t\big(w_t(\boldsymbol{x}_i) - \dot{U}_{t_i}(t)\big)\xi_i \,\mathrm{d}\boldsymbol{s} - \mathcal{F}\int_{\Gamma_c^h} \tilde{\lambda}_n\big(\,|w_t(\boldsymbol{x}_i)| - \big|\dot{U}_{t_i}(t)\big|\big)\xi_i \,\mathrm{d}\boldsymbol{s} \geq 0 \quad \forall i \in \mathcal{I}_c \,\forall t \in \mathbb{T},$$

or componentwisely:

$$\big(\boldsymbol{\lambda}_t(t)\big)_i\big(w_i - \big(\mathsf{B}_t\dot{\boldsymbol{U}}(t)\big)_i\big) - \mathcal{F}\big(\boldsymbol{\lambda}_n(t)\big)_i\big(\big|w_i\big| - \big|\big(\mathsf{B}_t\dot{\boldsymbol{U}}(t)\big)_i\big|\big) \geq 0$$

$$\forall \boldsymbol{w} \in \mathbb{R}^m \,\forall i \leq m \,\forall t \in \mathbb{T}. \quad (2.9)$$

Here B_t is the matrix composed from the vectors $\boldsymbol{T}_i$, $\boldsymbol{\lambda}_t(t)$ is the vector with the components given by $\Lambda_{t_i}(t)$ and $m = \operatorname{card}\mathcal{I}_c$. Defining the finite-dimensional approximation of the subdifferential of $j(\lambda_n, \dot{u}_t)$ by

$$\partial_2 j(\boldsymbol{\lambda}_n(t), \mathsf{B}_t\dot{\boldsymbol{U}}(t))$$

$$:= \Big\{\boldsymbol{\mu} \in \mathbb{R}^m \,|\, \mu_i\big(w_i - \big(\mathsf{B}_t\dot{\boldsymbol{U}}(t)\big)_i\big) \leq -\mathcal{F}\,(\boldsymbol{\lambda}_n(t))_i\,\big(|w_i| - \big|\big(\mathsf{B}_t\dot{\boldsymbol{U}}(t)\big)_i\big|\big)\,\forall \boldsymbol{w} \in \mathbb{R}^m \,\forall i \leq m\Big\},$$

we may write (2.9) equivalently in the form $-\boldsymbol{\lambda}_t(t) \in \partial_2 j\big(\boldsymbol{\lambda}_n(t), \mathsf{B}_t\dot{\boldsymbol{U}}(t)\big)$. For simplicity, we use the same notation for both continuous and discrete form of the subdifferential. Finally, (2.9) is equivalent to

$$\begin{cases} \dot{U}_{t_i}(t) = 0 & \Rightarrow \quad |\Lambda_{t_i}(t)| \leq -\mathcal{F}\Lambda_{n_i}(t) & \forall i \in \mathcal{I}_c, \forall t \in \mathbb{T}, \\ \dot{U}_{t_i}(t) \neq 0 & \Rightarrow \quad \Lambda_{t_i}(t) = \mathcal{F}\Lambda_{n_i}(t)\operatorname{sgn}\dot{U}_{t_i}(t) & \forall i \in \mathcal{I}_c, \forall t \in \mathbb{T}. \end{cases}$$

Remember that we used the constitutive law (1.23). The derivation of the discrete form of (1.22) or the law used in (1.19) is similar.

2.1.4 Summary: matrix formulation of the problem

At this point we are able to sum up results of the previous sections and to present the semi-discrete matrix formulation of the contact problem. It remains to define the discrete initial displacement and velocity vector as

$$\boldsymbol{U}_0 = (\boldsymbol{u}_0(\boldsymbol{x}_1)^\top, \boldsymbol{u}_0(\boldsymbol{x}_2)^\top, \ldots, \boldsymbol{u}_0(\boldsymbol{x}_n)^\top)^\top,$$

and

$$\dot{\boldsymbol{U}}_0 = (\boldsymbol{v}_0(\boldsymbol{x}_1)^\top, \boldsymbol{v}_0(\boldsymbol{x}_2)^\top, \ldots, \boldsymbol{v}_0(\boldsymbol{x}_n)^\top)^\top.$$

Until now we ignored the Dirichlet boundary conditions and the fact that the test functions in the space of virtual displacements $\mathcal{V}$ are identically equal to zero on Γ_u^h. To include these conditions into the formulation, let $\mathcal{I}_u := \left\{ i \,|\, \boldsymbol{x}_i \in \overline{\Gamma_u^h} \right\}$ be the set of indices of the nodes of $\mathcal{T}_h$ lying on the Dirichlet boundary. We set the elements of the $2i$-th and $(2i-1)$-th, $i \in \mathcal{I}_u$, rows and columns of the matrices M and K to zero. Next we set the diagonal elements of these rows of the matrix K to one and the respective components of the right-hand side vector to the value of the boundary condition at $\boldsymbol{x}_i$ given by $\hat{\boldsymbol{U}}(\boldsymbol{x}_i)$. For simplicity, we will denote these modified matrices and vector by the same symbols as the original ones, i.e. M, K and $\boldsymbol{L}(t)$, respectively.

In conclusion, the matrix formulation of the problem reads as follows:

$$\begin{cases} \text{Find } \boldsymbol{U}(t)\colon \mathbb{T} \mapsto \mathbb{R}^{2n}, \boldsymbol{\lambda}_n(t)\colon \mathbb{T} \mapsto \mathbb{R}^m, \boldsymbol{\lambda}_t(t)\colon \mathbb{T} \mapsto \mathbb{R}^m \text{ such that } \forall t \in \mathbb{T} \\ \mathsf{M}\ddot{\boldsymbol{U}}(t) + \mathsf{K}\boldsymbol{U}(t) = \boldsymbol{L}(t) + \mathsf{B}_n^\top \boldsymbol{\lambda}_n(t) + \mathsf{B}_t^\top \boldsymbol{\lambda}_t(t), \\ -\boldsymbol{\lambda}_n(t) \in N_{\mathbb{R}^m_-}(\mathsf{B}_n \boldsymbol{U}(t)), \\ -\boldsymbol{\lambda}_t(t) \in \partial_2 j\big(\boldsymbol{\lambda}_n(t), \mathsf{B}_t \dot{\boldsymbol{U}}(t)\big), \\ \boldsymbol{U}(0) = \boldsymbol{U}_0, \dot{\boldsymbol{U}}(0) = \dot{\boldsymbol{U}}_0. \end{cases} \tag{2.10}$$

2.2 Time-stepping algorithms

In Section 2.1 we have presented the spatially discretized form of the problem with the time dimension kept continuous. In the next paragraphs we shall use some of the time-stepping procedures to complete a total discretization. For this purpose let us divide the time interval $\mathbb{T}$ into non-overlapping subintervals of equal length such that

$$\mathbb{T} = \bigcup_{k=0}^{L-1} [t_k, t_{k+1}],$$

where $t_k < t_{k+1}$ and $t_0 = 0, t_L = T$. Let $\Delta t := t_{k+1} - t_k$. For the simplicity of notation we will write $\boldsymbol{u}^k := \boldsymbol{U}(t_k), \boldsymbol{v}^k := \dot{\boldsymbol{U}}(t_k), \boldsymbol{a}^k := \ddot{\boldsymbol{U}}(t_k)$. We will find the solution satisfying (2.10) only in a finite number of time-steps defined by t_k. Thus the totally discretized problem reads as follows:

$$\begin{cases} \forall k \in \{0, 1, \ldots, L-1\} \text{ find } \boldsymbol{u}^{k+1} \in \mathbb{R}^{2n}, \boldsymbol{\lambda}_n^{k+1} \in \mathbb{R}^m, \boldsymbol{\lambda}_t^{k+1} \in \mathbb{R}^m \text{ such that} \\ \mathsf{M}\boldsymbol{a}^{k+1} + \mathsf{K}\boldsymbol{u}^{k+1} = \boldsymbol{L}^{k+1} + \mathsf{B}_n^\top \boldsymbol{\lambda}_n^{k+1} + \mathsf{B}_t^\top \boldsymbol{\lambda}_t^{k+1}, \\ -\boldsymbol{\lambda}_n^{k+1} \in N_{\mathbb{R}^m_-}(\mathsf{B}_n \boldsymbol{u}^{k+1}), \\ -\boldsymbol{\lambda}_t^{k+1} \in \partial_2 j(\boldsymbol{\lambda}_n^{k+1}, \mathsf{B}_t \boldsymbol{v}^{k+1}), \\ \boldsymbol{u}^0 = \boldsymbol{U}_0, \boldsymbol{v}^0 = \dot{\boldsymbol{U}}_0, \end{cases} \tag{2.11}$$

For the solution of this problem we will use direct integration algorithms, which may be derived from Taylor's expansion of the displacement $\boldsymbol{U}$ and the velocity $\dot{\boldsymbol{U}}$ at t_k with respect to time. We distinguish explicit and implicit schemes.

- *Explicit methods* enable us to compute $\boldsymbol{u}^{k+1}, \boldsymbol{v}^{k+1}$ and $\boldsymbol{a}^{k+1}$ directly from the values at the previous time-step without any need to solve a coupled system of equations. The typical examples of this kind of integrators are the mid-point method or, for the specific choice of the real parameters, the Newmark integration scheme. However, explicit schemes are only conditionally stable (see Definition 2.2), i.e. the stability is guaranteed only for Δt lower than some value. It has been shown for linear systems, that a limit value for stability may be estimated by h/c, where h is a 'diameter' of the largest element and c is the speed of sound in a given material[6]. For this reason, explicit methods are appropriate for the simulation of processes with high frequency and short duration (e.g. impacts) [19].
- *Implicit methods* provide a system of implicit statements for $\boldsymbol{u}^{k+1}, \boldsymbol{v}^{k+1}$ and $\boldsymbol{a}^{k+1}$. For their evaluation, one has to solve a non-linear system of equations in each time-step. Widely used Wilson-Theta method or the Newmark method belong to this class. We will present some of them in the following sections.

For the study of the accuracy of the methods we define the *local discretization error* d_k as the error caused by used approximations in one time-step. The *global discretization error* is caused by the accumulation of the local discretization errors and is defined by $e_k := y(t_k) - y_k$, where y_k is the approximation of $y(t_k)$. We say that the method is of order $p \in \mathbb{N}$ if $d_k = \mathcal{O}(\Delta t^{p+1})$. For one-step methods of order p it holds that $e_k = \mathcal{O}(\Delta t^p)$.

2.2.1 The energy of a dynamic system and the stability of a method

As mentioned in the beginning of this section, the energy behavior of the temporal integration schemes is crucial property deciding their applicability. The *total energy* of an elastic body at time t may be evaluated using the following definition.

Definition 2.1 (Energy functional)**.** The energy functional of an elastic body is given by

$$J(\boldsymbol{U}, \dot{\boldsymbol{U}}, t) := \frac{1}{2}\dot{\boldsymbol{U}}(t)^\top \mathsf{M}\dot{\boldsymbol{U}}(t) + \frac{1}{2}\boldsymbol{U}(t)^\top \mathsf{K}\boldsymbol{U}(t) - \boldsymbol{L}(t)^\top \boldsymbol{U}(t).$$

For the discretized time we write

$$J(\boldsymbol{u}^k, \boldsymbol{v}^k) := \frac{1}{2}{\boldsymbol{v}^k}^\top \mathsf{M}\boldsymbol{v}^k + \frac{1}{2}{\boldsymbol{u}^k}^\top \mathsf{K}\boldsymbol{u}^k - {\boldsymbol{L}^k}^\top \boldsymbol{u}^k.$$

The first term represents the kinetic energy, the second term is the strain energy and the last one stands for the energy caused by applied loads.

By the *stability* of a method we mean the boundedness of the energy functional, i.e. we want the energy of a body to remain bounded as the number of time-steps goes to infinity.

[6] We say that Δt must satisfy the so called *Courant-Friedrichs-Lewy (CFL) condition.* Let us also recall that the speed of longitudinal and transverse wave propagation in a given material may be calculated by $c_L = \sqrt{\frac{E(1-\nu)}{\varrho(1+\nu)(1-2\nu)}}$ and $c_T = \sqrt{\frac{E}{2\rho(1+\nu)}}$, respectively.

Definition 2.2 (Stability)**.** A temporal integration scheme is *unconditionally stable* if there exists a constant $c \in \mathbb{R}^+$ such that for all $k \in \mathbb{N}_0$ and for all $\Delta t > 0$ it holds

$$J(\boldsymbol{u}^k, \boldsymbol{v}^k) \leq c.$$

If the previous inequality holds only when $\Delta t \leq \tau$ for some $\tau \in \mathbb{R}^+$, we say that a scheme is *conditionally stable*.

The presence of a priori unknown contact forces disallows the stability analysis by eigenvalues [19], therefore the stability is studied using the variation of the energy functional in two consecutive time-steps. This approach is extensively used in [13] from which we borrow some notation. The *energy variation* is defined by

$$\Delta J := J(\boldsymbol{u}^{k+1}, \boldsymbol{v}^{k+1}) - J(\boldsymbol{u}^k, \boldsymbol{v}^k).$$

In particular for frictionless contact problems, the energy conservation law should hold. If the time integration method satisfies the condition $\Delta J = 0 \, \forall k \in \mathbb{N}_0$ we say that the method is *conservative*. The method satisfying condition $\Delta J \leq 0$ is called *dissipative*.

2.2.2 Newmark integration scheme

One of the most frequently used time integration methods was proposed in 1959 by American structural engineer Nathan M. Newmark. It belongs to one-step methods (meaning that for the evaluation of unknowns at time t_{k+1} we need only values in the previous time t_k) for solving differential equations of the second order. For dynamic problems without unilateral and friction constraints this scheme is given by the following definition.

Definition 2.3 (Newmark integration scheme)**.** Given $\boldsymbol{u}^k, \boldsymbol{v}^k, \boldsymbol{a}^k$ and $\beta, \gamma \in \mathbb{R}$ evaluate $\boldsymbol{u}^{k+1}, \boldsymbol{v}^{k+1}, \boldsymbol{a}^{k+1}$ by

$$\boldsymbol{u}^{k+1} = \boldsymbol{u}^k + \Delta t \boldsymbol{v}^k + \Delta t^2 \left(\left(\frac{1}{2} - \beta \right) \boldsymbol{a}^k + \beta \boldsymbol{a}^{k+1} \right), \tag{2.12}$$

$$\boldsymbol{v}^{k+1} = \boldsymbol{v}^k + \Delta t \left((1 - \gamma) \, \boldsymbol{a}^k + \gamma \boldsymbol{a}^{k+1} \right), \tag{2.13}$$

together with the energy equilibrium equation $\mathsf{M}\boldsymbol{a}^{k+1} + \mathsf{K}\boldsymbol{u}^{k+1} = \boldsymbol{L}^{k+1}$.

For the detailed derivation of this scheme see [5, 21, 23]. The choice of the constants β and γ affects the stability and the order of convergence of the method. The scheme is of order two for $\gamma = \frac{1}{2}$ and of order one otherwise. In the case without contact the scheme is unconditionally stable for $\beta \geq \frac{\left(\frac{1}{2}+\gamma\right)^2}{4}$ while the choice $2\beta = \gamma = \frac{1}{2}$ provides the energy conserving algorithm. For $\beta = \gamma = 0$ the displacement $\boldsymbol{u}^{k+1}$ and the velocity $\boldsymbol{v}^{k+1}$ are expressed explicitly (see [23]).

We will now modify this method for the solution of contact problems. From (2.12) we can express $\boldsymbol{a}^{k+1}$ by means of $\boldsymbol{u}^{k+1}$ as follows:

$$\boldsymbol{a}^{k+1} = \frac{1}{\Delta t^2 \beta}\left(\boldsymbol{u}^{k+1} - \boldsymbol{u}^k\right) - \frac{1}{\Delta t \beta}\boldsymbol{v}^k - \frac{\frac{1}{2}-\beta}{\beta}\boldsymbol{a}^k,$$

and substitute it into (2.13):

$$\boldsymbol{v}^{k+1} = \frac{\gamma}{\Delta t \beta}\left(\boldsymbol{u}^{k+1} - \boldsymbol{u}^k\right) + \frac{\beta-\gamma}{\beta}\boldsymbol{v}^k + \frac{\beta-\frac{\gamma}{2}}{\beta}\Delta t \boldsymbol{a}^k.$$

Replacing $\boldsymbol{a}^{k+1}$ in the equilibrium equation in (2.11) we get

$$\underbrace{\left(\frac{1}{\beta \Delta t^2}\mathsf{M} + \mathsf{K}\right)}_{=:\hat{\mathsf{K}}}\boldsymbol{u}^{k+1} = \underbrace{\boldsymbol{L}^{k+1} + \frac{1}{\beta \Delta t^2}\mathsf{M}\boldsymbol{u}^k + \frac{1}{\beta \Delta t}\mathsf{M}\boldsymbol{v}^k + \frac{\frac{1}{2}-\beta}{\beta}\mathsf{M}\boldsymbol{a}^k}_{=:\hat{\boldsymbol{L}}^{k+1}} + \mathsf{B}_n^\top \boldsymbol{\lambda}_n^{k+1} + \mathsf{B}_t^\top \boldsymbol{\lambda}_t^{k+1}.$$

Here $\hat{\mathsf{K}} := \hat{\mathsf{K}}(\Delta t, \beta)$ is the so-called *effective stiffness matrix* and $\hat{\boldsymbol{L}}^{k+1}$ is the *effective load vector*. Similarly we replace $\boldsymbol{v}^{k+1}$ in the friction condition in (2.11):

$$-\boldsymbol{\lambda}_t^{k+1} \in \partial_2 j\Bigg(\boldsymbol{\lambda}_n^{k+1}, \underbrace{\frac{\gamma}{\beta \Delta t}}_{=:\alpha}\mathsf{B}_t\boldsymbol{u}^{k+1} \underbrace{- \frac{\gamma}{\beta \Delta t}\mathsf{B}_t\boldsymbol{u}^k + \frac{\beta-\gamma}{\beta}\mathsf{B}_t\boldsymbol{v}^k + \frac{\beta-\frac{\gamma}{2}}{\beta}\Delta t \mathsf{B}_t\boldsymbol{a}^k}_{=:-\boldsymbol{C}_t}\Bigg).$$

With this notation, the Newmark scheme for contact problems with Coulomb friction reads as follows:

$$\begin{cases} \forall k \in \{0, 1, \ldots, L-1\} \text{ find } \boldsymbol{u}^{k+1} \in \mathbb{R}^{2n}, \boldsymbol{\lambda}_n^{k+1} \in \mathbb{R}^m, \boldsymbol{\lambda}_t^{k+1} \in \mathbb{R}^m \text{ such that} \\ \hat{\mathsf{K}}\boldsymbol{u}^{k+1} = \hat{\boldsymbol{L}}^{k+1} + \mathsf{B}_n^\top \boldsymbol{\lambda}_n^{k+1} + \mathsf{B}_t^\top \boldsymbol{\lambda}_t^{k+1}, \\ -\boldsymbol{\lambda}_n^{k+1} \in N_{\mathbb{R}^m_-}(\mathsf{B}_n\boldsymbol{u}^{k+1}), \\ -\boldsymbol{\lambda}_t^{k+1} \in \partial_2 j(\boldsymbol{\lambda}_n^{k+1}, \alpha \mathsf{B}_t\boldsymbol{u}^{k+1} - \boldsymbol{C}_t), \\ \boldsymbol{u}^0 = \boldsymbol{U}_0, \boldsymbol{v}^0 = \dot{\boldsymbol{U}}_0. \end{cases} \tag{2.14}$$

From the previous sections we know that the explicit form of the non-penetration conditions is:

$$\begin{cases} \left(\mathsf{B}_n\boldsymbol{u}^{k+1}\right)_i &\leq 0, \\ \left(\boldsymbol{\lambda}_n^{k+1}\right)_i &\leq 0, \\ \left(\boldsymbol{\lambda}_n^{k+1}\right)_i \left(\mathsf{B}_n\boldsymbol{u}^{k+1}\right)_i &= 0 \quad \forall i = 1, 2, \ldots, m. \end{cases}$$

We may also explicitly express the friction conditions in (2.14) for $i = 1, 2, \ldots, m$:

$$\begin{cases} (\mathsf{B}_t\boldsymbol{u}^{k+1})_i = \frac{1}{\alpha}(\boldsymbol{C}_t)_i &\Rightarrow \quad |(\boldsymbol{\lambda}_t^{k+1})_i| \leq -\mathcal{F}(\boldsymbol{\lambda}_n^{k+1})_i, \\ (\mathsf{B}_t\boldsymbol{u}^{k+1})_i \neq \frac{1}{\alpha}(\boldsymbol{C}_t)_i &\Rightarrow \quad (\boldsymbol{\lambda}_t^{k+1})_i = \mathcal{F}(\boldsymbol{\lambda}_n^{k+1})_i \operatorname{sgn}(\alpha \mathsf{B}_t\boldsymbol{u}^{k+1} - \boldsymbol{C}_t)_i. \end{cases}$$

Therefore, we transformed the dynamic problem to a sequence of static frictional contact problems. In friction condition the tangential displacement at $t = t_{k+1}$ is not compared with zero, but with the value

$$\frac{1}{\alpha}\boldsymbol{C}_t =: \mathsf{B}_t\boldsymbol{u}^k + \Delta t\left(\mathsf{B}_t\boldsymbol{v}^k - \frac{\beta}{\gamma}\mathsf{B}_t\boldsymbol{v}^k\right) + \frac{1}{2}\Delta t^2\left(\mathsf{B}_t\boldsymbol{a}^k - \frac{2\beta}{\gamma}\mathsf{B}_t\boldsymbol{a}^k\right).$$

One can note that the previous relation is Taylor's expansion of the displacement at time $t = t_k$ with the velocity and the acceleration modified by the constants β and γ. Contrary to some other methods (e.g., the mid-point method presented in the following paragraphs) the choice of these constants may affect the contact behavior of the method.

The following proposition gives us the information about the energy variation which is useful for the stability considerations.

Proposition 2.1. Let $\boldsymbol{L}(t) \equiv \boldsymbol{L}$ be constant in t. Then the energy variation of the Newmark method is

$$\begin{aligned}\Delta J = &\left(\frac{1}{2} - \gamma\right)\left(\boldsymbol{u}^{k+1} - \boldsymbol{u}^k\right)^\top \mathsf{K}\left(\boldsymbol{u}^{k+1} - \boldsymbol{u}^k\right)\\
&+ \Delta t\left(\beta - \frac{\gamma}{2}\right)\left(\boldsymbol{v}^{k+1} - \boldsymbol{v}^k\right)^\top \mathsf{K}\left(\boldsymbol{u}^{k+1} - \boldsymbol{u}^k\right)\\
&- \Delta t\left(\beta - \frac{\gamma}{2}\right)\left(\boldsymbol{v}^{k+1} - \boldsymbol{v}^k\right)^\top \left(\left(\mathsf{B}_n^\top\boldsymbol{\lambda}_n^{k+1} + \mathsf{B}_t^\top\boldsymbol{\lambda}_t^{k+1}\right) - \left(\mathsf{B}_n^\top\boldsymbol{\lambda}_n^k + \mathsf{B}_t^\top\boldsymbol{\lambda}_t^k\right)\right)\\
&+ \left(\boldsymbol{u}^{k+1} - \boldsymbol{u}^k\right)^\top \left((1-\gamma)\left(\mathsf{B}_n^\top\boldsymbol{\lambda}_n^k + \mathsf{B}_t^\top\boldsymbol{\lambda}_t^k\right) + \gamma\left(\mathsf{B}_n^\top\boldsymbol{\lambda}_n^{k+1} + \mathsf{B}_t^\top\boldsymbol{\lambda}_t^{k+1}\right)\right).\end{aligned}$$

Proof. This proof corrects mistakes in the one presented in [13]. From the definition of the energy variation we get:

$$\begin{aligned}\Delta J = J(\boldsymbol{u}^{k+1}, \boldsymbol{v}^{k+1}) - J(\boldsymbol{u}^k, \boldsymbol{v}^k) = \frac{1}{2}(\boldsymbol{v}^{k+1} - \boldsymbol{v}^k)\mathsf{M}(\boldsymbol{v}^{k+1} + \boldsymbol{v}^k)\\
+ \frac{1}{2}(\boldsymbol{u}^{k+1} - \boldsymbol{u}^k)\mathsf{K}(\boldsymbol{u}^{k+1} + \boldsymbol{u}^k) - (\boldsymbol{u}^{k+1} - \boldsymbol{u}^k)^\top\boldsymbol{L}.\end{aligned} \tag{2.15}$$

Multiplying (2.12) and (2.13) by M we obtain:

$$\mathsf{M}(\boldsymbol{u}^{k+1} - \boldsymbol{u}^k - \Delta t\boldsymbol{v}^k) = \Delta t^2\left(\left(\frac{1}{2} - \beta\right)\mathsf{M}\boldsymbol{a}^k + \beta\mathsf{M}\boldsymbol{a}^{k+1}\right), \tag{2.16}$$

$$\mathsf{M}(\boldsymbol{v}^{k+1} - \boldsymbol{v}^k) = \Delta t\left((1-\gamma)\,\mathsf{M}\boldsymbol{a}^k + \gamma\mathsf{M}\boldsymbol{a}^{k+1}\right). \tag{2.17}$$

Since the energy equilibrium equation $\mathsf{M}\boldsymbol{a}^k = \boldsymbol{L} + \mathsf{B}_n\boldsymbol{\lambda}_n^k + \mathsf{B}_t^k - \mathsf{K}\boldsymbol{u}^k$ holds we can write (2.16) and (2.17) as:

$$\begin{aligned}\mathsf{M}(\boldsymbol{u}^{k+1} - \boldsymbol{u}^k - \Delta t\boldsymbol{v}^k) &= \Delta t^2\Bigg(\left(\frac{1}{2} - \beta\right)\left(\boldsymbol{L} + \mathsf{B}_n^\top\boldsymbol{\lambda}_n^k + \mathsf{B}_t^\top\boldsymbol{\lambda}_t^k - \mathsf{K}\boldsymbol{u}^k\right)\\ &\quad + \beta\left(\boldsymbol{L} + \mathsf{B}_n^\top\boldsymbol{\lambda}_n^{k+1} + \mathsf{B}_t^\top\boldsymbol{\lambda}_t^{k+1} - \mathsf{K}\boldsymbol{u}^{k+1}\right)\Bigg)\\ &= \frac{\Delta t^2}{2}\boldsymbol{L} - \Delta t^2\left(\left(\frac{1}{2} - \beta\right)\mathsf{K}\boldsymbol{u}^k + \beta\mathsf{K}\boldsymbol{u}^{k+1}\right)\\ &\quad + \Delta t^2\left(\left(\frac{1}{2} - \beta\right)\left(\mathsf{B}_n^\top\boldsymbol{\lambda}_n^k + \mathsf{B}_t^\top\boldsymbol{\lambda}_t^k\right) + \beta\left(\mathsf{B}_n^\top\boldsymbol{\lambda}_n^{k+1} + \mathsf{B}_t^\top\boldsymbol{\lambda}_t^{k+1}\right)\right)\end{aligned} \tag{2.18}$$

and

$$\begin{aligned}\mathsf{M}(\boldsymbol{v}^{k+1} - \boldsymbol{v}^k) &= \Delta t\,(1-\gamma)\left(\boldsymbol{L} + \mathsf{B}_n^\top\boldsymbol{\lambda}_n^k + \mathsf{B}_t^\top\boldsymbol{\lambda}_t^k - \mathsf{K}\boldsymbol{u}^k\right)\\ &\quad + \Delta t\gamma\left(\boldsymbol{L} + \mathsf{B}_n^\top\boldsymbol{\lambda}_n^{k+1} + \mathsf{B}_t^\top\boldsymbol{\lambda}_t^{k+1} - \mathsf{K}\boldsymbol{u}^{k+1}\right)\\ &= \Delta t\boldsymbol{L} - \Delta t\left((1-\gamma)\,\mathsf{K}\boldsymbol{u}^k + \gamma\mathsf{K}\boldsymbol{u}^{k+1}\right)\\ &\quad + \Delta t\left((1-\gamma)\left(\mathsf{B}_n^\top\boldsymbol{\lambda}_n^k + \mathsf{B}_t^\top\boldsymbol{\lambda}_t^k\right) + \gamma\left(\mathsf{B}_n^\top\boldsymbol{\lambda}_n^{k+1} + \mathsf{B}_t^\top\boldsymbol{\lambda}_t^{k+1}\right)\right).\end{aligned} \tag{2.19}$$

Multiplying (2.19) by $\frac{\Delta t}{2}$ and subtracting from (2.18) we get after some modifications:

$$\begin{aligned}\mathsf{M}(\boldsymbol{u}^{k+1} - \boldsymbol{u}^k) &= -\Delta t^2\left(\beta - \frac{\gamma}{2}\right)\mathsf{K}\left(\boldsymbol{u}^{k+1} - \boldsymbol{u}^k\right) + \frac{\Delta t}{2}\mathsf{M}\left(\boldsymbol{v}^{k+1} + \boldsymbol{v}^k\right)\\ &\quad + \Delta t^2\left(\beta - \frac{\gamma}{2}\right)\Bigg(\left(\mathsf{B}_n^\top\boldsymbol{\lambda}_n^{k+1} + \mathsf{B}_t^\top\boldsymbol{\lambda}_t^{k+1}\right) - \left(\mathsf{B}_n^\top\boldsymbol{\lambda}_n^k + \mathsf{B}_t^\top\boldsymbol{\lambda}_t^k\right)\Bigg).\end{aligned}$$

Expressing $\mathsf{M}(\boldsymbol{v}^{k+1} + \boldsymbol{v}^k)$ from the previous equation and substituting it into (2.15) we have:

$$\begin{aligned}\Delta J &= \frac{1}{2}(\boldsymbol{u}^{k+1} - \boldsymbol{u}^k)^\top\mathsf{K}(\boldsymbol{u}^{k+1} + \boldsymbol{u}^k) + \frac{1}{\Delta t}(\boldsymbol{v}^{k+1} - \boldsymbol{v}^k)^\top\mathsf{M}(\boldsymbol{u}^{k+1} - \boldsymbol{u}^k)\\ &\quad + \Delta t\left(\beta - \frac{\gamma}{2}\right)(\boldsymbol{v}^{k+1} - \boldsymbol{v}^k)^\top\mathsf{K}(\boldsymbol{u}^{k+1} - \boldsymbol{u}^k)\\ &\quad - \Delta t\left(\beta - \frac{\gamma}{2}\right)(\boldsymbol{v}^{k+1} - \boldsymbol{v}^k)^\top\left(\left(\mathsf{B}_n^\top\boldsymbol{\lambda}_n^{k+1} + \mathsf{B}_t^\top\boldsymbol{\lambda}_t^{k+1}\right) - \left(\mathsf{B}_n^\top\boldsymbol{\lambda}_n^k + \mathsf{B}_t^\top\boldsymbol{\lambda}_t^k\right)\right)\\ &\quad - (\boldsymbol{u}^{k+1} - \boldsymbol{u}^k)^\top\boldsymbol{L}.\end{aligned} \tag{2.20}$$

Next, let us multiply (2.19) by $(\boldsymbol{u}^{k+1} - \boldsymbol{u}^k)$ and express $(\boldsymbol{u}^{k+1} - \boldsymbol{u}^k)^\top\boldsymbol{L}$:

$$\begin{aligned}(\boldsymbol{u}^{k+1} - \boldsymbol{u}^k)^\top\boldsymbol{L} &= \frac{1}{\Delta t}(\boldsymbol{u}^{k+1} - \boldsymbol{u}^k)^\top\mathsf{M}(\boldsymbol{v}^{k+1} - \boldsymbol{v}^k)\\ &\quad + (\boldsymbol{u}^{k+1} - \boldsymbol{u}^k)^\top\left((1-\gamma)\,\mathsf{K}\boldsymbol{u}^k + \gamma\mathsf{K}\boldsymbol{u}^{k+1}\right)\\ &\quad - (\boldsymbol{u}^{k+1} - \boldsymbol{u}^k)^\top\left((1-\gamma)\left(\mathsf{B}_n^\top\boldsymbol{\lambda}_n^k + \mathsf{B}_t^\top\boldsymbol{\lambda}_t^k\right) + \gamma\left(\mathsf{B}_n^\top\boldsymbol{\lambda}_n^{k+1} + \mathsf{B}_t^\top\boldsymbol{\lambda}_t^{k+1}\right)\right).\end{aligned}$$

Finally substituting the previous expression to 2.20 we get after some modifications:

$$\begin{aligned}\Delta J = &\left(\frac{1}{2}-\gamma\right)\left(\boldsymbol{u}^{k+1}-\boldsymbol{u}^{k}\right)^{\top}\mathsf{K}\left(\boldsymbol{u}^{k+1}-\boldsymbol{u}^{k}\right)\\ &+\Delta t\left(\beta-\frac{\gamma}{2}\right)\left(\boldsymbol{v}^{k+1}-\boldsymbol{v}^{k}\right)^{\top}\mathsf{K}\left(\boldsymbol{u}^{k+1}-\boldsymbol{u}^{k}\right)\\ &-\Delta t\left(\beta-\frac{\gamma}{2}\right)\left(\boldsymbol{v}^{k+1}-\boldsymbol{v}^{k}\right)^{\top}\left(\left(\mathsf{B}_n^{\top}\boldsymbol{\lambda}_n^{k+1}+\mathsf{B}_t^{\top}\boldsymbol{\lambda}_t^{k+1}\right)-\left(\mathsf{B}_n^{\top}\boldsymbol{\lambda}_n^{k}+\mathsf{B}_t^{\top}\boldsymbol{\lambda}_t^{k}\right)\right)\\ &+\left(\boldsymbol{u}^{k+1}-\boldsymbol{u}^{k}\right)^{\top}\left((1-\gamma)\left(\mathsf{B}_n^{\top}\boldsymbol{\lambda}_n^{k}+\mathsf{B}_t^{\top}\boldsymbol{\lambda}_t^{k}\right)+\gamma\left(\mathsf{B}_n^{\top}\boldsymbol{\lambda}_n^{k+1}+\mathsf{B}_t^{\top}\boldsymbol{\lambda}_t^{k+1}\right)\right).\end{aligned}$$

□

From the previous proposition it is seen that for $\gamma > \frac{1}{2}$ the first term in ΔJ provides a strong dissipation of the energy (even when no contact occurs). Choosing, e.g., $2\beta = \gamma = 1$ we obtain:

$$\Delta J = -\frac{1}{2}\left(\boldsymbol{u}^{k+1}-\boldsymbol{u}^{k}\right)^{\top}\mathsf{K}\left(\boldsymbol{u}^{k+1}-\boldsymbol{u}^{k}\right)+\left(\boldsymbol{u}^{k+1}-\boldsymbol{u}^{k}\right)^{\top}\left(\mathsf{B}_n^{\top}\boldsymbol{\lambda}_n^{k+1}+\mathsf{B}_t^{\top}\boldsymbol{\lambda}_t^{k+1}\right).$$

The first term is clearly dissipative. To determine the sign of the last term at least approximately, let us write:

$$\left(\boldsymbol{u}^{k+1}-\boldsymbol{u}^{k}\right)^{\top}\left(\mathsf{B}_n^{\top}\boldsymbol{\lambda}_n^{k+1}+\mathsf{B}_t^{\top}\boldsymbol{\lambda}_t^{k+1}\right)=\left(\boldsymbol{u}^{k+1}-\boldsymbol{u}^{k}\right)^{\top}\mathsf{B}_t^{\top}\boldsymbol{\lambda}_t^{k+1}-\left(\mathsf{B}_n\boldsymbol{u}^{k}\right)^{\top}\boldsymbol{\lambda}_n^{k+1}.$$

Substituting for $\boldsymbol{u}^{k+1}$ from (2.12) with $2\beta = \gamma = 1$ we obtain:

$$\begin{aligned}\left(\boldsymbol{u}^{k+1}-\boldsymbol{u}^{k}\right)^{\top}\mathsf{B}_t^{\top}\boldsymbol{\lambda}_t^{k+1}-\left(\mathsf{B}_n\boldsymbol{u}^{k}\right)^{\top}\boldsymbol{\lambda}_n^{k+1}&=\left(\Delta t\boldsymbol{v}^{k}+\frac{\Delta t^2}{2}\boldsymbol{a}^{k+1}\right)^{\top}\mathsf{B}_t^{\top}\boldsymbol{\lambda}_t^{k+1}-\left(\mathsf{B}_n\boldsymbol{u}^{k}\right)^{\top}\boldsymbol{\lambda}_n^{k+1}\\ &\overset{(2.13)}{=}\left(\Delta t\boldsymbol{v}^{k+1}-\underbrace{\frac{\Delta t^2}{2}\boldsymbol{a}^{k+1}}_{\approx 0}\right)^{\top}\mathsf{B}_t^{\top}\boldsymbol{\lambda}_t^{k+1}-\left(\mathsf{B}_n\boldsymbol{u}^{k}\right)^{\top}\boldsymbol{\lambda}_n^{k+1}\\ &\approx \Delta t\underbrace{\left(\mathsf{B}_t\boldsymbol{v}^{k+1}\right)^{\top}\boldsymbol{\lambda}_t^{k+1}}_{\leq 0}-\left(\mathsf{B}_n\boldsymbol{u}^{k}\right)^{\top}\boldsymbol{\lambda}_n^{k+1}.\end{aligned}$$

The sign in the last term follows from the Coulomb's law. This term therefore also contributes to the energy dissipation. Although it is not possible to determine the sign of the last term, from $\left(\mathsf{B}_n\boldsymbol{u}^{k+1}\right)^{\top}\boldsymbol{\lambda}_n^{k+1}=0$ one can assume that its value is close to zero if $\|\boldsymbol{u}^{k+1}-\boldsymbol{u}^{k}\|$ is small enough. Then the method is stable and very dissipative for this choice of the parameters.

2.2.3 Mid-point method

This time integration method is based on classical Euler's method for solving differential equations

$$y'(t) = f(t, y(t)).$$

Whereas Euler's method is based on the approximation $y'(t) \approx (y(t+\Delta t) - y(t))/\Delta t$ from which one can easily obtain the scheme

$$y_{k+1} = y_k + \Delta t f(t_k, y_k),$$

the mid-point scheme is derived from the expression

$$y'(t + \frac{1}{2}\Delta t) \approx (y(t + \Delta t) - y(t))/\Delta t.$$

From this we get

$$y_{k+1} = y_k + \Delta t f\left(t_{k+\frac{1}{2}}, y_{k+\frac{1}{2}}\right),$$

where $t_{k+\frac{1}{2}} := (t_{k+1} + t_k)/2$ and $y_{k+\frac{1}{2}} := y(t_{k+\frac{1}{2}})$. One can also derive this scheme from Taylor's expansion of $y(t)$. Using this way it is easier to derive the error of the method:

$$\begin{aligned}
y(t + \Delta t) &= y(t) + \Delta t y'(t) + \frac{\Delta t^2}{2} y''(t) + \mathcal{O}(\Delta t^3) \\
&= y(t) + \Delta t \underbrace{\left(y'(t) + \frac{\Delta t}{2} y''(t) \right)}_{= y'\left(t + \frac{\Delta t}{2}\right) + \mathcal{O}(\Delta t^2)} + \mathcal{O}(\Delta t^3) \\
&= y(t) + \Delta t y'\left(t + \frac{\Delta t}{2}\right) + \mathcal{O}(\Delta t^3) \\
&= y(t) + \Delta t f\left(t + \frac{\Delta t}{2}, y\left(t + \frac{\Delta t}{2}\right)\right) + \mathcal{O}(\Delta t^3).
\end{aligned}$$

The unknown expression $y\left(t + \frac{\Delta t}{2}\right)$ appearing in the argument of f may be approximated similarly:

$$\begin{aligned}
y\left(t + \frac{\Delta t}{2}\right) &= y(t) + \frac{\Delta t}{2} y'(t) + \mathcal{O}(\Delta t^2) \\
&= y(t) + \frac{\Delta t}{2}\left(\frac{y(t + \Delta t) - y(t)}{\Delta t} + \mathcal{O}(\Delta t) \right) + \mathcal{O}(\Delta t^2) \\
&= y(t) + \frac{y(t + \Delta t) - y(t)}{2} + \mathcal{O}(\Delta t^2) \\
&= \frac{y(t) + y(t + \Delta t)}{2} + \mathcal{O}(\Delta t^2),
\end{aligned}$$

where we used the finite difference to estimate $y'(t)$. We see that the global discretization error is of order two.

In the next definition we apply this approach to the system of equations to our dynamic elasticity problem without unilateral and friction conditions.

Definition 2.4 (Mid-point scheme)**.** Given $\boldsymbol{u}^k, \boldsymbol{v}^k, \boldsymbol{a}^k$ evaluate $\boldsymbol{u}^{k+1}, \boldsymbol{v}^{k+1}, \boldsymbol{a}^{k+1}$ such that it holds

$$\begin{cases} \boldsymbol{u}^{k+1} &= \boldsymbol{u}^k + \Delta t \boldsymbol{v}^{k+\frac{1}{2}}, \\ \boldsymbol{u}^{k+\frac{1}{2}} &= \frac{\boldsymbol{u}^k + \boldsymbol{u}^{k+1}}{2}, \\ \boldsymbol{v}^{k+1} &= \boldsymbol{v}^k + \Delta t \boldsymbol{a}^{k+\frac{1}{2}}, \\ \boldsymbol{v}^{k+\frac{1}{2}} &= \frac{\boldsymbol{v}^k + \boldsymbol{v}^{k+1}}{2}, \end{cases} \tag{2.21}$$

together with the energy equilibrium equation $\mathsf{M}\boldsymbol{a}^{k+\frac{1}{2}} + \mathsf{K}\boldsymbol{u}^{k+\frac{1}{2}} = \boldsymbol{L}^{k+\frac{1}{2}}$ satisfied at time $t = t_{k+\frac{1}{2}}$.

We will now use (2.21) for our contact problem. From the first two equations we express $\boldsymbol{v}^{k+\frac{1}{2}}$ in terms of $\boldsymbol{u}^{k+\frac{1}{2}}$ by

$$\boldsymbol{v}^{k+\frac{1}{2}} = \frac{2}{\Delta t}\boldsymbol{u}^{k+\frac{1}{2}} - \frac{2}{\Delta t}\boldsymbol{u}^k$$

Combining this with the third and the fourth equation in (2.21) we get

$$\boldsymbol{a}^{k+\frac{1}{2}} = \frac{4}{\Delta t^2}\boldsymbol{u}^{k+\frac{1}{2}} - \frac{4}{\Delta t^2}\boldsymbol{u}^k - \frac{2}{\Delta t}\boldsymbol{v}^k.$$

Finally we insert these expressions into the equilibrium equation

$$\mathsf{M}\boldsymbol{a}^{k+\frac{1}{2}} + \mathsf{K}\boldsymbol{u}^{k+\frac{1}{2}} = \boldsymbol{L}^{k+\frac{1}{2}} + \mathsf{B}_n^\top \boldsymbol{\lambda}_n^{k+\frac{1}{2}} + \mathsf{B}_t^\top \boldsymbol{\lambda}_t^{k+\frac{1}{2}}$$

and the friction inclusion (both at time $t = t_{k+\frac{1}{2}}$) to obtain:

$$\underbrace{\left(\frac{4}{\Delta t^2}\mathsf{M} + \mathsf{K}\right)}_{=:\hat{\mathsf{K}}} \boldsymbol{u}^{k+\frac{1}{2}} = \underbrace{\boldsymbol{L}^{k+\frac{1}{2}} + \frac{4}{\Delta t^2}\mathsf{M}\boldsymbol{u}^k + \frac{2}{\Delta t}\mathsf{M}\boldsymbol{v}^k}_{=:\hat{\boldsymbol{L}}^{k+\frac{1}{2}}} + \mathsf{B}_n^\top \boldsymbol{\lambda}_n^{k+\frac{1}{2}} + \mathsf{B}_t^\top \boldsymbol{\lambda}_t^{k+\frac{1}{2}},$$

and

$$-\boldsymbol{\lambda}_t^{k+\frac{1}{2}} \in \partial_2 j\Big(\boldsymbol{\lambda}_n^{k+\frac{1}{2}}, \frac{2}{\Delta t}\mathsf{B}_t\boldsymbol{u}^{k+\frac{1}{2}} - \frac{2}{\Delta t}\mathsf{B}_t\boldsymbol{u}^k\Big).$$

Here again, $\hat{\mathsf{K}}$ is the effective stiffness matrix and $\hat{\boldsymbol{L}}^{k+\frac{1}{2}}$ is the effective load vector. Denoting $\alpha := \frac{2}{\Delta t}$ and $\boldsymbol{C}_t := \frac{2}{\Delta t}\mathsf{B}_t\boldsymbol{u}^k$ one can write the whole problem as

$$\begin{cases} \forall k \in \{0, 1, \ldots, L-1\} \text{ find } \boldsymbol{u}^{k+\frac{1}{2}} \in \mathbb{R}^{2n}, \boldsymbol{\lambda}_n^{k+\frac{1}{2}} \in \mathbb{R}^m, \boldsymbol{\lambda}_t^{k+\frac{1}{2}} \in \mathbb{R}^m \text{ such that} \\ \hat{\mathsf{K}}\boldsymbol{u}^{k+\frac{1}{2}} = \hat{\boldsymbol{L}}^{k+\frac{1}{2}} + \mathsf{B}_n^\top \boldsymbol{\lambda}_n^{k+\frac{1}{2}} + \mathsf{B}_t^\top \boldsymbol{\lambda}_t^{k+\frac{1}{2}}, \\ -\boldsymbol{\lambda}_n^{k+\frac{1}{2}} \in N_{\mathbb{R}^m_-}\big(\mathsf{B}_n\boldsymbol{u}^{k+\frac{1}{2}}\big), \\ -\boldsymbol{\lambda}_t^{k+\frac{1}{2}} \in \partial_2 j\big(\boldsymbol{\lambda}_n^{k+\frac{1}{2}}, \alpha\mathsf{B}_t\boldsymbol{u}^{k+\frac{1}{2}} - \boldsymbol{C}_t\big), \\ \boldsymbol{u}^0 = \boldsymbol{U}_0, \boldsymbol{v}^0 = \dot{\boldsymbol{U}}_0, \\ \text{and set} \\ \boldsymbol{u}^{k+1} = \boldsymbol{u}^k + \Delta t \boldsymbol{v}^{k+\frac{1}{2}}, \text{ where } \boldsymbol{v}^{k+\frac{1}{2}} = \frac{2}{\Delta t}\boldsymbol{u}^{k+\frac{1}{2}} - \frac{2}{\Delta t}\boldsymbol{u}^k, \\ \boldsymbol{v}^{k+1} = \boldsymbol{v}^k + \Delta t \boldsymbol{a}^{k+\frac{1}{2}}, \text{ where } \boldsymbol{a}^{k+\frac{1}{2}} = \frac{4}{\Delta t^2}\boldsymbol{u}^{k+\frac{1}{2}} - \frac{4}{\Delta t^2}\boldsymbol{u}^k - \frac{2}{\Delta t}\boldsymbol{v}^k. \end{cases} \tag{2.22}$$

Similarly to the Newmark scheme, the unilateral and the friction constraints at $t = t_{k+\frac{1}{2}}$ may be written explicitly in the following way:

$$\begin{cases} \left(\mathsf{B}_n \boldsymbol{u}^{k+\frac{1}{2}}\right)_i & \leq & 0, \\ \left(\boldsymbol{\lambda}_n^{k+\frac{1}{2}}\right)_i & \leq & 0, \\ \left(\boldsymbol{\lambda}_n^{k+\frac{1}{2}}\right)_i \left(\mathsf{B}_n \boldsymbol{u}^{k+\frac{1}{2}}\right)_i & = & 0 \quad \forall i = 1, 2, \ldots, m, \end{cases} \tag{2.23}$$

and

$$\begin{cases} \left(\mathsf{B}_t \boldsymbol{u}^{k+\frac{1}{2}}\right)_i = \left(\mathsf{B}_t \boldsymbol{u}^{k}\right)_i & \Rightarrow & \left|\left(\boldsymbol{\lambda}_t^{k+\frac{1}{2}}\right)_i\right| \leq -\mathcal{F}\left(\boldsymbol{\lambda}_n^{k+\frac{1}{2}}\right)_i \\ \left(\mathsf{B}_t \boldsymbol{u}^{k+\frac{1}{2}}\right)_i \neq \left(\mathsf{B}_t \boldsymbol{u}^{k}\right)_i & \Rightarrow & \left(\boldsymbol{\lambda}_t^{k+\frac{1}{2}}\right)_i = \mathcal{F}\left(\boldsymbol{\lambda}_n^{k+\frac{1}{2}}\right)_i \operatorname{sgn}\left(\alpha \mathsf{B}_t \boldsymbol{u}^{k+\frac{1}{2}} - \boldsymbol{C}_t\right)_i, \end{cases}$$

for $i = 1, 2, \ldots, m$ taking into account the definition of α and $\boldsymbol{C}_t$. Note that unlike the Newmark method, the friction condition now takes into account solely the displacement at the previous time-step.

The energy variation of the mid-point method is described by the next proposition (see [13]).

Proposition 2.2. Let $\boldsymbol{L}(t) \equiv \boldsymbol{L}$ be constant in t. Then the energy variation of the mid-point method is

$$\Delta J = \Delta t \left(\boldsymbol{v}_n^{k+\frac{1}{2}}\right)^\top \boldsymbol{\lambda}_n^{k+\frac{1}{2}} + \Delta t \left(\boldsymbol{v}_t^{k+\frac{1}{2}}\right)^\top \boldsymbol{\lambda}_t^{k+\frac{1}{2}} \leq -2 \left(\boldsymbol{u}_n^{k}\right)^\top \boldsymbol{\lambda}_n^{k+\frac{1}{2}}. \tag{2.24}$$

Since the contact conditions in (2.22) are imposed at time $t = t_{k+\frac{1}{2}}$, one cannot determine the sign of the last term in (2.24). Therefore it is not possible to have the definite statement on the stability of the mid-point method. It may even happen that the unilateral conditions are not satisfied at $t = t_k$, i.e. the body interpenetrates the obstacle. A possible treatment of this problem is described in the following section.

2.2.4 Modified mid-point method

The modification of the mid-point method is based on the implicit treatment of the contact force. The acceleration of the body due to the contact effects is treated separately at time-step $k + 1$:

$$\begin{cases} \boldsymbol{u}^{k+1} & = \boldsymbol{u}^k + \Delta t \boldsymbol{v}^{k+\frac{1}{2}}, \\ \boldsymbol{u}^{k+\frac{1}{2}} & = \frac{\boldsymbol{u}^k + \boldsymbol{u}^{k+1}}{2}, \\ \boldsymbol{v}^{k+1} & = \boldsymbol{v}^k + \Delta t \boldsymbol{a}^{k+\frac{1}{2}} + \Delta t \boldsymbol{a}_n^{k+1}, \\ \boldsymbol{v}^{k+\frac{1}{2}} & = \frac{\boldsymbol{v}^k + \boldsymbol{v}^{k+1}}{2}, \end{cases} \tag{2.25}$$

where $\boldsymbol{a}_n^{k+1}$ is the normal acceleration at time $t = t_{k+1}$, i.e. $\mathsf{M}\boldsymbol{a}_n^{k+1} = \mathsf{B}_n^\top \boldsymbol{\lambda}_n^{k+1}$. The equilibrium equation at $t = t_{k+\frac{1}{2}}$ has the following form:

$$\mathsf{M}\boldsymbol{a}^{k+\frac{1}{2}} + \mathsf{K}\boldsymbol{u}^{k+\frac{1}{2}} = \boldsymbol{L}^{k+\frac{1}{2}} + \mathsf{B}_t^\top \boldsymbol{\lambda}_t^{k+\frac{1}{2}}.$$

The condition $-\boldsymbol{\lambda}_n^{k+\frac{1}{2}} \in N_{\mathbb{R}^m_-}(\mathsf{B}_n \boldsymbol{u}^{k+\frac{1}{2}})$ is now replaced by $-\boldsymbol{\lambda}_n^{k+1} \in N_{\mathbb{R}^m_-}(\mathsf{B}_n \boldsymbol{u}^{k+1})$. From (2.25) we can express $\boldsymbol{u}^{k+1}$ in terms of $\boldsymbol{u}^k$ and $\boldsymbol{u}^{k+\frac{1}{2}}$:

$$\boldsymbol{u}^{k+1} = 2\boldsymbol{u}^{k+\frac{1}{2}} - \boldsymbol{u}^k, \tag{2.26}$$

therefore the unilateral condition becomes:

$$-\boldsymbol{\lambda}_n^{k+1} \in N_{\mathbb{R}^m_-}\left(\mathsf{B}_n\left(2\boldsymbol{u}^{k+\frac{1}{2}} - \boldsymbol{u}^k\right)\right).$$

For the velocity at the time t_{k+1} it follows from (2.25):

$$\boldsymbol{v}^{k+1} = 2\boldsymbol{v}^{k+\frac{1}{2}} - \boldsymbol{v}^k = 2\frac{\boldsymbol{u}^{k+1} - \boldsymbol{u}^k}{\Delta t} - \boldsymbol{v}^k = 4\frac{\boldsymbol{u}^{k+\frac{1}{2}} - \boldsymbol{u}^k}{\Delta t} - \boldsymbol{v}^k. \tag{2.27}$$

Expressing $\boldsymbol{v}^{k+\frac{1}{2}}$ and $\boldsymbol{a}^{k+\frac{1}{2}}$ from (2.25):

$$\boldsymbol{v}^{k+\frac{1}{2}} = \frac{\boldsymbol{u}^{k+1} - \boldsymbol{u}^k}{\Delta t} \overset{(2.26)}{=} \frac{2}{\Delta t}\boldsymbol{u}^{k+\frac{1}{2}} - \frac{2}{\Delta t}\boldsymbol{u}^k,$$

$$\boldsymbol{a}^{k+\frac{1}{2}} = \frac{\boldsymbol{v}^{k+1} - \boldsymbol{v}^k}{\Delta t} - \boldsymbol{a}_n^{k+1} \overset{(2.27)}{=} \frac{4}{\Delta t^2}\boldsymbol{u}^{k+\frac{1}{2}} - \frac{4}{\Delta t^2}\boldsymbol{u}^k - \frac{2}{\Delta t}\boldsymbol{v}^k - \boldsymbol{a}_n^{k+1},$$

substituting them into the energy equilibrium equations and using $\mathsf{M}\boldsymbol{a}_n^{k+1} = \mathsf{B}_n^\top \boldsymbol{\lambda}_n^{k+1}$ we get:

$$\begin{cases} \forall k \in \{0, 1, \ldots, L-1\} \text{ find } \boldsymbol{u}^{k+\frac{1}{2}} \in \mathbb{R}^{2n}, \boldsymbol{\lambda}_n^{k+1} \in \mathbb{R}^m, \boldsymbol{\lambda}_t^{k+\frac{1}{2}} \in \mathbb{R}^m \text{ such that} \\ \hat{\mathsf{K}}\boldsymbol{u}^{k+\frac{1}{2}} = \hat{\boldsymbol{L}}^{k+\frac{1}{2}} + \mathsf{B}_n^\top \boldsymbol{\lambda}_n^{k+1} + \mathsf{B}_t^\top \boldsymbol{\lambda}_t^{k+\frac{1}{2}}, \\ -\boldsymbol{\lambda}_n^{k+1} \in N_{\mathbb{R}^m_-}\big(\mathsf{B}_n\big(2\boldsymbol{u}^{k+\frac{1}{2}} - \boldsymbol{u}^k\big)\big), \\ -\boldsymbol{\lambda}_t^{k+\frac{1}{2}} \in \partial_2 j(\boldsymbol{\lambda}_n^{k+\frac{1}{2}}, \alpha \mathsf{B}_t \boldsymbol{u}^{k+\frac{1}{2}} - \boldsymbol{C}_t), \\ \boldsymbol{u}^0 = \boldsymbol{U}_0, \boldsymbol{v}^0 = \dot{\boldsymbol{U}}_0, \\ \text{and set} \\ \boldsymbol{u}^{k+1} = \boldsymbol{u}^k + \Delta t \boldsymbol{v}^{k+\frac{1}{2}}, \text{ where } \boldsymbol{v}^{k+\frac{1}{2}} = \frac{2}{\Delta t}\boldsymbol{u}^{k+\frac{1}{2}} - \frac{2}{\Delta t}\boldsymbol{u}^k, \\ \boldsymbol{v}^{k+1} = \boldsymbol{v}^k + \Delta t \boldsymbol{a}^{k+\frac{1}{2}} + \Delta t \boldsymbol{a}_n^{k+1}, \text{ where } \boldsymbol{a}^{k+\frac{1}{2}} = \frac{4}{\Delta t^2}\boldsymbol{u}^{k+\frac{1}{2}} - \frac{4}{\Delta t^2}\boldsymbol{u}^k - \frac{2}{\Delta t}\boldsymbol{v}^k - \boldsymbol{a}_n^{k+1}. \end{cases} \tag{2.28}$$

with the same notation as in the previous section. The explicit form of the non-penetration conditions is:

$$\begin{cases} \big(\mathsf{B}_n \boldsymbol{u}^{k+\frac{1}{2}} - \frac{1}{2}\mathsf{B}_n \boldsymbol{u}^k\big)_i &\leq 0, \\ \big(\boldsymbol{\lambda}_n^{k+1}\big)_i &\leq 0, \\ \big(\boldsymbol{\lambda}_n^{k+1}\big)_i \big(\mathsf{B}_n \boldsymbol{u}^{k+\frac{1}{2}} - \frac{1}{2}\mathsf{B}_n \boldsymbol{u}^k\big)_i &= 0 \quad \forall i = 1, 2, \ldots, m. \end{cases} \tag{2.29}$$

The advantage of this modification is easily seen from the next proposition.

Proposition 2.3. Let $\boldsymbol{L}(t) \equiv \boldsymbol{L}$ be constant in t. Then the energy variation of the scheme (2.28) is given by

$$\Delta J = \Delta t\big(\boldsymbol{v}_n^{k+\frac{1}{2}}\big)^\top \boldsymbol{\lambda}_n^{k+1} + \Delta t\big(\boldsymbol{v}_t^{k+\frac{1}{2}}\big)^\top \boldsymbol{\lambda}_t^{k+\frac{1}{2}} \leq -\big(\boldsymbol{u}_n^k\big)^\top \boldsymbol{\lambda}_n^{k+1} \leq 0. \tag{2.30}$$

Proof. For the proof see [13]. □

We see that with the modified contact conditions the mid-point method is stable and dissipative.

2.3 Solution of static contact problems with Coulomb friction

In Section 2.2 we presented the time discretization methods for dynamic contact problems with Coulomb friction and arrived at a sequence of static problems. In this section we will briefly discuss how to realize these problems. The method we use is described e.g. in [12]. For the detailed theoretical analysis of static contact problems with Coulomb's law of friction we refer to [11].

2.3.1 Fixed point formulation of frictional contact problems

We will search for the solution of static problems represented by the systems (2.14), (2.22) or (2.28) using the *fixed point formulation*. Then in each time step we will use the method of successive approximations to find fixed points of an appropriate mapping. For simplicity of this presentation we will restrict ourselves to the problem (2.14) arising from the Newmark scheme and we will omit the temporal indexes k. Again we suppose that $\mathcal{F}$ is constant on Γ_c.

Replacing the unknown normal contact stress $\boldsymbol{\lambda}_n$ in the friction condition by a-priori known slip stress $\hat{\boldsymbol{g}} \in \mathbb{R}^m_-$, we arrive at the formulation of the contact problem with Tresca friction:

$$\begin{cases} \text{Find } \boldsymbol{u} \in \mathbb{R}^{2n}, \boldsymbol{\lambda}_n \in \mathbb{R}^m, \boldsymbol{\lambda}_t \in \mathbb{R}^m \text{ such that} \\ \hat{\mathsf{K}}\boldsymbol{u} = \hat{\boldsymbol{L}} + \mathsf{B}_n^\top \boldsymbol{\lambda}_n + \mathsf{B}_t^\top \boldsymbol{\lambda}_t, \\ -\boldsymbol{\lambda}_n \in N_{\mathbb{R}^m_-}(\mathsf{B}_n \boldsymbol{u}), \\ -\boldsymbol{\lambda}_t \in \partial_2 j(\hat{\boldsymbol{g}}, \alpha \mathsf{B}_t \boldsymbol{u} - \boldsymbol{C}_t). \end{cases} \tag{2.31}$$

This problem is much simpler since the unilateral and friction conditions are now decoupled.

Let us define the mapping $\boldsymbol{\Psi}\colon \mathbb{R}^m_- \mapsto \mathbb{R}^m_-$ by

$$\boldsymbol{\Psi}(\hat{\boldsymbol{g}}) = \boldsymbol{\lambda}_n, \quad \hat{\boldsymbol{g}} \in \mathbb{R}^m_-,$$

where $(\boldsymbol{u}, \boldsymbol{\lambda}_n, \boldsymbol{\lambda}_t)$ is the solution of (2.31). From this it is obvious that $(\boldsymbol{u}, \boldsymbol{\lambda}_n, \boldsymbol{\lambda}_t)$ is the solution of the contact problem with Coulomb's law of friction, iff $\boldsymbol{\lambda}_n$ is the fixed point of $\boldsymbol{\Psi}$ in $\mathbb{R}^m_-$, i.e. $\boldsymbol{\Psi}(\boldsymbol{\lambda}_n) = \boldsymbol{\lambda}_n$. It has been shown (see [11]) that $\boldsymbol{\Psi}$ has at least one fixed point for any friction coefficient $\mathcal{F}$.

Algorithm 2.1 Method of successive approximations

Choose $\boldsymbol{\lambda}_n^{(0)} \in \mathbb{R}^m_-$.
while stopping criterion is not satisfied **do**
  Solve (2.31) with $\hat{\boldsymbol{g}} := \boldsymbol{\lambda}_n^{(k)}$.
  $k := k + 1$
end while
return $(\boldsymbol{u} = \boldsymbol{u}^{(k-1)}, \boldsymbol{\lambda}_n = \boldsymbol{\lambda}_n^{(k-1)}, \boldsymbol{\lambda}_t = \boldsymbol{\lambda}_t^{(k-1)})$.

2.3.2 Approximation of contact problems with given (Tresca) friction

For numerical realization of static contact problems with given friction arising from Algorithm 2.1 we use the duality approach. For this purpose let us define the sets:

$$\boldsymbol{\Lambda}_n := \mathbb{R}^m_-,$$

and

$$\boldsymbol{\Lambda}_t(\hat{\boldsymbol{g}}) := \{\boldsymbol{\mu} \in \mathbb{R}^m \mid |(\boldsymbol{\mu})_i| \leq -\mathcal{F}\,(\hat{\boldsymbol{g}})_i\,, i = 1, 2, \ldots, m\}\,.$$

From Section 1.4 (see (1.24) and (1.25)) we know that the variational inclusions in (2.31) are equivalent to:

$$-\mathsf{B}_n\boldsymbol{u} \in N_{\boldsymbol{\Lambda}_n}(\boldsymbol{\lambda}_n),$$

and

$$-\alpha\mathsf{B}_t\boldsymbol{u} + \boldsymbol{C}_t \in N_{\boldsymbol{\Lambda}_t(\hat{\boldsymbol{g}})}(\boldsymbol{\lambda}_t).$$

Using the definition of the normal cone, the problem (2.31) becomes:

$$\begin{cases} \text{Find } \boldsymbol{u} \in \mathbb{R}^{2n}, \boldsymbol{\lambda}_n \in \boldsymbol{\Lambda}_n, \boldsymbol{\lambda}_t \in \boldsymbol{\Lambda}_t(\hat{\boldsymbol{g}}) \text{ such that} \\ \hat{\mathsf{K}}\boldsymbol{u} = \hat{\boldsymbol{L}} + \mathsf{B}_n^\top\boldsymbol{\lambda}_n + \mathsf{B}_t^\top\boldsymbol{\lambda}_t, \\ (\boldsymbol{w}_n - \boldsymbol{\lambda}_n)^\top\mathsf{B}_n\boldsymbol{u} \geq 0 \quad \forall \boldsymbol{w}_n \in \boldsymbol{\Lambda}_n, \\ (\boldsymbol{w}_t - \boldsymbol{\lambda}_t)^\top\alpha\mathsf{B}_t\boldsymbol{u} \geq (\boldsymbol{w}_t - \boldsymbol{\lambda}_t)^\top\boldsymbol{C}_t \quad \forall \boldsymbol{w}_t \in \boldsymbol{\Lambda}_t(\hat{\boldsymbol{g}}), \end{cases} \tag{2.32}$$

or equivalently:

$$\begin{cases} \text{Find } \boldsymbol{u} \in \mathbb{R}^{2n}, \boldsymbol{\lambda}_n \in \boldsymbol{\Lambda}_n, \boldsymbol{\lambda}_t \in \boldsymbol{\Lambda}_t(\hat{\boldsymbol{g}}) \text{ such that} \\ \hat{\mathsf{K}}\boldsymbol{u} = \hat{\boldsymbol{L}} + \mathsf{B}_n^\top\boldsymbol{\lambda}_n + \mathsf{B}_t^\top\boldsymbol{\lambda}_t, \\ (\boldsymbol{w}_n - \boldsymbol{\lambda}_n)^\top\mathsf{B}_n\boldsymbol{u} + \alpha(\boldsymbol{w}_t - \boldsymbol{\lambda}_t)^\top\mathsf{B}_t\boldsymbol{u} \geq (\boldsymbol{w}_t - \boldsymbol{\lambda}_t)^\top\boldsymbol{C}_t \quad \forall \boldsymbol{w}_t \in \boldsymbol{\Lambda}_t(\hat{\boldsymbol{g}})\, \forall \boldsymbol{w}_n \in \boldsymbol{\Lambda}_n. \end{cases} \tag{2.33}$$

In what follows we shall derive the so-called *reciprocal variational formulation* in which the displacement $\boldsymbol{u}$ is eliminated and the problem is expressed only in terms of the contact stresses $\boldsymbol{\lambda}_t$ and $\boldsymbol{\lambda}_n$. This technique significantly reduces the number of unknowns, however it leads to the need of evaluating the inverse of $\hat{\mathsf{K}}$ as will be seen from the following.

From $(2.33)_1$ we get

$$\boldsymbol{u} = \hat{\mathsf{K}}^{-1}(\hat{\boldsymbol{L}} + \mathsf{B}_n^\top\boldsymbol{\lambda}_n + \mathsf{B}_t^\top\boldsymbol{\lambda}_t),$$

and substituting this expression into $(2.33)_2$ the inequality becomes:

$$\begin{aligned}(\mathsf{B}_n\hat{\mathsf{K}}^{-1}\mathsf{B}_n^\top\boldsymbol{\lambda}_n)^\top(\boldsymbol{w}_n-\boldsymbol{\lambda}_n)+(\mathsf{B}_n\hat{\mathsf{K}}^{-1}\mathsf{B}_t^\top\boldsymbol{\lambda}_t)^\top(\boldsymbol{w}_n-\boldsymbol{\lambda}_n)\\ +(\mathsf{B}_t\hat{\mathsf{K}}^{-1}\mathsf{B}_n^\top\boldsymbol{\lambda}_n)^\top(\boldsymbol{w}_t-\boldsymbol{\lambda}_t)+(\mathsf{B}_t\hat{\mathsf{K}}^{-1}\mathsf{B}_t^\top\boldsymbol{\lambda}_t)^\top(\boldsymbol{w}_t-\boldsymbol{\lambda}_t)\\ \geq -(\mathsf{B}_n\hat{\mathsf{K}}^{-1}\hat{\boldsymbol{L}})^\top(\boldsymbol{w}_n-\boldsymbol{\lambda}_n)-(\mathsf{B}_t\hat{\mathsf{K}}^{-1}\hat{\boldsymbol{L}}-\frac{1}{\alpha}\boldsymbol{C}_t)^\top(\boldsymbol{w}_t-\boldsymbol{\lambda}_t)\\ \forall\boldsymbol{w}_n\in\boldsymbol{\Lambda}_n\,\forall\boldsymbol{w}_t\in\boldsymbol{\Lambda}_t(\hat{\boldsymbol{g}}).\end{aligned}$$

Denoting

$$\mathsf{A}:=\begin{bmatrix}\mathsf{B}_n\hat{\mathsf{K}}^{-1}\mathsf{B}_n^\top & \mathsf{B}_n\hat{\mathsf{K}}^{-1}\mathsf{B}_t^\top\\ \mathsf{B}_t\hat{\mathsf{K}}^{-1}\mathsf{B}_n^\top & \mathsf{B}_t\hat{\mathsf{K}}^{-1}\mathsf{B}_t^\top\end{bmatrix},\qquad \boldsymbol{F}(\hat{\boldsymbol{L}}):=\begin{bmatrix}-\mathsf{B}_n\hat{\mathsf{K}}^{-1}\hat{\boldsymbol{L}}\\ \frac{1}{\alpha}\boldsymbol{C}_t-\mathsf{B}_t\hat{\mathsf{K}}^{-1}\hat{\boldsymbol{L}}\end{bmatrix},\tag{2.34}$$

and $\boldsymbol{\lambda}:=\left(\boldsymbol{\lambda}_n^\top,\boldsymbol{\lambda}_t^\top\right)^\top$, the problem (2.33) may be written as

$$\begin{cases}\text{Find }\boldsymbol{\lambda}\in\boldsymbol{\Lambda}_n\times\boldsymbol{\Lambda}_t(\hat{\boldsymbol{g}})\text{ such that}\\ \boldsymbol{\lambda}^\top\mathsf{A}(\boldsymbol{\mu}-\boldsymbol{\lambda})\geq\boldsymbol{F}(\hat{\boldsymbol{L}})(\boldsymbol{\mu}-\boldsymbol{\lambda})\quad\forall\boldsymbol{\mu}:=\left(\boldsymbol{\mu}_n^\top,\boldsymbol{\mu}_t^\top\right)^\top\in\boldsymbol{\Lambda}_n\times\boldsymbol{\Lambda}_t(\hat{\boldsymbol{g}}).\end{cases}\tag{2.35}$$

Note that A is $(2m\times 2m)$ matrix and $\boldsymbol{F}(\hat{\boldsymbol{L}})\in\mathbb{R}^{2m}$. It is well-known that (2.35) is equivalent to the following constrained minimization problem:

$$\begin{cases}\text{Find }\boldsymbol{\lambda}\in\boldsymbol{\Lambda}_n\times\boldsymbol{\Lambda}_t(\hat{\boldsymbol{g}})\text{ such that}\\ \mathcal{J}(\boldsymbol{\lambda})=\min\limits_{\boldsymbol{\mu}\in\boldsymbol{\Lambda}_n\times\boldsymbol{\Lambda}_t(\hat{\boldsymbol{g}})}\mathcal{J}(\boldsymbol{\mu}),\end{cases}\tag{2.36}$$

where $\boldsymbol{\mu}:=\left(\boldsymbol{\mu}_n^\top,\boldsymbol{\mu}_t^\top\right)^\top$ and

$$\mathcal{J}(\boldsymbol{\mu}):=\frac{1}{2}\boldsymbol{\mu}^\top\mathsf{A}\boldsymbol{\mu}-\boldsymbol{\mu}^\top\boldsymbol{F}(\hat{\boldsymbol{L}}).$$

Proposition 2.4. Let $\hat{\mathsf{K}}$ be symmetric and positive definite. Then the matrix A defined in (2.34) is symmetric and positive definite, too.

Proof. If the matrix $\hat{\mathsf{K}}$ is symmetric and positive definite, then its inverse $\hat{\mathsf{K}}^{-1}$ must be symmetric, positive definite, as well. The proof of the symmetry of A is straightforward. Indeed, for the first diagonal block we have

$$\left(\mathsf{B}_n\hat{\mathsf{K}}^{-1}\mathsf{B}_n^\top\right)^\top=\mathsf{B}_n\left(\hat{\mathsf{K}}^{-1}\right)^\top\mathsf{B}_n^\top=\mathsf{B}_n\hat{\mathsf{K}}^{-1}\mathsf{B}_n^\top.$$

Similarly one can prove the symmetry of the second diagonal block. For the non-diagonal blocks it holds:

$$\left(\mathsf{B}_n\hat{\mathsf{K}}^{-1}\mathsf{B}_t^\top\right)^\top=\mathsf{B}_t\left(\hat{\mathsf{K}}^{-1}\right)^\top\mathsf{B}_n^\top=\mathsf{B}_t\hat{\mathsf{K}}^{-1}\mathsf{B}_n^\top.$$

Thus the matrix A is symmetric. The positive definiteness of A follows from the relations:

$$\begin{aligned}\boldsymbol{x}^\top \mathsf{A}\boldsymbol{x} &= \begin{bmatrix}\boldsymbol{x}_1^\top & \boldsymbol{x}_2^\top\end{bmatrix}\begin{bmatrix}\mathsf{B}_n\hat{\mathsf{K}}^{-1}\mathsf{B}_n^\top & \mathsf{B}_n\hat{\mathsf{K}}^{-1}\mathsf{B}_t^\top \\ \mathsf{B}_t\hat{\mathsf{K}}^{-1}\mathsf{B}_n^\top & \mathsf{B}_t\hat{\mathsf{K}}^{-1}\mathsf{B}_t^\top\end{bmatrix}\begin{bmatrix}\boldsymbol{x}_1 \\ \boldsymbol{x}_2\end{bmatrix} \\ &= \boldsymbol{x}_1^\top\mathsf{B}_n\hat{\mathsf{K}}^{-1}\mathsf{B}_n^\top\boldsymbol{x}_1 + 2\boldsymbol{x}_1^\top\mathsf{B}_n\hat{\mathsf{K}}^{-1}\mathsf{B}_t^\top\boldsymbol{x}_2 + \boldsymbol{x}_2^\top\mathsf{B}_t\hat{\mathsf{K}}^{-1}\mathsf{B}_t^\top\boldsymbol{x}_2 \\ &= \left(\mathsf{B}_n^\top\boldsymbol{x}_1 + \mathsf{B}_t^\top\boldsymbol{x}_2\right)^\top\hat{\mathsf{K}}^{-1}\left(\mathsf{B}_n^\top\boldsymbol{x}_1 + \mathsf{B}_t^\top\boldsymbol{x}_2\right) > 0 \quad \forall\boldsymbol{x}\in\mathbb{R}^{2m}, \boldsymbol{x}\neq\mathbf{0}.\end{aligned}$$

□

The matrix $\hat{\mathsf{K}}$ defined in Section 2.2.2 is apparently symmetric and positive definite. The importance of the previous proposition consists in the fact that it enables us to use the *conjugate gradient* based algorithm *MPRGP* (Modified Proportioning with Reduced Gradient Projections) for the solution of (2.36).

2.3.3 Modified Proportioning with Reduced Gradient Projections

Algorithm MPRGP (see Algorithm 2.2) is used for minimizing the quadratic functional with box constraints:

$$\min_{\boldsymbol{x}\in\Omega_B} f(\boldsymbol{x}),$$

where $\Omega_B := \{\boldsymbol{x}\in\mathbb{R}^n \,|\, \boldsymbol{\ell}\leq\boldsymbol{x}\leq\boldsymbol{q}\}$, $f(x) := \frac{1}{2}\boldsymbol{x}^\top\mathsf{A}\boldsymbol{x} - \boldsymbol{x}^\top\boldsymbol{b}$ with A being symmetric, positive definite and $\boldsymbol{\ell},\boldsymbol{q}\in\mathbb{R}^n, \boldsymbol{\ell}\leq\boldsymbol{q}$ given. The algorithm combines the method of conjugate gradients together with the method of gradient projections.

To clarify notation used in Algorithm 2.2 presented below let $\mathcal{N} := \{1,2,\ldots,n\}$ be the set of all indices of the vectors $\boldsymbol{x},\boldsymbol{q},\boldsymbol{\ell}$ etc. We can divide this set into two disjoint subsets:

$$\mathcal{A}(\boldsymbol{x}) := \{i\in\mathcal{N} \,|\, x_i = \ell_i \vee x_i = u_i\},$$

$$\mathcal{F}(\boldsymbol{x}) := \{i\in\mathcal{N} \,|\, x_i \neq \ell_i \wedge x_i \neq u_i\},$$

termed the *active* and the *free set*, respectively. Using them, one can split the *gradient* $\boldsymbol{g} := \mathsf{A}\boldsymbol{x} - \boldsymbol{b}$ into two parts:

$$\varphi_i(\boldsymbol{x}) := g_i(\boldsymbol{x}) \text{ for } i\in\mathcal{F}(\boldsymbol{x}), \quad \varphi_i(\boldsymbol{x}) := 0 \text{ for } i\in\mathcal{A}(\boldsymbol{x}),$$

$$\beta(\boldsymbol{x}) := 0 \text{ for } i\in\mathcal{F}(\boldsymbol{x}), \quad \beta_i(\boldsymbol{x}) := g_i^{\pm}(\boldsymbol{x}) \text{ for } i\in\mathcal{A}(\boldsymbol{x}),$$

where $g_i^{\pm} := \min\{g_i, 0\}$ if $x_i = l_i$, or $g_i^{\pm} := \max\{g_i, 0\}$ if $x_i = u_i$. The *projected gradient* is defined as:

$$\boldsymbol{g}^P(\boldsymbol{x}) := \boldsymbol{\varphi}(\boldsymbol{x}) + \boldsymbol{\beta}(\boldsymbol{x}).$$

Finally, we define the projection of a vector $\boldsymbol{x}\in\mathbb{R}^n$ on Ω_B by

$$\left(P_{\Omega_B}(\boldsymbol{x})\right)_i := \max\{l_i, \min\{q_i, x_i\}\} \quad \forall i\in\mathcal{N}.$$

The main advantage of the presented algorithm is the fact that it finds a solution with an *R-linear rate of convergence*[7] and the bound on the speed of convergence depends only on the spectral number $\kappa(\mathsf{A}) := \frac{\lambda_{\max}(\mathsf{A})}{\lambda_{\min}(\mathsf{A})}$. However the detailed analysis of the algorithm exceeds the range of this text, thus we refer reader to [6].

[7]We say that a sequence (a_k) converges *Q-linearly* to a iff there exists $\eta \in (0,1)$ and $k_0 \in \mathbb{N}$ such that:

$$\frac{|a_{k+1} - a|}{|a_k - a|} \leq \eta \quad \forall k \geq k_0.$$

A sequence (x_k) converges *R-linearly* to x iff

$$|x_k - x| \leq \mu_k \quad \forall k \geq k_0,$$

where (μ_k) is a sequence of nonnegative scalars converging Q-linearly to zero.

Algorithm 2.2 Modified Proportioning with Reduced Gradient Projection

Require: Symmetric positive definite matrix $\mathsf{A} \in \mathbb{R}^{n\times n}$, vectors $\boldsymbol{b}, \boldsymbol{\ell}, \boldsymbol{q} \in \mathbb{R}^n$,
$\Omega_B := \{\boldsymbol{x} \in \mathbb{R}^n \,|\, \boldsymbol{\ell} \le \boldsymbol{x} \le \boldsymbol{q}\}$.
{Initialization}
Choose $\Gamma > 0, \overline{\alpha} \in \left(0, 2\|\mathsf{A}\|^{-1}\right\rangle$, set $k := 0$, $\boldsymbol{g} := \mathsf{A}\boldsymbol{x}^0 - \boldsymbol{b}, \boldsymbol{p} := \varphi(\boldsymbol{x}^{\boldsymbol{0}})$.
while $\|\boldsymbol{g}^P(\boldsymbol{x}^k)\|$ not small enough **do**
  if $\|\beta(\boldsymbol{x}^k)\|^2 \le \Gamma^2 \widetilde{\varphi}(\boldsymbol{x}^k)^T \varphi(\boldsymbol{x}^k)$ **then**
    {$\boldsymbol{x}^k$ proportional, conjugate gradients testing step.}
    $\alpha_{cg} := \boldsymbol{g}^T\boldsymbol{p}/\boldsymbol{p}^T\mathsf{A}\boldsymbol{p}, \boldsymbol{y} := \boldsymbol{x}^k - \alpha_{cg}\boldsymbol{p}$
    $\alpha_f := \max\left\{\alpha \,|\, \boldsymbol{x}^k - \alpha\boldsymbol{p} \in \Omega_B\right\}$
    if $\alpha_{cg} \ge \alpha_f$ **then**
      {Conjugate gradients step.}
      $\boldsymbol{x}^{k+1} := \boldsymbol{y}, \boldsymbol{g} := \boldsymbol{g} - \alpha_{cg}\mathsf{A}\boldsymbol{p}$
      $\beta := \varphi(\boldsymbol{y})^T\mathsf{A}\boldsymbol{p}/\boldsymbol{p}^T\mathsf{A}\boldsymbol{p}, \boldsymbol{p} := \varphi(\boldsymbol{y}) - \beta\boldsymbol{p}$
    else
      {Active set expansion step}
      $\boldsymbol{x}_1 := \boldsymbol{x}^k - \alpha_f\boldsymbol{p}, \boldsymbol{x}_2 := P_{\Omega_B}(\boldsymbol{x}^k - \alpha_{cg}\boldsymbol{p})$
      if $f(\boldsymbol{x}_1) \le f(\boldsymbol{x}_2)$ **then**
        $\boldsymbol{x}^{k+\frac{1}{2}} := \boldsymbol{x}_1, \boldsymbol{g} := \boldsymbol{g} - \alpha_f\mathsf{A}\boldsymbol{p}$
      else
        $\boldsymbol{x}^{k+\frac{1}{2}} := \boldsymbol{x}_2, \boldsymbol{g} := \mathsf{A}\boldsymbol{x}^{k+\frac{1}{2}} - \boldsymbol{b}$
      end if
      $\boldsymbol{x}^{k+1} := P_{\Omega_B}(\boldsymbol{x}^{k+\frac{1}{2}} - \bar{\alpha}\varphi(\boldsymbol{x}^{k+\frac{1}{2}}))$
    end if
  else
    {Proportioning step}
    $\boldsymbol{d} := \beta(\boldsymbol{x}^k), \alpha_{cg} := \boldsymbol{g}^T\boldsymbol{d}/\boldsymbol{d}^T\mathsf{A}\boldsymbol{d}$
    $\alpha_f := \max\left\{\alpha \,|\, \boldsymbol{x}^k - \alpha\boldsymbol{d} \in \Omega_b\right\}$
    $\alpha_p := \min\left\{\alpha_f, \alpha_{cg}\right\}$
    $\boldsymbol{x}^{k+1} := \boldsymbol{x}^k - \alpha_{cg}\boldsymbol{d}, \boldsymbol{g} := \boldsymbol{g} - \alpha_{cg}\mathsf{A}\boldsymbol{d}, \boldsymbol{p} = \varphi(\boldsymbol{x}^{k+1})$
  end if
  $k := k + 1$
end while
return $\widetilde{x} = x^k$

3 Mass redistribution method

Here we restrict ourselves to frictionless contact problems. As mentioned in the previous section, the classical time discretization schemes usually fail in the case of contact problems. The reason is that in the standard mass matrix, the contact nodes have their own mass and therefore also the inertia and the kinetic energy. However when a contact occurs and a node is stopped, all its kinetic energy vanishes. On the other hand time discretization algorithm tries to preserve the energy, causing the artificial oscillations, even energy blow-ups. In addition, because of the contact mass the spatially semi-discrete formulation of the problem (2.10) is ill-posed and possesses multiple solutions, as was shown in [14].

The mass redistribution method proposed by Khenous et al. [13, 14] modifies the mass matrix in such a way that the contact nodes are weightless, while it preserves the total mass, the center of gravity and the moment of inertia of the body. Such discretization corresponds better to the continuous setting in which the contact boundary has zero mass.

3.1 Computing the new mass matrix

Recall that $\boldsymbol{N}_i, i \in \mathcal{I}_c$, are the normal vectors defined in Section 2.1.3 and denote $\mathcal{N} := \operatorname{span}\{\boldsymbol{N}_i\}_{i\in\mathcal{I}_c} \subset \mathbb{R}^{2n}$. The elimination of the mass of the contact nodes can be expressed by the following condition on the redistributed matrix M_r:

$$\ker \mathsf{M}_r = \mathcal{N}.$$

For simplicity let us assume that all the vectors $\boldsymbol{N}_i$ have only one non-zero entry (i.e. the normal vectors to Γ_c are parallel to the x or y axes). Reordering the unknowns in the displacement vector $\boldsymbol{U}(t)$ in such a way that the ones corresponding to the normal displacement of the contact nodes are listed last we can write the matrix M_r as:

$$\mathsf{M}_r = \begin{bmatrix} \bar{\mathsf{M}} & 0 \\ 0 & 0 \end{bmatrix},$$

where $\bar{\mathsf{M}}$ is the matrix of the order $2n - m$ (recall that $m = \operatorname{card}\mathcal{I}_c$).

To preserve the mechanical properties of the modeled system, the matrix M_r must have the same mass, center of gravity and moments of inertia as the original mass matrix which will be now denoted by M_0. Denoting the vector $\boldsymbol{X} := (1, \ldots, 1)^\top \in \mathbb{R}^{2n}$ one can approximate the total mass of the body Ω by:

$$m := \int_\Omega \varrho \, \mathrm{d}\boldsymbol{x} \approx \frac{1}{2}\boldsymbol{X}^\top \mathsf{M}_0 \boldsymbol{X} =: \tilde{m}.$$

Let $\boldsymbol{Y}_1 \in \mathbb{R}^{2n}$ be the vector whose the $(2i-1)$ components are equal to $(\boldsymbol{x}_i)_1$, where $\boldsymbol{x}_i, i = 1, \cdots, n$ are the nodes of $\mathcal{T}^h$, while all even components are equal to zero, i.e. $\boldsymbol{Y}_1 = ((\boldsymbol{x}_p \cdot \boldsymbol{e}_1)\boldsymbol{e}_1)_{p\in\mathcal{P}^h}$. Similarly, let $\boldsymbol{Y}_2 = ((\boldsymbol{x}_p \cdot \boldsymbol{e}_2)\boldsymbol{e}_2)_{p\in\mathcal{P}^h}$. Here $\boldsymbol{e}_1$ and $\boldsymbol{e}_2$ are the

vectors of the standard canonical basis of $\mathbb{R}^2$. Then the coordinates of the center of gravity of Ω may be approximated by:

$$\frac{1}{m}\int_\Omega \varrho x_k \,\mathrm{d}\boldsymbol{x} \approx \frac{1}{\tilde{m}}\boldsymbol{X}^\top \mathsf{M}_0 \boldsymbol{Y}_k, \quad k = 1, 2.$$

Finally, we get the approximations of the moments of inertia from the relations

$$\int_\Omega \varrho x_k x_l \,\mathrm{d}\boldsymbol{x} \approx \frac{1}{2}\boldsymbol{Y}_k \mathsf{M}_0 \boldsymbol{Y}_l, \quad k, l = 1, 2.$$

Therefore the new mass matrix M_r must satisfy the following conditions:

$$\begin{cases} \boldsymbol{X}^\top(\mathsf{M}_r - \mathsf{M}_0)\boldsymbol{X} &= 0, \\ \boldsymbol{X}^\top(\mathsf{M}_r - \mathsf{M}_0)\boldsymbol{Y}_k &= 0, \quad k = 1, 2, \\ \boldsymbol{Y}_k^\top(\mathsf{M}_r - \mathsf{M}_0)\boldsymbol{Y}_l &= 0, \quad k, l = 1, 2. \end{cases} \tag{3.1}$$

The new matrix should also preserve the symmetry ($\mathsf{M}_r = \mathsf{M}_r^\top$). Let $\mathcal{N}^\perp$ denote the orthogonal complement of $\mathcal{N}$ in $\mathbb{R}^{2n}$. Then M_r must satisfy:

$$\boldsymbol{v}^\top \mathsf{M}_r \boldsymbol{v} > 0 \quad \forall \boldsymbol{v} \in \mathcal{N}^\perp,$$

i.e. it should be positive definite in $\mathcal{N}^\perp$. However due to the computational complexity, this condition will not be explicitly enforced in what follows.

As proposed in [13, 14], it is possible to find the redistributed mass matrix M_r by minimizing the distance between M_r and the standard mass matrix M_0 with respect to the Frobenius norm $\|\cdot\|_F$ and subject to the constraints (3.1). This problem can be solved by the augmented Lagrangian method (see Algorithm 3.1), e.g. Setting

$$\boldsymbol{h}(\mathsf{M}) := \begin{bmatrix} \boldsymbol{X}^\top(\mathsf{M} - \mathsf{M}_0)\boldsymbol{X} \\ \boldsymbol{X}^\top(\mathsf{M} - \mathsf{M}_0)\boldsymbol{Y}_1 \\ \boldsymbol{X}^\top(\mathsf{M} - \mathsf{M}_0)\boldsymbol{Y}_2 \\ \boldsymbol{Y}_1^\top(\mathsf{M} - \mathsf{M}_0)\boldsymbol{Y}_1 \\ \boldsymbol{Y}_1^\top(\mathsf{M} - \mathsf{M}_0)\boldsymbol{Y}_2 \\ \boldsymbol{Y}_2^\top(\mathsf{M} - \mathsf{M}_0)\boldsymbol{Y}_2 \end{bmatrix}$$

one can write the Lagrangian in the form

$$\mathcal{L}(\mathsf{M}, \boldsymbol{\lambda}_r) := \frac{1}{2}\|\mathsf{M} - \mathsf{M}_0\|_F^2 + \boldsymbol{\lambda}_r^\top \boldsymbol{h}(\mathsf{M}),$$

where $\boldsymbol{\lambda}_r \in \mathbb{R}^6$ is the vector of Lagrange multipliers. Computations are simplified by assuming that the position of the non-zero elements in the redistributed matrix is the same as in the original one (except for the contact nodes that are explicitly set to zero).

Due to the symmetry it is sufficient to redistribute only the upper triangular part of the mass matrix. The non-zero elements of the matrix are converted to a vector and the minimization part of Algorithm 3.1 is performed by the steepest descent method. At the end of computations the vector is converted back to the matrix by mapping its elements to their original location. For further implementation details we refer reader to the source code enclosed to this work.

Algorithm 3.1 Augmented Lagrangian method

Choose $\boldsymbol{\lambda}_r^{(0)} \in \mathbb{R}^6, \mathsf{M}^{(0)}, \rho \geq 0$.
while stopping criterion is not satisfied **do**
$\mathsf{M}^{(k+1)} := \arg\min_{\mathsf{M}} \left(\mathcal{L}(\mathsf{M}, \boldsymbol{\lambda}_r^{(k)}) + \frac{\rho}{2} (\boldsymbol{h}(\mathsf{M}))^\top \boldsymbol{h}(\mathsf{M}) \right)$
$\boldsymbol{\lambda}_r^{(k+1)} := \boldsymbol{\lambda}_r^{(k)} + \rho \boldsymbol{h}(\mathsf{M})$
$k := k + 1$
end while
return $\mathsf{M}^{(k-1)}$.

3.2 Stability analysis

The analysis presented in [13] unveils that the described method not only restores the well-posedness of frictionless semi-discrete contact problems, but also guarantees the energy conservation (in the case when the load vector is constant over the whole time interval).

We will now briefly outline the proof of the uniqueness of the solution as presented in [13]. We use notation of Section 3.1. Recall that the normal components of the displacement vector $\boldsymbol{U}(t)$ are listed last. Thus we divide the stiffness matrix K and the matrix B_n into the following block structure:

$$\mathsf{K} = \begin{bmatrix} \bar{\mathsf{K}} & \mathsf{C}^\top \\ \mathsf{C} & \mathsf{K}_c \end{bmatrix}, \quad \mathsf{B}_n^\top = \begin{bmatrix} \mathsf{0} \\ \mathsf{B}_{c_n}^\top \end{bmatrix},$$

where $\bar{\mathsf{K}}$ is the $(2n - m) \times (2n - m)$ block. Further $\mathsf{C} \in \mathbb{R}^{m \times (2n-m)}, \mathsf{K}_c \in \mathbb{R}^{m \times m}$ and $\mathsf{B}_{c_n} \in \mathbb{R}^{m \times m}$.

Since $\mathbb{R}^{2n} = \mathcal{N} \oplus \mathcal{N}^\perp$ one can decompose any displacement vector $\boldsymbol{v} \in \mathbb{R}^{2n}$ into the sum $\boldsymbol{v} = \boldsymbol{v}_* + \boldsymbol{v}_c$, where $\boldsymbol{v}_* \in \mathcal{N}^\perp, \boldsymbol{v}_c \in \mathcal{N}$. The displacement vector may be written as:

$$\boldsymbol{U}(t) = \underbrace{\begin{bmatrix} \boldsymbol{U}_*(t) \\ \mathbf{0} \end{bmatrix}}_{\in \mathcal{N}^\perp} + \underbrace{\begin{bmatrix} \mathbf{0} \\ \boldsymbol{U}_c(t) \end{bmatrix}}_{\in \mathcal{N}} = \begin{bmatrix} \boldsymbol{U}_*(t) \\ \boldsymbol{U}_c(t) \end{bmatrix},$$

with $\boldsymbol{U}_*(t) \in \mathbb{R}^{2n-m}$ and $\boldsymbol{U}_c(t) \in \mathbb{R}^m$. Using this decomposition one can write the semi-discrete frictionless contact problem in the form:

$$\begin{cases} \text{Find } \boldsymbol{U}(t) := \begin{bmatrix} \boldsymbol{U}_*^\top(t) & \boldsymbol{U}_c^\top(t) \end{bmatrix}^\top : \mathbb{T} \mapsto \mathbb{R}^{2n}, \boldsymbol{\lambda}_n(t) \colon \mathbb{T} \mapsto \mathbb{R}^m, \text{ such that } \forall t \in \mathbb{T} \\ \begin{bmatrix} \bar{\mathsf{M}} & \mathsf{0} \\ \mathsf{0} & \mathsf{0} \end{bmatrix} \begin{bmatrix} \ddot{\boldsymbol{U}}_*(t) \\ \ddot{\boldsymbol{U}}_c(t) \end{bmatrix} + \begin{bmatrix} \bar{\mathsf{K}} & \mathsf{C}^\top \\ \mathsf{C} & \mathsf{K}_c \end{bmatrix} \begin{bmatrix} \boldsymbol{U}_*(t) \\ \boldsymbol{U}_c(t) \end{bmatrix} = \begin{bmatrix} \boldsymbol{L}_*(t) \\ \boldsymbol{L}_c(t) \end{bmatrix} + \begin{bmatrix} \mathsf{0} \\ \mathsf{B}_{c_n}^\top \end{bmatrix} \boldsymbol{\lambda}_n(t), \\ -\boldsymbol{\lambda}_n(t) \in N_{\mathbb{R}_-^m}\big(\mathsf{B}_{c_n} \boldsymbol{U}_c(t)\big), \\ \boldsymbol{U}(0) = \boldsymbol{U}_0, \dot{\boldsymbol{U}}(0) = \dot{\boldsymbol{U}}_0, \end{cases}$$

or equivalently

$$\left\{\begin{array}{l} \text{Find } \boldsymbol{U}(t) := \left[\boldsymbol{U}_*^\top(t) \quad \boldsymbol{U}_c^\top(t)\right]^\top : \mathbb{T} \mapsto \mathbb{R}^{2n}, \boldsymbol{\lambda}_n(t) \colon \mathbb{T} \mapsto \mathbb{R}^m, \text{ such that } \forall t \in \mathbb{T} \\ \bar{\mathsf{M}}\ddot{\boldsymbol{U}}_*(t) + \bar{\mathsf{K}}\boldsymbol{U}_*(t) = \boldsymbol{L}_*(t) + \mathsf{C}^\top \boldsymbol{U}_c(t) \\ \mathsf{C}\boldsymbol{U}_*(t) + \mathsf{K}_c\boldsymbol{U}_c(t) = \boldsymbol{L}_c(t) + \mathsf{B}_{c_n}^\top \boldsymbol{\lambda}_n(t) \\ -\boldsymbol{\lambda}_n(t) \in N_{\mathbb{R}^m_-}\left(\mathsf{B}_{c_n}\boldsymbol{U}_c(t)\right), \\ \boldsymbol{U}(0) = \boldsymbol{U}_0, \dot{\boldsymbol{U}}(0) = \dot{\boldsymbol{U}}_0. \end{array}\right. \tag{3.2}$$

This makes it possible to decompose the problem into the subproblems for $\boldsymbol{U}_*(t)$ and $\boldsymbol{U}_c(t)$. The equation $(3.2)_2$ with the constraints $(3.2)_3$ can be written for all $t \in \mathbb{T}$ in the form of the elliptic variational inequality in which time t plays the role of a parameter:

$$\text{Find } \boldsymbol{U}_c(t) \in K_c(t): \quad a(\boldsymbol{U}_c(t), \boldsymbol{V}_c(t) - \boldsymbol{U}_c(t)) \geq l_{\boldsymbol{U}_*(t)}(\boldsymbol{V}_c(t) - \boldsymbol{U}_c(t)) \quad \forall \boldsymbol{V}_c(t) \in K_c(t),$$

where

$$K_c(t) := \left\{\boldsymbol{V}_c(t) \in \mathbb{R}^m \mid \boldsymbol{N}_{c_i}^\top \boldsymbol{V}_c(t) \leq 0 \, \forall i \in \mathcal{I}_c\right\},$$

with $a(\boldsymbol{U}, \boldsymbol{V}) := \boldsymbol{V}^\top \mathsf{K}_c \boldsymbol{U}$, $l_{\boldsymbol{U}_*(t)}(\boldsymbol{V}) := \boldsymbol{V}^\top \boldsymbol{L}_c(t) - \boldsymbol{V}^\top \mathsf{C}\boldsymbol{U}_*(t)$ and $\boldsymbol{N}_{c_i}$ are the rows of the matrix B_{c_n}. For given $\boldsymbol{U}_*(t)$ this inequality has a unique solution $\boldsymbol{U}_c(t)$. Moreover, the function $t \mapsto \boldsymbol{U}_c(t)$ is Lipschitz continuous in $\mathbb{T}$ therefore the second order ordinary differential equation $(3.2)_1$ with the Lipschitz right-hand side has a unique solution. Then the semi-discrete frictionless contact problem has a unique solution. Assuming that $\boldsymbol{L}_c(t)$ is Lipschitz continuous then $\boldsymbol{\lambda}_n(t)$ is Lipschitz continuous too.

The following two theorems hold for the solution of the system (3.2).

Theorem 3.1. The solution $(\boldsymbol{U}(t), \boldsymbol{\lambda}_n(t))$ of (3.2) satisfies the so-called *persistency condition*:

$$(\boldsymbol{\lambda}_n)_i(\boldsymbol{N}_{c_i}^\top \dot{\boldsymbol{U}}(t)) = 0 \quad \forall i \in \mathcal{I}_c \forall t \in \mathbb{T}.$$

Proof. See [13]. □

Theorem 3.2. Let $\boldsymbol{L}(t) \equiv \boldsymbol{L}$ be constant in $\mathbb{T}$. Then the solution of the system (3.2) is energy conserving, i.e.

$$J(\boldsymbol{U}(t), \dot{\boldsymbol{U}}(t)) = J(\boldsymbol{U}(0), \dot{\boldsymbol{U}}(0)) \quad \forall t \in \mathbb{T}.$$

Proof. We multiply the equilibrium equation

$$\mathsf{M}_r \ddot{\boldsymbol{U}}(s) + \mathsf{K}\boldsymbol{U}(s) = \boldsymbol{L} + \mathsf{B}_n^\top \boldsymbol{\lambda}_n(s) \quad \forall s \in \mathbb{T}$$

by $\dot{\boldsymbol{U}}(s)$ and integrate from 0 to t:

$$\int_0^t \dot{\boldsymbol{U}}^\top(s) \mathsf{M}_r \ddot{\boldsymbol{U}}(s) \, \mathrm{d}s + \int_0^t \dot{\boldsymbol{U}}^\top(s) \mathsf{K}\boldsymbol{U}(s) \, \mathrm{d}s = \int_0^t \dot{\boldsymbol{U}}^\top(s)(\boldsymbol{L}(s) + \mathsf{B}_n^\top \boldsymbol{\lambda}_n(s)) \, \mathrm{d}s. \tag{3.3}$$

Then the left-hand side of (3.3) can be written as

$$\frac{1}{2}\int_0^t \frac{\mathrm{d}}{\mathrm{d}s}(\dot{\boldsymbol{U}}^\top(s)\mathsf{M}_r\dot{\boldsymbol{U}}(s))\,\mathrm{d}s + \frac{1}{2}\int_0^t \frac{\mathrm{d}}{\mathrm{d}s}(\boldsymbol{U}^\top(s)\mathsf{K}\boldsymbol{U}(s))\,\mathrm{d}s.$$

We have:

$$\frac{1}{2}\dot{\boldsymbol{U}}^\top(t)\mathsf{M}_r\dot{\boldsymbol{U}}(t) - \frac{1}{2}\dot{\boldsymbol{U}}^\top(0)\mathsf{M}_r\dot{\boldsymbol{U}}(0) + \frac{1}{2}\boldsymbol{U}^\top(t)\mathsf{K}\boldsymbol{U}(t) - \frac{1}{2}\boldsymbol{U}^\top(0)\mathsf{K}\boldsymbol{U}(0) = \int_0^t \dot{\boldsymbol{U}}^\top(s)(\boldsymbol{L} + \mathsf{B}_n^\top\boldsymbol{\lambda}_n(s))\,\mathrm{d}s,$$

therefore

$$\frac{1}{2}\dot{\boldsymbol{U}}^\top(t)\mathsf{M}_r\dot{\boldsymbol{U}}(t) + \frac{1}{2}\boldsymbol{U}^\top(t)\mathsf{K}\boldsymbol{U}(t) - \frac{1}{2}\dot{\boldsymbol{U}}^\top(0)\mathsf{M}_r\dot{\boldsymbol{U}}(0) - \frac{1}{2}\boldsymbol{U}^\top(0)\mathsf{K}\boldsymbol{U}(0) = \boldsymbol{U}(t)^\top\boldsymbol{L} - \boldsymbol{U}(0)^\top\boldsymbol{L} + \int_0^t \dot{\boldsymbol{U}}^\top(s)\mathsf{B}_n^\top\boldsymbol{\lambda}_n(s)\,\mathrm{d}s.$$

Taking into account the definition of the energy functional (see Definition 2.1) we see that:

$$J(\boldsymbol{U}(t),\dot{\boldsymbol{U}}(t)) = J(\boldsymbol{U}(0),\dot{\boldsymbol{U}}(0)) + \int_0^t \dot{\boldsymbol{U}}^\top(s)\mathsf{B}_n^\top\boldsymbol{\lambda}_n(s)\,\mathrm{d}s = J(\boldsymbol{U}(0),\dot{\boldsymbol{U}}(0)).$$

in virtue of Theorem 3.1. □

Remark 3.1. In the previous text we assumed that the normal vectors have only one non-zero element. This simplification enabled us to annihilate the mass on the contact boundary in the normal direction by setting the appropriate rows and columns of the mass matrix to zero. In a general case one can use a transformation of variables for the contact displacements in such a way, that a local coordinate system at every contact node can be introduced, such that the normal direction plays the role of the x-axis and the tangential direction plays the role of y-axis, and to measure the displacement of this node in this local coordinate system. Another possibility is to simply remove the mass in both the normal and the tangential directions. However the next remark indicates that this technique may not be suitable in all cases.

Remark 3.2. In the case of the frictional contact problem the situation is more complicated. In [20] it has been shown that the total annihilation of the mass on the contact boundary may lead to the ill-posedness of the frictional contact problem. The mass matrix redistribution method should be therefore applied only to the unilateral conditions (i.e the mass matrix should be redistributed in such a way that $\ker \mathsf{M}_r = \mathcal{N}$). However the numerical experiments presented in the same work did not show any significant differences between these two approaches. We will perform several numerical tests in the last part of this work to compare these methods, too.

3.3 Redistribution of the mass matrix by modification of quadrature formulas

A main drawback of the described method is a necessity to solve a global constrained minimization problem to obtain the redistributed mass matrix. This gives rise to extra computational costs which may forbid its usage for large problems. Another method for the construction of the redistributed mass matrix has been proposed in [9, 10]. It is based on a modification of a quadrature formula that allows us to assemble the new mass matrix without a necessity to solve a global optimization problem. Let us only briefly describe the main idea of the method.

Using the approach presented in [9] one can construct the new mass matrix M_r which satisfies conditions (3.1). However there is a need to use the second triangulation with macro-elements along the contact boundary. A construction of such triangulation may be rather complicated for general meshes. Therefore we will use a simpler approach described in [10], which is directly applicable to any shape-regular triangulation, however it preserves only the mass of a body but not the moments of inertia.

Let us denote $\overline{\Omega^c} := \bigcup_{i\in\mathcal{I}_c} \operatorname{supp}\varphi_i$ and $\Omega^n := \Omega^h \setminus \overline{\Omega^c}$, where φ_i are the Courant basis functions. Thus $\overline{\Omega^c}$ is a stripe of triangles with at least one vertex on the contact boundary (see Figure 3.1a). The main idea of the method is to approximate the integral over a triangle $T \subset \overline{\Omega^c}$ by:

$$\int_T \varrho N_i(\boldsymbol{x}) N_j(\boldsymbol{x})\,\mathrm{d}\boldsymbol{x} \approx Q_T(\varrho N_i(\boldsymbol{x}) N_j(\boldsymbol{x})), \quad i,j = 1,2,3,$$

where $N_i\colon \mathbb{R}^2 \mapsto \mathbb{R}$ are the element shape functions and Q_T is a modified quadrature formula satisfying the following conditions:

1. No quadrature point is placed on $\Omega_c \setminus \Gamma_h$, where $\Gamma_h := \partial\Omega^c \cap \partial\Omega^h$.
2. Let $S^H := \operatorname{span}\left\{\varphi_i^H\right\}_{i\in\mathcal{P}^h\setminus\mathcal{I}_c}$ be the finite dimensional space spanned by the modified nodal basis functions φ_i^H which satisfy additional conditions listed in [10]. Then Q_T is exact on each $T \in \mathcal{T}^h$ for all functions of the form $\chi^H\eta^H$ with $\chi^H, \eta^H \in S^H$.[8]

The integrals over elements $T \in \overline{\Omega^n}$ are evaluated in the standard way. The example of the appropriate quadrature points and weights for the elements from $\overline{\Omega_c}$ is given in Figure 3.2. The quadrature formula then reads as:

$$Q_T(f(\boldsymbol{x})) = \Delta f(\boldsymbol{q}_1) \tag{3.4}$$

for the situation depicted in Figure 3.2a and

$$Q_T(f(\boldsymbol{x})) = \frac{1}{12}\Delta f(\boldsymbol{q}_1) + \frac{5}{6}\Delta f(\boldsymbol{q}_2) + \frac{1}{12}\Delta f(\boldsymbol{q}_3) \tag{3.5}$$

[8] The set of possible modified nodal functions spanning S^H for elements from Ω^c (as used in [10]) is depicted in Figure 3.1b. The rest of the basis consists of the standard piece-wise linear Courant basis functions.

for the situation described in Figure 3.2b. Recall that Δ denotes the area of a given triangle T.

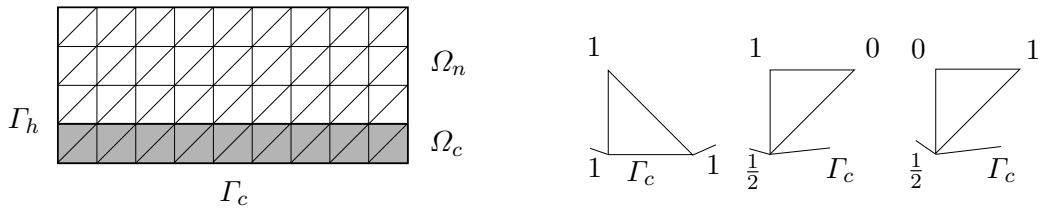

(a) Partition of Ω into Ω_c and Ω_n (b) Modified nodal basis functions

Figure 3.1: Partition of Ω and modified basis functions

Formulas (3.4), (3.5) yield the following form of the element mass matrices for the triangles from $\overline{\Omega_c}$:

$$\mathsf{M}_r^e = \varrho\Delta \begin{bmatrix} 1 & 0 & 0 & 0 & 0 & 0 \\ 0 & 1 & 0 & 0 & 0 & 0 \\ 0 & 0 & 0 & 0 & 0 & 0 \\ 0 & 0 & 0 & 0 & 0 & 0 \\ 0 & 0 & 0 & 0 & 0 & 0 \\ 0 & 0 & 0 & 0 & 0 & 0 \end{bmatrix}, \quad \mathsf{M}_r^e = \frac{\varrho\Delta}{24} \begin{bmatrix} 7 & 0 & 5 & 0 & 0 & 0 \\ 0 & 7 & 0 & 5 & 0 & 0 \\ 5 & 0 & 7 & 0 & 0 & 0 \\ 0 & 5 & 0 & 7 & 0 & 0 \\ 0 & 0 & 0 & 0 & 0 & 0 \\ 0 & 0 & 0 & 0 & 0 & 0 \end{bmatrix},$$

respectively (assuming that the contact nodes displacements are listed last). For the remaining triangles the element mass matrix remains the same as defined in Section 2.1.1. Assembling the global mass matrix using these element matrices assigns zeros to the nodes on the contact boundary whereas the total mass remains the same as in the standard case. However note that the mass is reduced in both, normal and tangential directions.

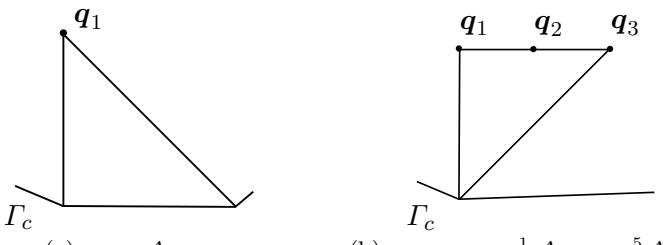

(a) $w_1 = \Delta$ (b) $w_1 = w_3 = \frac{1}{12}\Delta, w_2 = \frac{5}{6}\Delta$

Figure 3.2: Example of the quadrature points and weights for $T \subset \overline{\Omega^c}$

4 Numerical experiments

In this section we present several numerical experiments to confirm the theoretical results of the previous chapters. All experiments were realized using the programming environment Matlab. A spatial discretization of the second example was generated by Comsol Multiphysics simulation software.

Let us sum up the workflow necessary to solve the problems:

1. Spatial discretization of a problem by a finite element method;
2. Redistribution of a mass matrix (optional);
3. Time discretization of a problem by a suitable scheme;
4. For all time-steps do:
   (a) Transformation of a resulting static contact problem to the dual formulation;
   (b) Solution of a static contact problem with Coulomb friction;
      - Solution of a series of static contact problems with Tresca friction;
   (c) Transformation of a result to the primal variables;
5. Visualization of results.

The mass matrix redistribution is performed by the method presented in Section 3.1 unless stated otherwise. For realization of (4b) we use the implementation of the algorithm MPRGP from MatSol library developed at the Department of Applied Mathematics of Technical University of Ostrava [18].

Let us also mention that within this section outward normal unit vectors to the contact boundary are approximated by the relation (1.5).

4.1 Example 1: Contact of a brick on a rigid foundation

In the first example we simulate the behaviour of a 2-dimensional elastic brick $\Omega = (0, 0.4) \times (0, 0.4)$ supported by the rigid foundation represented by the half-plane $S = \mathbb{R} \times \mathbb{R}_-$ (see Figure 4.1). The brick of unit thickness is made from a material with the density $\varrho = 7000\,\mathrm{kg} \cdot \mathrm{m}^{-3}$, Young's modulus $E = 1.5 \cdot 10^6\,\mathrm{Pa}$ and Poisson's ratio $\nu = 0.3$. The friction coefficient is $\mathcal{F} = 0.2$. There is no initial gap between Ω and S and the brick is fixed on its top Γ_u. The tractions $\boldsymbol{P}_1 := (7 \cdot 10^4, 2 \cdot 10^4)$ and $\boldsymbol{P}_2 := (-4 \cdot 10^4, 2 \cdot 10^4)$ are prescribed on the lateral parts Γ_σ^1, Γ_σ^2 respectively (the values are in Pa). The initial displacement and velocity are $\boldsymbol{u}_{|t=0}(\boldsymbol{x}) = \boldsymbol{0}, \dot{\boldsymbol{u}}_{|t=0}(\boldsymbol{x}) = \boldsymbol{0}$ for all $\boldsymbol{x} \in \Omega$.

The brick was divided into small squares of size $h = 0.02\,\mathrm{m}$ and then each square by its diagonal into two triangles. This leads to 882 primal and 42 dual variables. Unless explicitly stated otherwise, all simulations use the time-step $\Delta t = 0.001\,\mathrm{s}$ which satisfies the CFL condition (see Section 2.2).

4.1.1 Newmark method

At first we demonstrate the behavior of the classical Newmark method. Choosing $\beta = \frac{1}{2}, \gamma = 1$ we obtain a very dissipative scheme (see Figure 4.2) with smooth normal and tangential contact stresses (see Figure 4.3). However the drawback of this choice of β, γ is the fact that the method is only of the first order.

For $\beta = \gamma = \frac{1}{2}$ the method behaves steadily too. The energy oscillations visible in Figure 4.4 are caused especially by the second and the third term in the expression for ΔJ in Proposition 2.1. From Figure 4.4b one can see that the oscillation can be damped by choosing a smaller time-step. The solution of the problem using this method is depicted in Figure 4.17. From Figure 4.5 we see that although the method is stable for this choice of β, γ, the Lagrange multipliers show spurious oscillations.

In the classical case (without contact and friction) the choice $2\beta = \gamma = \frac{1}{2}$ leads to the energy conserving scheme. As seen from Figure 4.6a the presence of contact makes this algorithm unstable and the energy grows.

4.1.2 Mid-point and modified mid-point method

The standard mid-point method presented in Section 2.2.3 is not suitable for contact problems as was confirmed by the numerical experiment. The energy blow-up and the normal stress oscillations are clearly visible in Figure 4.7.

To overcome these drawbacks the modified mid-point method described in Section 2.2.4 was used. This modification leads to the dissipative scheme as seen from Figure 4.8.

4.1.3 Stabilization by the modified mass matrix approach

From Section 3.2 we know that the method of mass matrix redistribution represents a very promising tool for stabilizing some of the presented methods. In this part we will use a fully redistributed (i.e. in both, the normal and tangential direction) mass matrix to confirm

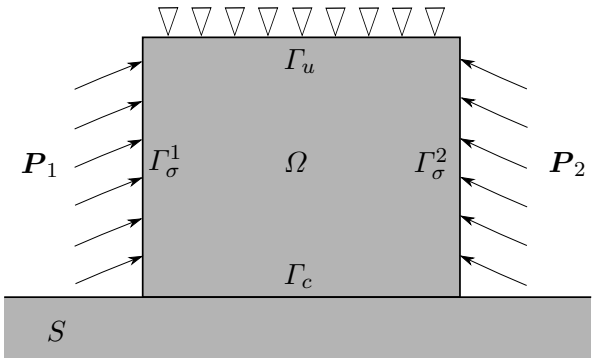

Figure 4.1: Setting of the first example

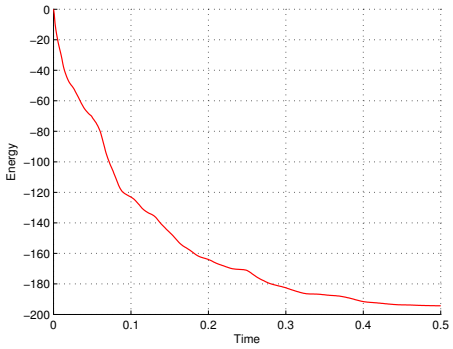

Figure 4.2: Evolution of the energy (Newmark scheme with $\beta = 0.5, \gamma = 1$)

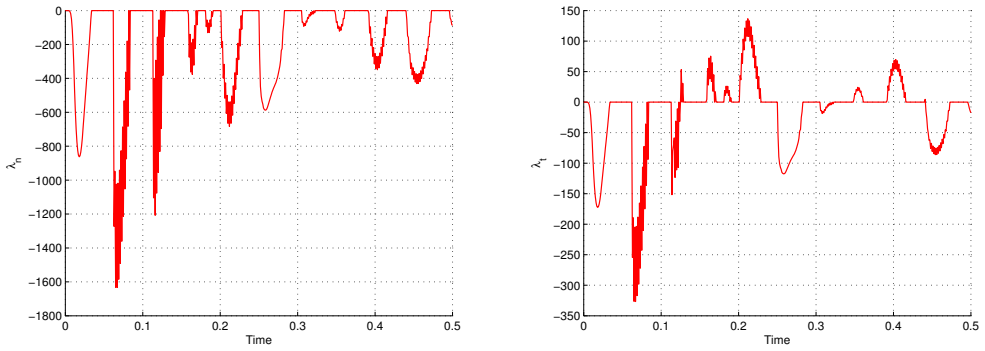

(a) Normal contact stress

(b) Tangential contact stress

Figure 4.3: Evolution of the Lagrange multipliers at the mid-point of Γ_c^h (Newmark scheme with $\beta = 0.5, \gamma = 1$)

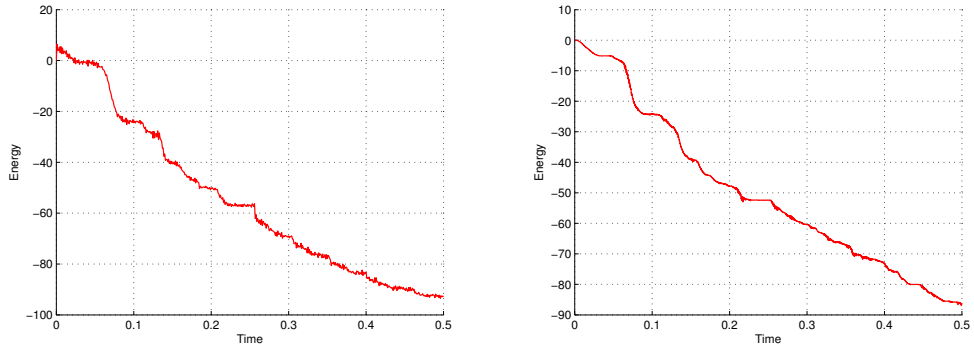

(a) $\Delta t = 0.001\,\mathrm{s}$ (b) $\Delta t = 0.0001\,\mathrm{s}$

Figure 4.4: Evolution of the energy (Newmark scheme with $\beta = \gamma = 0.5$)

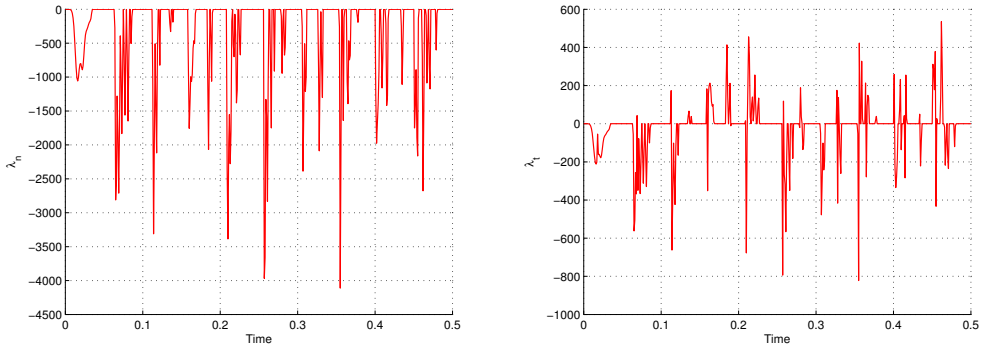

(a) Normal contact stress (b) Tangential contact stress

Figure 4.5: Evolution of the Lagrange multipliers at the mid-point of Γ_c^h (Newmark scheme with $\beta = \gamma = 0.5$)

this statement. Figure 4.10 illustrating the evolution of the energy for the Newmark scheme with $2\beta = \gamma = \frac{1}{2}$ confirms a stabilization (compare with Figure 4.6a). Figures 4.11 and 4.12 compare the normal and tangential contact stress with and without mass matrix redistribution. A significant improvement is visible as the artificial oscillations of the Lagrange multipliers are suppressed. A similar improvement for the mid-point method is depicted in Figure 4.13.

Figure 4.14 compares the energy and normal stress distribution for a fully and a partially redistributed mass matrix. No significant difference is apparent from these figures. However from Figure 4.15 one can see that the number of iterations of the algorithm MPRGP is higher in the case of the fully redistributed mass matrix.

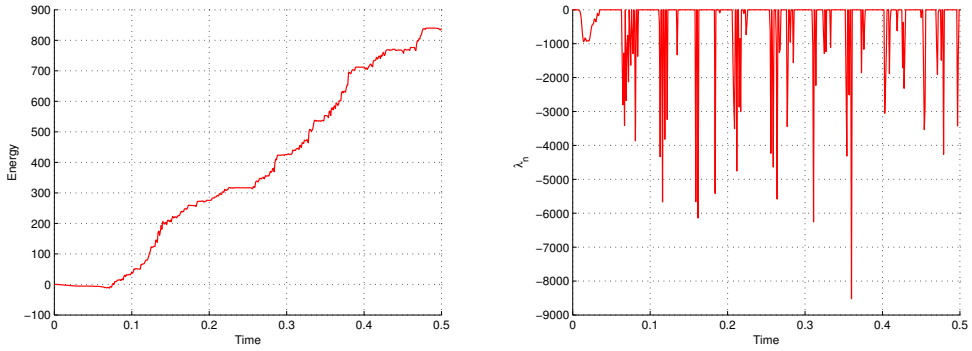

(a) Energy (b) Normal contact stress

Figure 4.6: Energy and the normal stress at the mid-point of Γ_c^h (Newmark scheme with $\beta = 0.25, \gamma = 0.5$)

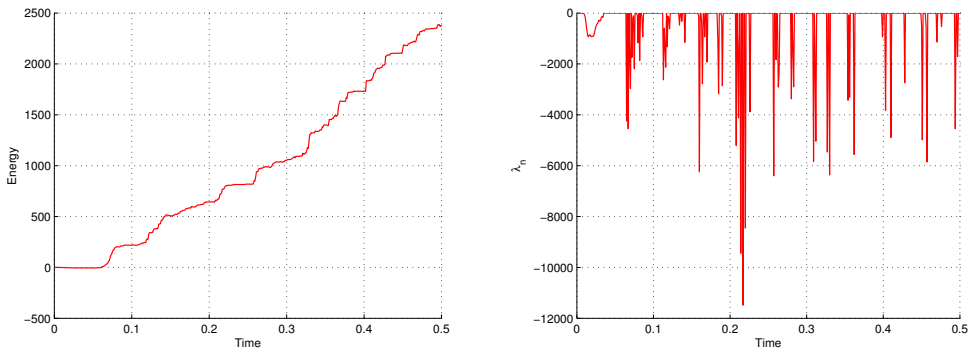

(a) Energy (b) Normal contact stress

Figure 4.7: Energy and the normal stress at the mid-point of Γ_c^h (the mid-point method)

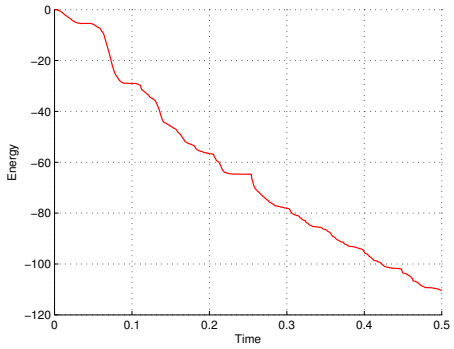

Figure 4.8: Evolution of the energy (the modified mid-point method)

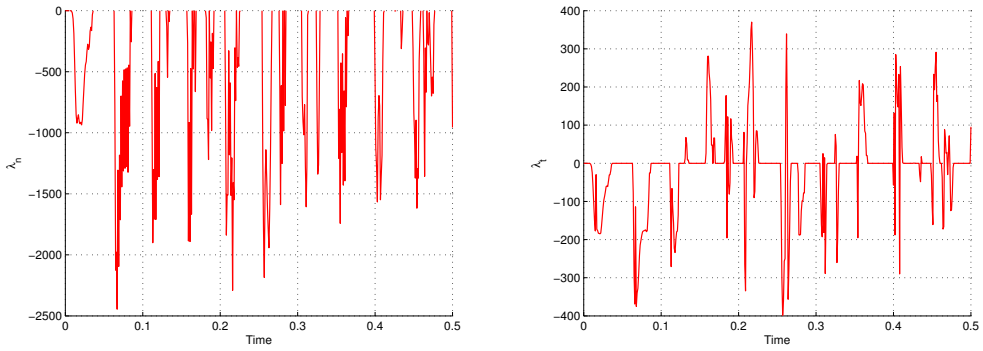

(a) Normal contact stress (b) Tangential contact stress

Figure 4.9: Evolution of the Lagrange multipliers at the mid-point of Γ_c^h (the modified mid-point method)

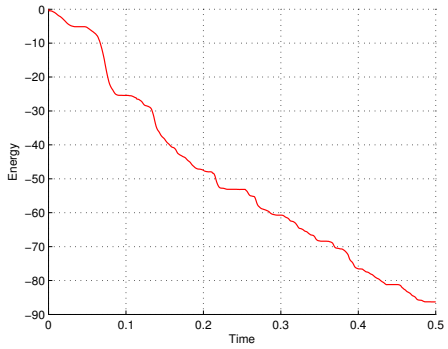

Figure 4.10: Evolution of the energy (Newmark scheme with the redistributed mass matrix, $\beta = 0.25, \gamma = 0.5$)

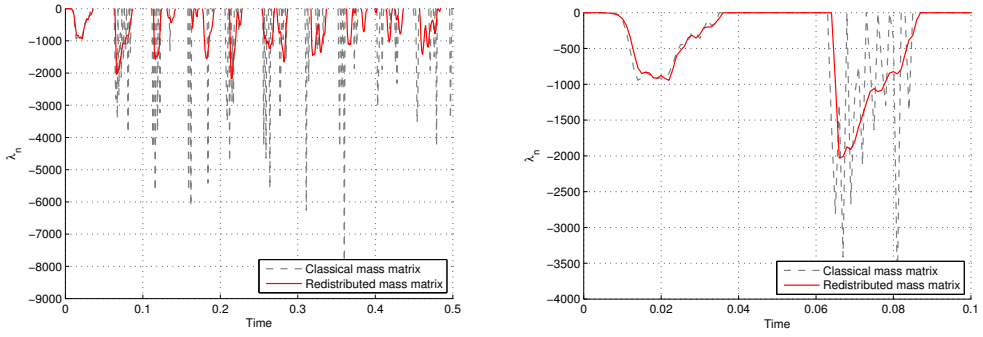

(a) $T = 0.5\,\mathrm{s}$ (b) $T = 0.1\,\mathrm{s}$

Figure 4.11: Comparison of the normal contact stress at the mid-point of Γ_c^h with the classical and the redistributed mass matrix (Newmark scheme with $\beta = 0.25, \gamma = 0.5$)

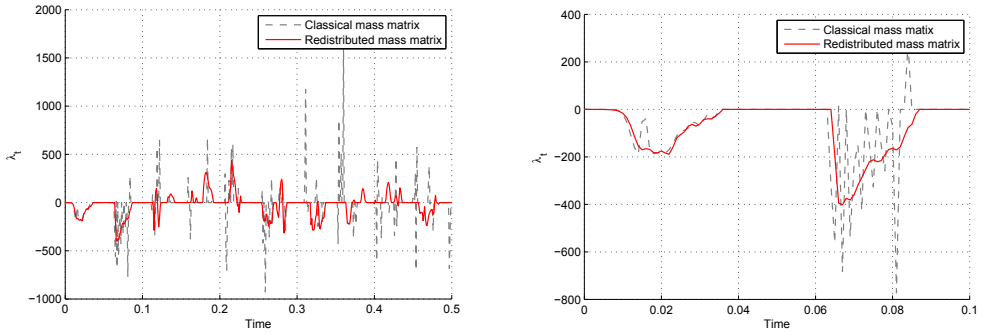

(a) $T = 0.5\,\mathrm{s}$ (b) $T = 0.1\,\mathrm{s}$

Figure 4.12: Comparison of the tangential contact stress at the mid-point of Γ_c^h with the classical and the redistributed mass matrix (Newmark scheme with $\beta = 0.25, \gamma = 0.5$)

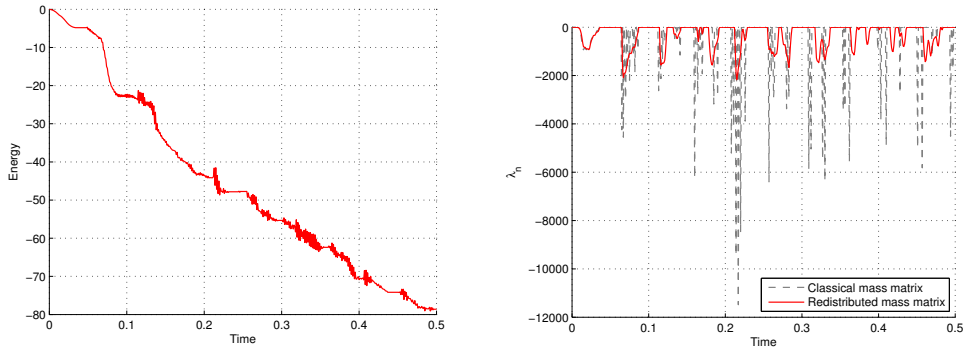

(a) Energy (b) Normal contact stress

Figure 4.13: Energy and the normal contact stress at the mid-point of Γ_c^h with and without mass matrix redistribution (the mid-point method)

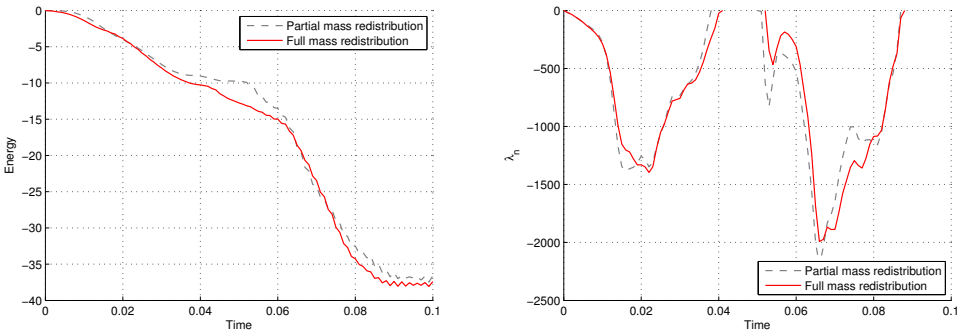

(a) Energy (b) Normal contact stress

Figure 4.14: Comparison between a full and a partial mass redistribution (Newmark method with $\beta = \gamma = 0.5$)

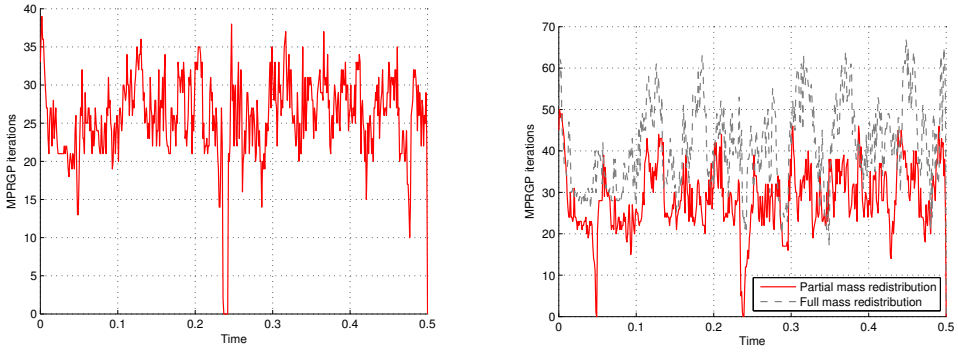

(a) Without a mass redistribution (b) With a mass redistribution

Figure 4.15: Iterations of MPRGP algorithm (Newmark method with $\beta = \gamma = 0.5$)

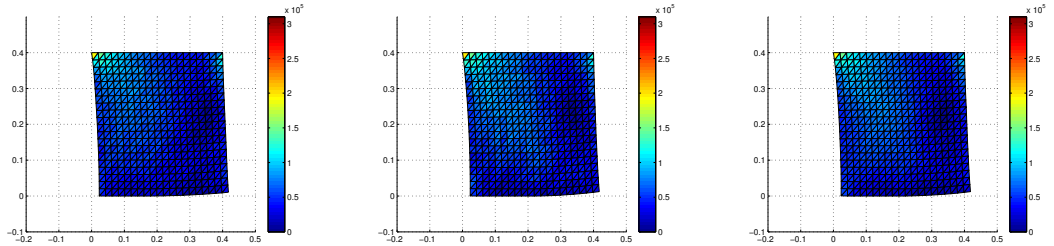

(a) Newmark method ($\beta = \gamma = 0.5$) (b) Newmark method with the redistributed mass matrix ($2\beta = \gamma = 0.5$) (c) Modified mid-point method

Figure 4.16: Deformation and von Misses stress at $t = 5\,\mathrm{s}$

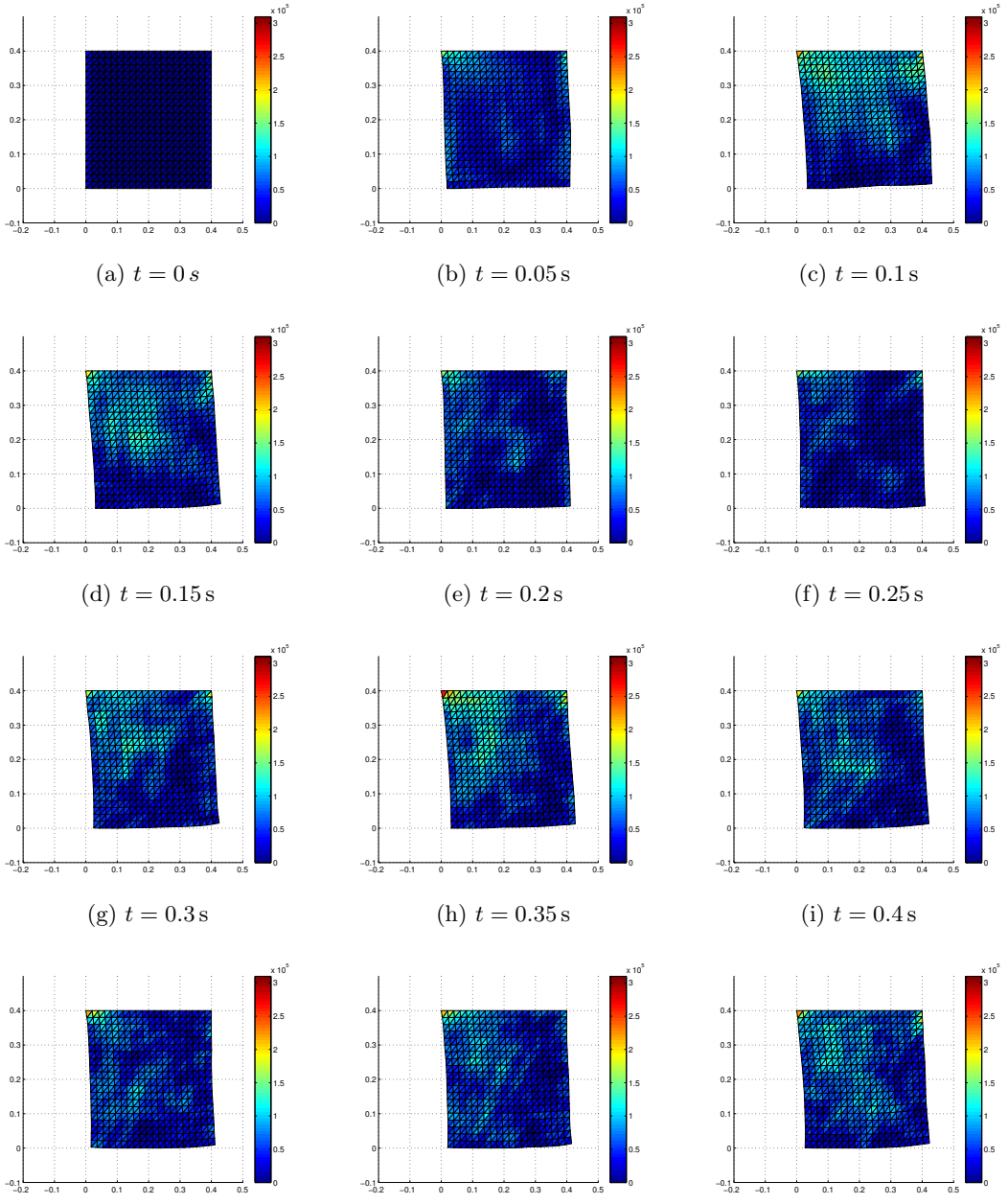

(a) $t = 0\,s$ (b) $t = 0.05\,\mathrm{s}$ (c) $t = 0.1\,\mathrm{s}$

(d) $t = 0.15\,\mathrm{s}$ (e) $t = 0.2\,\mathrm{s}$ (f) $t = 0.25\,\mathrm{s}$

(g) $t = 0.3\,\mathrm{s}$ (h) $t = 0.35\,\mathrm{s}$ (i) $t = 0.4\,\mathrm{s}$

(j) $t = 0.45\,\mathrm{s}$ (k) $t = 0.5\,\mathrm{s}$ (l) $t = 0.55\,\mathrm{s}$

Figure 4.17: Deformation and von Mises stress (Newmark scheme with $\beta = \gamma = 0.5$)

4.2 Example 2: Contact of a disc on a rigid foundation

The setting of the second example is depicted in Figure 4.18a. We simulate the behaviour of a disc Ω supported by a rigid foundation $S = \mathbb{R} \times \mathbb{R}_-$. The disc is made from a material with the density $\varrho = 1200\,\mathrm{kg} \cdot \mathrm{m}^{-3}$, Young's modulus $E = 10^7\,\mathrm{Pa}$ and Poisson's ratio 0.45. Its diameter is 0.8 m and it has a unit thickness. The friction coefficient is $\mathcal{F} = 0.3$. There is the initial gap of 2 cm between the obstacle and the lowest point of the disc. The initial displacement of the disc is $\boldsymbol{u}_{|t=0}(\boldsymbol{x}) = \mathbf{0}$ for all $\boldsymbol{x} \in \Omega$ while the initial velocity is $\dot{\boldsymbol{u}}_{|t=0}(\boldsymbol{x}) = (0, -1)$ for all $\boldsymbol{x} \in \Omega$ (in $\mathrm{m} \cdot \mathrm{s}^{-1}$). Moreover the disc is subject to its own weight. One can easily calculate that due to the gravitational acceleration, the velocity at the moment of contact is approximately $-1.17\,\mathrm{m} \cdot \mathrm{s}^{-1}$ in the vertical direction.

The triangulation of the disc is shown in Figure 4.18b. The minimal 'diameter' of a triangle is $h = 0.01\,\mathrm{m}$. Due to the symmetry one can model only one half of the disc. On the axe of symmetry the condition $u_1 = 0$ is prescribed. The contact boundary Γ_c^h consists of nine nodes at the lowest part of the $\partial\Omega^h$. After the spatial discretization we obtain the problem with 1030 primal and 18 dual unknowns. For the time discretization Newmark and mid-point scheme with time-step $\Delta t = 10^{-4}\,\mathrm{s}$ satisfying the CFL condition is used.

Similarly to the previous subsection one can see that the Newmark method with $\beta = \frac{1}{2}$ and $\gamma = 1$ provides a dissipative scheme (see Figure 4.19) with smooth Lagrange multipliers (Figure 4.20) whereas for $2\beta = \gamma = \frac{1}{2}$ the scheme is unstable with the standard mass matrix. The effects of this instability and the stabilization by the full mass matrix redistribution are presented in Figure 4.21 and Figure 4.22. One can see that the redistribution leads to a dissipative scheme.

Finally, the evolution of the energy of the solution computed by the mid-point method is shown in Figure 4.23 while Figure 4.24 displays the Lagrange multipliers for the same

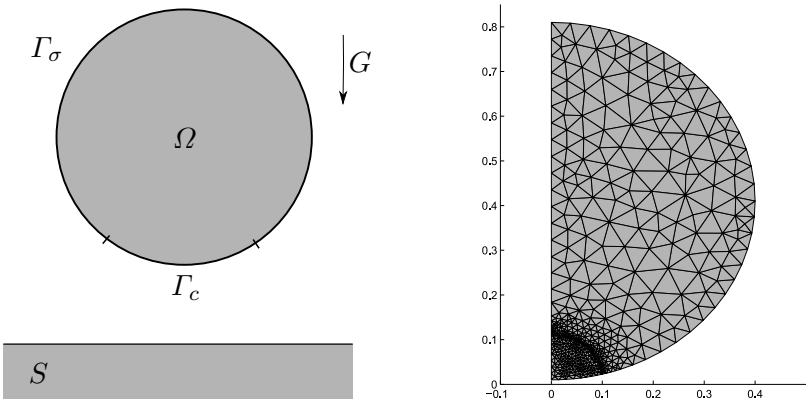

(a) Setting of Example 2 (b) Discretization of the disc

Figure 4.18: Example 2

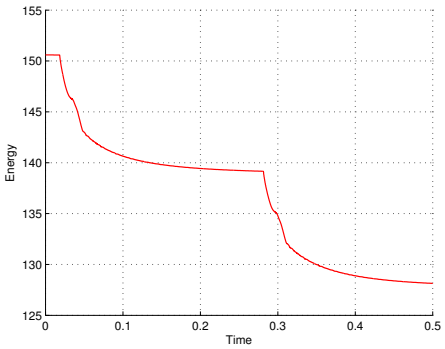

Figure 4.19: Evolution of the energy (Newmark scheme with $\beta = 0.5, \gamma = 1$)

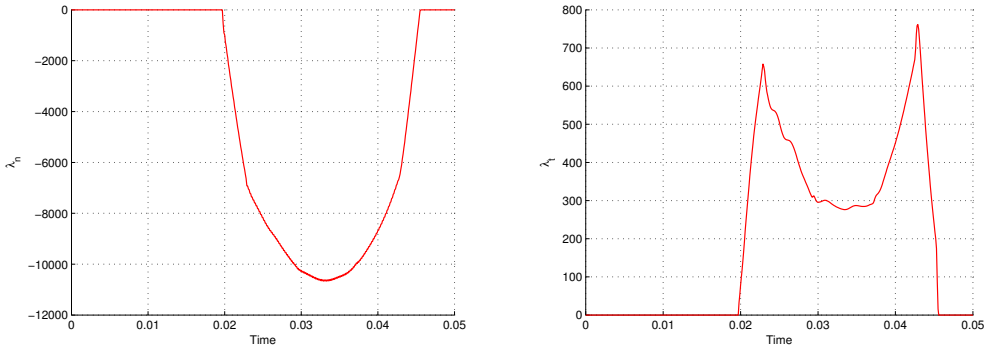

(a) Normal contact stress

(b) Tangential contact stress

Figure 4.20: Evolution of the Lagrange multipliers at the mid-point of Γ_c^h (Newmark scheme with $\beta = 0.5, \gamma = 1$)

case. Again a significant improvement is clearly visible however the energy oscillates during the contact, as seen from Figure 4.23b, and the scheme is not conservative.

For completeness Figure 4.25 and Figure 4.26 show the evolution of the energy and the Lagrange multipliers for the redistribution by modified quadrature formulas. We have not observed any significant difference between this approach and the latter one.

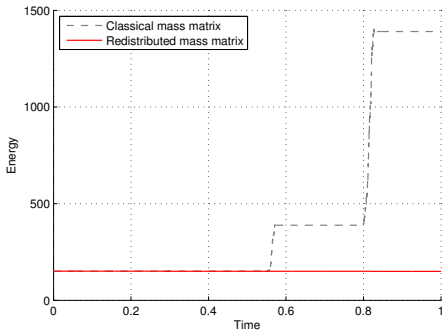

Figure 4.21: Evolution of the energy (Newmark scheme with $\beta = 0.25, \gamma = 0.5$)

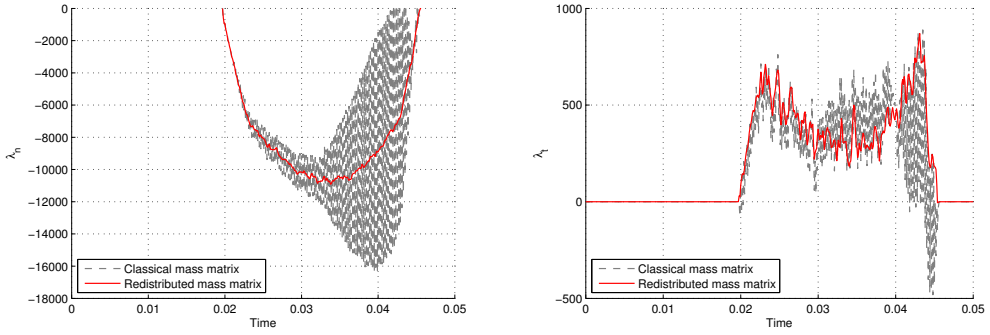

(a) Normal contact stress

(b) Tangential contact stress

Figure 4.22: Evolution of the Lagrange multipliers at the mid-point of Γ_c^h (Newmark scheme with $\beta = 0.25, \gamma = 0.5$)

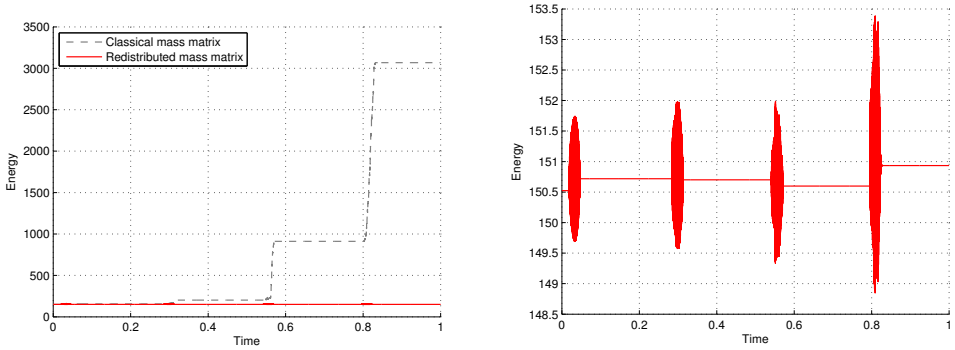

(a) Comparison between the classical and redistributed mass matrix

(b) Redistributed mass matrix

Figure 4.23: Evolution of the energy (mid-point method)

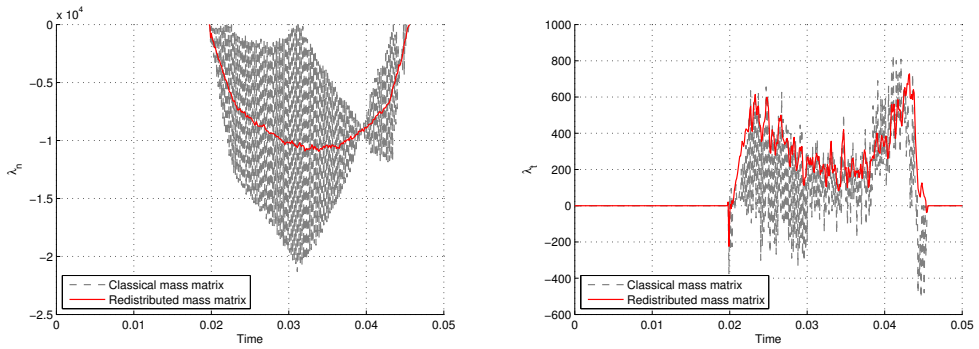

(a) Normal contact stress (b) Tangential contact stress

Figure 4.24: Evolution of the Lagrange multipliers at the mid-point of Γ_c^h (mid-point method)

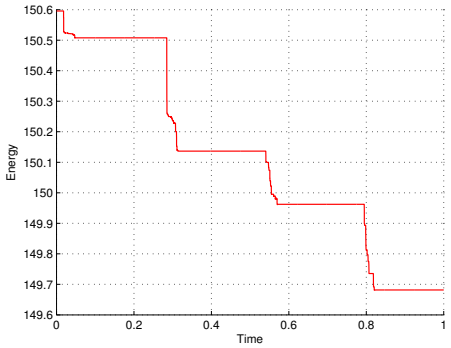

Figure 4.25: Evolution of the energy (Newmark scheme with $\beta = 0.25, \gamma = 0.5$, redistribution by modified quadrature formula)

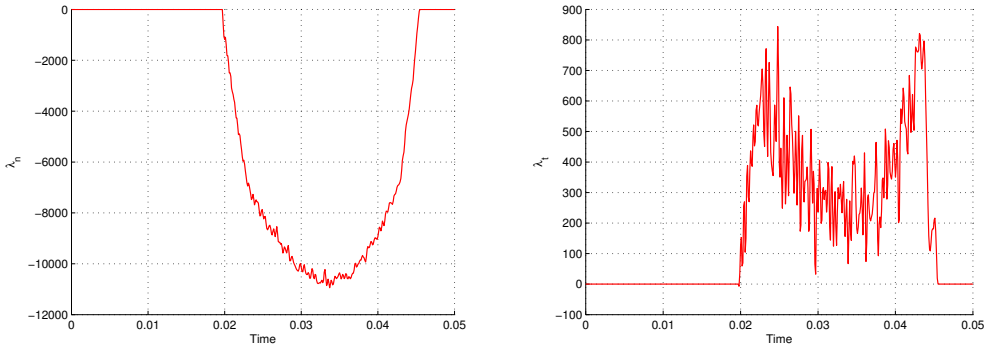

(a) Normal contact stress (b) Tangential contact stress

Figure 4.26: Evolution of the Lagrange multipliers at the mid-point of Γ_c^h (Newmark method with $\beta = 0.25, \gamma = 0.5$, redistribution by modified quadratic formula)

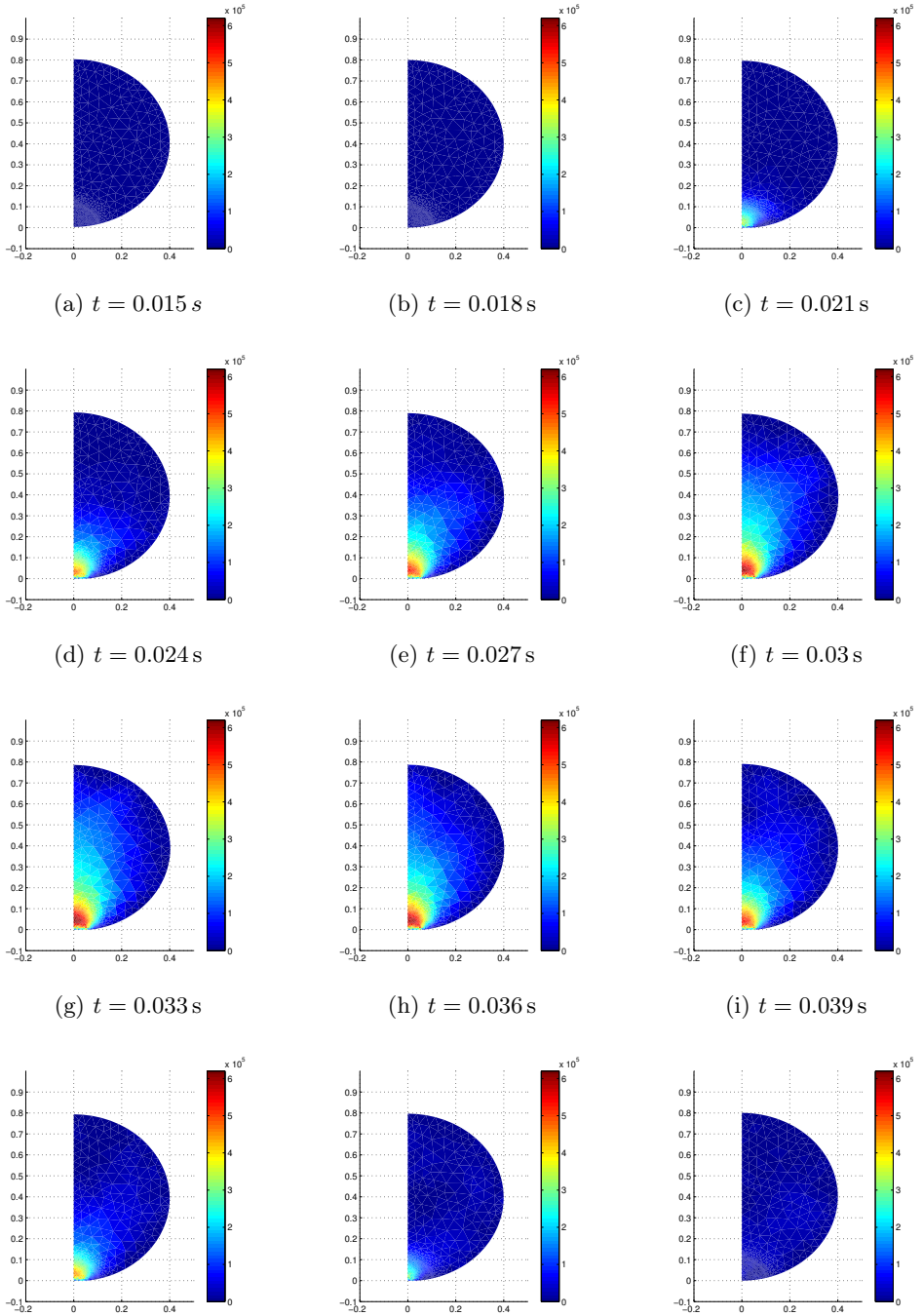

(a) $t = 0.015\,s$ (b) $t = 0.018\,\mathrm{s}$ (c) $t = 0.021\,\mathrm{s}$

(d) $t = 0.024\,\mathrm{s}$ (e) $t = 0.027\,\mathrm{s}$ (f) $t = 0.03\,\mathrm{s}$

(g) $t = 0.033\,\mathrm{s}$ (h) $t = 0.036\,\mathrm{s}$ (i) $t = 0.039\,\mathrm{s}$

(j) $t = 0.042\,\mathrm{s}$ (k) $t = 0.045\,\mathrm{s}$ (l) $t = 0.048\,\mathrm{s}$

Figure 4.27: Deformation and von Mises stress during the first contact between the disc and the obstacle (Newmark scheme with $\beta = 0.25, \gamma = 0.5$)

4.3 Example 3: Sliding of a brick on a rigid foundation

In the last numerical example we focus especially on the frictional behaviour of a 2-dimensional elastic brick $\Omega = (0, 0.4) \times (0, 0.4)$ sliding on a rigid foundation $S = \mathbb{R} \times \mathbb{R}_-$ (see Figure 4.28). The material constants correspond to the steel, i.e. Young's modulus $E = 200 \cdot 10^9\,\mathrm{Pa}$, Poisson's ratio $\nu = 0.3$ and the density $\varrho = 8000\,\mathrm{kg} \cdot \mathrm{m}^{-3}$. The brick has a unit thickness. There is no initial gap between the brick and the obstacle and the friction coefficient is $\mathcal{F} = 0.5$. The initial displacement of the brick is $\boldsymbol{u}_{|t=0}(\boldsymbol{x}) = \boldsymbol{0}$ for all $\boldsymbol{x} \in \Omega$ and the initial velocity is $\dot{\boldsymbol{u}}_{|t=0}(\boldsymbol{x}) = (4, 0)$ in $\mathrm{m} \cdot \mathrm{s}^{-1}$. The brick is subjected to the traction $\boldsymbol{P} := (0, -10^5)$ on Γ_σ^1 (in Pa) and Earth's gravitation force.

The spatial discretization with step $h = 0.02\,\mathrm{m}$ leads to 882 primal and 42 dual variables. We will use the time-step $\Delta t = 10^{-3}\,\mathrm{s}$ unless stated otherwise. Since we will use only implicit time-stepping schemes there is no necessity for the satisfaction of the CFL condition.

In what follows we use the following relation for the evaluation of the total energy dissipated by friction up to the time-step k:

$$J_F^k := \sum_{i=0}^{k} (\mathsf{B}_t \boldsymbol{v}^i)^\top \boldsymbol{\lambda}_t^i \Delta t.$$

We start with the Newmark scheme with $2\beta = \gamma = \frac{1}{2}$ and observe some interesting behaviour of the method. For $\Delta t = 0.001\,\mathrm{s}$ the method is unstable even with the mass redistribution (see Figure 4.29). As seen from Figure 4.30 using the time-step $\Delta t = 10^{-4}\,\mathrm{s}$ the method behaves steadily for both the standard and redistributed mass matrix although the graph of the difference of the total energy and the energy dissipated by friction suggests that it is not conservative. Finally in Figure 4.31 one can see that due to friction the tangential velocity of the body decreases and starts to oscillate around zero.

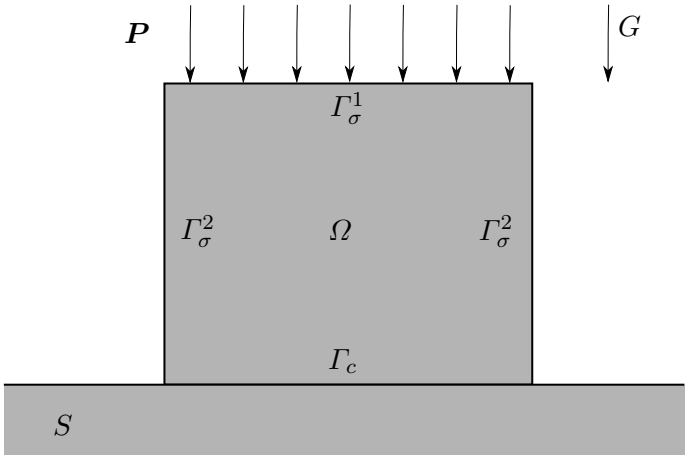

Figure 4.28: Setting of the third experiment

Choosing $\beta = \gamma = \frac{1}{2}$ we obtain much better results. Since for this example the method is stable with the classical mass matrix we do not use the mass redistribution. The evolution of the energy for various friction coefficients is depicted in Figure 4.32. We see that in the case without friction the energy is conserved. To have a better idea on the energetic behaviour of the scheme itself (without the influence of friction) we subtract the energy dissipated by friction from the total energy. In Figure 4.33 one can see that the energy oscillations may be damped by choosing a smaller time-step. Contrary to the previous example the tangential velocity of the contact nodes does not show such oscillations (compare Figure 4.31 with Figure 4.34a). Due to friction we observe a linear decrease of the velocity.

For the last test we choose the modified mid-point method. At first we use a frictionless problem. Since the body is sliding on the foundation and the normal velocity of the nodes of the triangulation is zero, according to the expression (2.30) we should get a conservative behaviour. This is confirmed in Figure 4.35a. In Figure 4.35b one can see that the method is dissipative for the frictional case. Again the tangential velocity of the contact nodes does not show any oscillations and decreases linearly to zero for $\mathcal{F} > 0$ (see Figure 4.36a).

In this last set of experiments there was no need for the stabilization by the mass redistribution. This is not very surprising since instabilities are mainly caused by rapid changes of the normal velocity of contact nodes which remains approximately zero during the whole simulation.

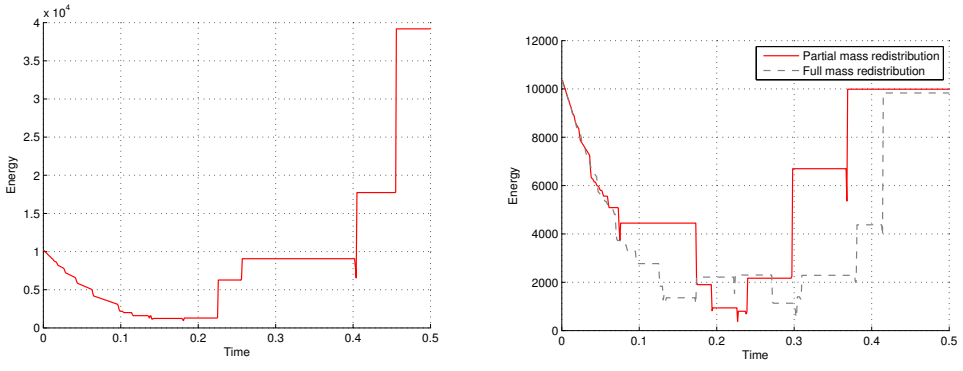

(a) Without mass redistribution (b) With mass redistribution

Figure 4.29: Evolution of the energy (Newmark scheme with $\beta = 0.25, \gamma = 0.5, \Delta t = 0.001\,\mathrm{s}$)

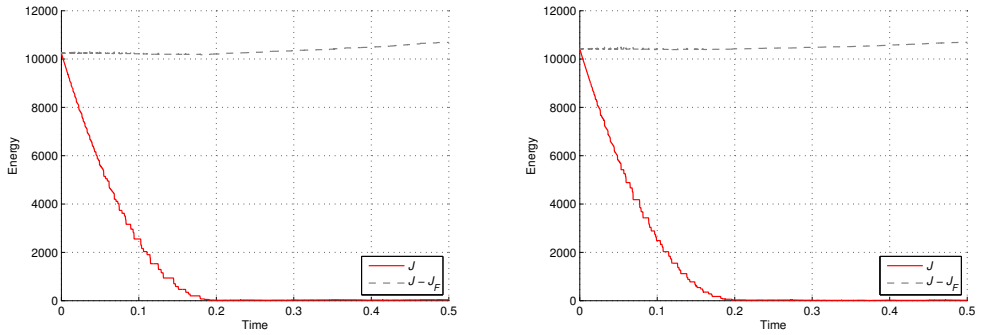

(a) Without mass redistribution (b) With mass redistribution

Figure 4.30: Evolution of the energy and the difference between the total energy J and the energy dissipated by friction J_F (Newmark scheme with $\beta = 0.25, \gamma = 0.5, \Delta t = 10^{-4}\,\mathrm{s}$)

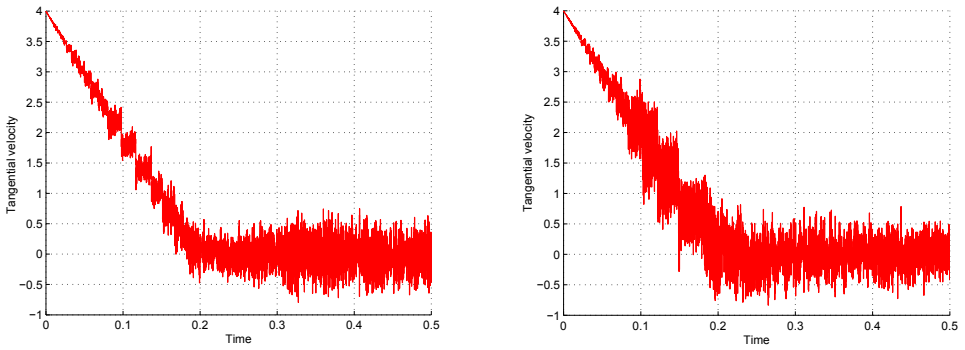

(a) Without mass redistribution (b) With mass redistribution

Figure 4.31: Tangential velocity at the mid-point of Γ_c^h (Newmark scheme with $\beta = 0.25, \gamma = 0.5, \Delta t = 10^{-4}\,\mathrm{s}$)

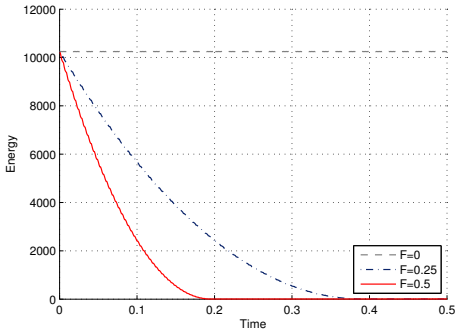

Figure 4.32: Evolution of the energy (Newmark scheme with $\beta = \gamma = 0.5$)

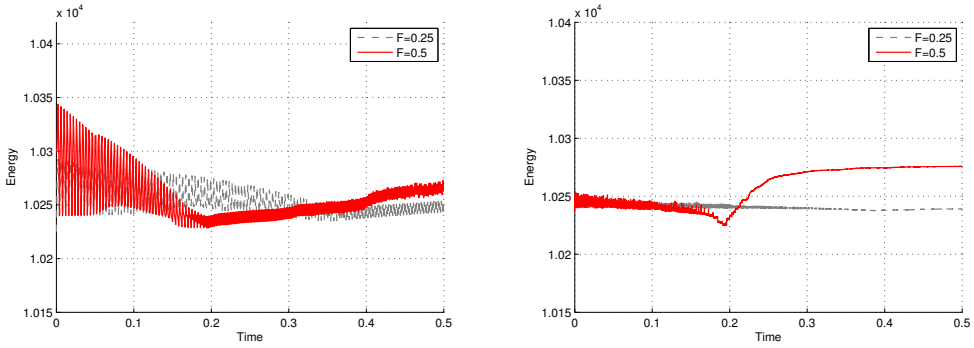

(a) $\Delta t = 10^{-3}\,\mathrm{s}$ (b) $\Delta t = 10^{-4}\,\mathrm{s}$

Figure 4.33: Difference betweet the total energy and the energy dissipated by friction (Newmark scheme with $\beta = \gamma = 0.5$)

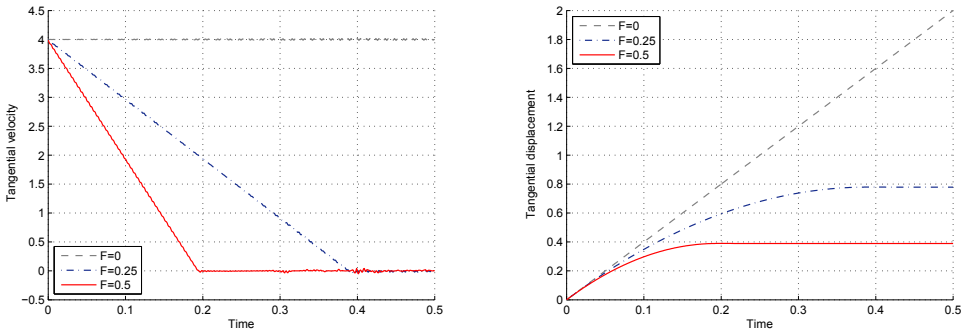

(a) Tangential velocity (b) Tangential displacement

Figure 4.34: Tangential velocity and displacement at the mid-point of Γ_c^h (Newmark scheme with $\beta = \gamma = 0.5$)

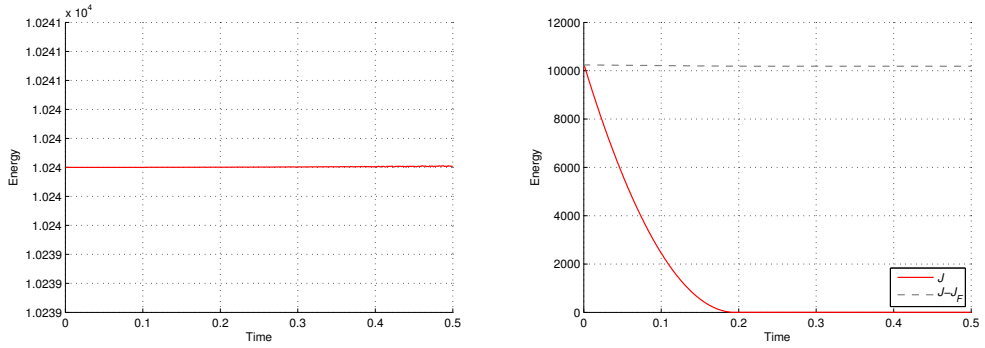

(a) $\mathcal{F} = 0$ (b) $\mathcal{F} = 0.5$

Figure 4.35: Evolution of the energy and the difference between the total energy J and the energy dissipated by friction J_F (modified mid-point method)

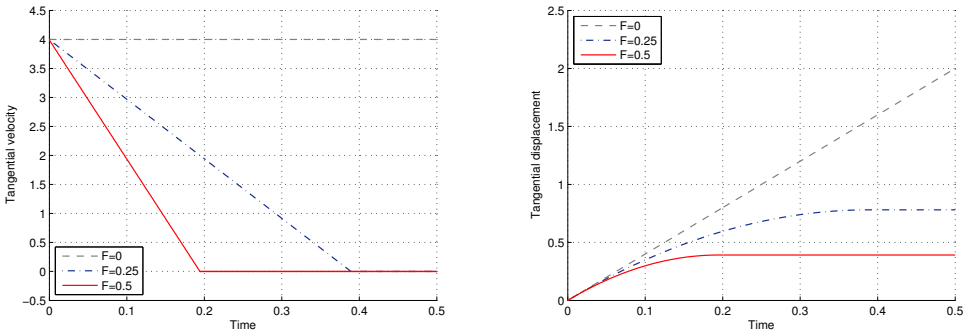

(a) Tangential velocity (b) Tangential displacement

Figure 4.36: Tangential velocity and displacement at the mid-point of Γ_c^h (modified mid-point method)

Conclusion

The aim of this thesis was to present an overview of the current state in the field of numerical realization of dynamical contact problems with friction. We introduced the strong formulation of the problem and derived the weak formulation with the unilateral and the friction conditions in the form of the variational inclusions. In the next part the spatial discretization by the finite element method and several time-stepping algorithms were presented. Since most of these algorithms show an unstable behaviour, some kind of stabilization is almost always necessary. In this work we chose the method of the mass redistribution in order to eliminate the mass on the contact boundary. The main advantage of this method is its applicability to practically any existing time-stepping algorithm. The redistribution itself was mainly performed by the method of Khenous [13] consisting in minimization of a distance between a standard and a redistributed mass matrix. However, it turns out that its implementation may be rather complicated and the solution of the global minimization problem is time-consuming. Therefore the use of this method for larger problems is questionable. Although the redistribution by modified quadrature formulas was mentioned only marginally in this work, it represents a promising less computational demanding alternative to the previous method. On the other hand it has its own drawbacks, namely a need of a special triangulation with macro-elements along the contact boundary. Here we presented only a simpler version of this method not preserving the moments of inertia. The last section was devoted to numerical experiments where we confirmed the positive effects of the mass redistribution on the behaviour of the energy and the Lagrange multipliers. However, the last example showed that the redistribution is not always necessary and that in specific cases it does not solve problems with instability.

Besides the implementation of the presented algorithms in Matlab environment and the testing of their properties, the contribution of this thesis also lies in the correction of some mistakes in [13]. In addition, this work may hopefully become the starting point for future research in this field at the Department of Applied Mathematics of Technical University of Ostrava, where the effective solution of problems from nonlinear contact mechanics is one of the main research areas.

For solution of larger real world problems the parallelization and processing on parallel computers is almost always necessary. Therefore, concerning the future work, there is a possibility to continue the study of this topic combined with domain decomposition methods and effective quadratic programming solvers like presented in [2]. The implementation in MatSol library [18] is one of the future concerns too.

References

[1] BRDIČKA, Miroslav; SAMEK, Ladislav; SOPKO, Bruno. *Mechanika kontinua*. 3., revidované vydání. Praha : Academia, 2005. 799 p. ISBN 80-200-1344-X.

[2] BRZOBOHATÝ, Tomáš. *Škálovatelné metody rozložení oblasti k řešení dynamických úloh mechaniky*. Ostrava, 2009. xi, 93 p. Dissertation thesis. VŠB-TU Ostrava.

[3] CHANDRUPATLA, Tirupathi R.; BELEGUNDU, Ashok D. *Introduction to finite elements in engineering*. Englewood Cliffs : Prentice Hall, c1991. xiv, 414 p.

[4] DEUFLHARD, Peter; KRAUSE, Rolf; ERTEL, Susanne. A Contact-Stabilized Newmark Method for Dynamical Contact Problems. *Int. J. Numer. Meth. Engng.*. 2007, 73, pp. 1274–1290.

[5] DHATT, Gouri, TOUZOT, Gilbert. *The Finite Element Method Displayed*. Gilles Cantin. Norwich : John Wiley & Sons, 1984. 509 p.

[6] DOSTÁL, Zdeněk. *Optimal Quadratic Programming Algorithms : With Applications to Variational Inequalities*. New York : Springer, c2009. xvii, 284 p. ISBN 978-0-387-84805-1.

[7] DUVAUT, G.; LIONS, J. L. *Les Inéquations en Mécanique et en Physique*. Paris : Dunod, 1972. 387 p.

[8] EKELAND, Ivar; TÉMAM, Roger. *Convex Analysis and Variational Problems*. Philadelphia : Society for Industrial and Applied Mathematics, 1999. 402 p. ISBN 0-89871-450-8.

[9] HAGER, C.; HÜEBER, S; WOHLMUTH, B. I. A stable energy-conserving approach for frictional contact problems based on quadrature formulas. *International Journal for Numerical Methods in Engineering*. 2008, 73, s. 205-225. Accessible from: <http://dx.doi.org/10.1002/nme.2069>. ISSN :0029-5981.

[10] HAGER, C.; WOHLMUTH, B. I. Fachbereich Mathematik Institut für Angewandte Analysis und Numerische Simulation. *Analysis of Modified Mass Lumping Method for the Stabilization of Frictional Contact Problems*. To appear. Accessible from: <http://preprints.ians.uni-stuttgart.de/downloads/2007/2007-003.pdf>.

[11] HASLINGER, Jaroslav; HLAVÁČEK, Ivan; NEČAS, Jindřich. Numerical Methods for Unilateral Problems in Solid Mechanics. In CIARLET, P. G.; LIONS, J. L. *Handbook of Numerical Analysis : Volume IV.*. Amsterdam : Elsevier, 1996. pp. 313-485. ISBN 0-444-81794-8.

[12] HASLINGER, Jaroslav; VLACH, Oldřich. Approximation and Numerical Realization of 2D Contact Problems with Coulomb Friction and a Solution-Dependent Coefficient of Friction. *Journal of Computational and Applied Mathematics*. 2006, 197, pp.

421-436. Accessible from <http://www.sciencedirect.com/science/article/B6TYH-4HX47FM-2/2/a17a5a25e5deb58ecb5075b9a00f8109>. ISSN 0377-0427.

[13] KHENOUS, Houari B. *Problèmes de contact unilatéral avec frottement de Coulomb en élastostatique et élastodynamique : Etude mathématique et résolution numérique.* Toulouse, 2005. 134 p. Dissertation thesis. Institut National des Sciences Appliquées de Toulouse.

[14] KHENOUS, Houari B.; LABORDE, Patrick; RENARD, Yves. Mass Redistribution Method for Finite Element Contact Problems in Elastodynamics. *European Journal of Mechanics A/Solids.* 2008, 27, pp. 918-932. Accessible from: <http://www.sciencedirect.com/science/article/B6VKW-4RSBY0M-2/2/f5fdc61817633616f52850e279ca7a83>. ISSN 0997-7538.

[15] KHENOUS, Houari B.; POMMIER, Julien; RENARD, Yves. Hybrid discretization of the Signorini problem with Coulomb friction : Theoretical aspects and comparison of some numerical solvers. *Applied Numerical Mathematics.* 2006, 56, pp. 163-192. Accessible from: <http://www.sciencedirect.com/science/article/B6TYD-4FXNRB0-3/2/9aec163be25e07bb9ca9df22440296f0>. ISSN 0168-9274.

[16] KIKUCHI, Naboru; ODEN, J. Tinsley. *Contact Problems in Elasticity : A Study of Variational Inequalities and Finite Element Method.* Philadelphia : Society for Industrial and Applied Mathematics, 1988. xiii, 495 p. s. ISBN 0-89871-468-0.

[17] KRAUSE, Rolf; WALLOTH, Mirjam. A Time Discretization Scheme Based on Rothe's Method for Dynamical Contact Problems with Friction. *Comput. Methods Appl. Mech. Engrg..* 2009, 199, pp. 1-19. Accessible from <http://www.sciencedirect.com/science/article/B6V29-4X4RWMP-2/2/93ccfb241c8c756dc97110c054ed4795>. ISSN 0045-7825.

[18] KOZUBEK, Tomáš; BRZOBOHATÝ, Tomáš; MARKOPOULOS, Alexandros. *MatSol* [online]. 2011 [cit. 2011-04-02]. Accessible from: <http://matsol.vsb.cz>.

[19] LAURSEN, Tod A. *Computational Contact and Impact Mechanics : Fundamentals of Modeling Interfacial Phenomena in Nonlinear Finite Element Analysis.* 1st ed., Corr. 2nd print. Berlin : Springer, 2003. xv, 454 p. ISBN 3-540-42906-9.

[20] LIGURSKÝ, Tomáš; RENARD Yves. A Well-Posed Semi-Discretization of Elastodynamic Contact Problems with Friction. To appear in *Q. J. Mech. Appl. Math.*

[21] MERTA, Michal. *Newmarkova metoda pro numerické řešení počátečních problémů 2. řádu.* Ostrava, 2009. 41 p. Bachelor thesis. VŠB - Technical University of Ostrava.

[22] NEČAS, Jindřich, HLAVÁČEK, Ivan. *Mathematical Theory of Elastic and Elasto-Plastic Bodies: An Introduction.* Elsevier, New York 1981. 342 p.

[23] RAVIART, Pierre-Arnaud, THOMAS, Jean-Marie. *Introduction à l'analyse numérique des équations aux dérivées partielles.* [s.l.] : Masson, 1988. 224 p.

[24] ZIENKIEWICZ, O. C.; TAYLOR, R. L.; ZHU, J. Z. *The Finite Element Method : Its Basis and Fundamentals*. Sixth ed. Oxford : Elsevier, 2005. xiv, 733 p. ISBN 0-7506-6320-0.